Republic of Iraq
Ministry of Higher Education and Scientific Research
University of Misan/College of Engineering
Civil Engineering Department

STRUCTURAL BEHAVIOR OF SIMPLY SUPPORTED REINFORCED CONCRETE BEAMS WITH NON PRISMATIC FLANGES

A THESIS
SUBMITTED TO THE COLLEGE OF ENGINEERING OF MISAN UNIVERSITY IN PARTIAL FULFILLMENT OF THE REQUIREMENTS FOR THE DEGREE OF MASTER IN CIVIL ENGINEERING
(STRUCTURES)

By
Jassim Kadhem Zamel AL-IbadI
(B.Sc. University of Basrh, 1991)

Supervised By
Assist. Prof. Dr. Sa'ad Fahad Resan

September 2019 **Muharam 1441**

۞وَقُلِ اعْمَلُوا فَسَيَرَى اللَّهُ عَمَلَكُمْ وَرَسُولُهُ وَالْمُؤْمِنُونَ وَسَتُرَدُّونَ إِلَى عَالِمِ الْغَيْبِ وَالشَّهَادَةِ فَيُنَبِّئُكُمْ بِمَا كُنْتُمْ تَعْمَلُونَ» ۞

سورة التوبة الآية (١٠٥)

Certification of the supervisor

*We certify that this thesis entitled "**STRCTURAL BEHAVIOR OF SIMPLY SUPPORTED RIENFORCED CONCRETE BEAMS WITH NON PRISMATIC FLANGES**", which is being submitted by "JASSIM KADHEM ZAMEL AL-IBADI", was made under my supervision at University of Misan / College of Engineering, in partial fulfillment of the requirements for the Degree of Master of Science in Civil Engineering structures.*

Signature:

Name: Assist. Prof. Dr. Sa'ad Fahad Resan

(Supervisor)

Date: / /2020

In view of the available recommendations, I forward this thesis for debate by the examining committee.

Signature:

Name: Dr. Samir. M. Chassib

Head of the Civil Engineering Department/University of Misan

Date: / / 2020

EXAMINING COMMITTTEE'S REPORT

We certify that we, the examining committee, have read the thesis titled (**Structural Behavior of Simply Supported Reinforced Concrete Beams with Non Prismatic Flanges)** which is being submitted by (**Jassim Kadhem Zamel Al-Ibadi**), and examined the student in its content and in what is concerned with it, and that in our opinion, it meets the standard of a thesis for the degree of Master of Science in Civil Engineering (Structures).

Signature:

Name: **Assist. Prof. Dr. Sa'ad F. Resan**

(Supervisor)

Date: / /2020

Signature:

Name: **Dr. Samir M. Chassib**

(Member)

Date: / /2020

Signature:

Name: **Assist. Prof. Dr. Abdulkhaliq A. Jaafer**

(Member)

Date: / /2020

Signature:

Name: **Prof. Dr. Haitham H. Muteb**

(Chairman)

Date: / /2020

Approval of the College of Engineering:

Signature:

Name: **Assist. Prof. Dr. Abbas O. Dawood**

Dean, College of Engineering

Date: / /2020

DEDICATION

First, all my thanks to Allah for blessing me and giving me the ability to get where I am now.

I would like to express my great and deep gratitude to my family: my deceased father for the favor he had made for me, my mother who surrounded me by her praying for the success and to the spirit of my wife who was the main motive for me and her wish was to attend when this work is completed, but she left before her wish came true.

My sincere gratitude also goes to my supervisor (Assist. Prof. Dr. Sa'ad Fahad Resan) for his support in my research work, his motivation, patience and extensive knowledge . His instruction and guidance supported me throughout the duration of the work and the writing of my dissertation.

Lastly, I would like to thank my brother Hassan for his help in this research during the writing of my dissertation.

ACKNOWLEDGEMENT

I would like to express my profound gratitude to my supervisor (Assist. Prof. Dr. Sa'ad Fahad Resan) for his guidance, encouragement, and fruitful discussion throughout supervision of this work.

My thanks and appreciation to Prof. Dr. Ahmed Alshara Dean of the college of Engineering for taking care of us throughout our stay at the University of Misan.

Sincere thanks are to Assist. Prof. Dr. Abbas A. Dawood head of Civil Engineering Department for his help and real support throughout the studies period.

Thanks are also to my teachers in Misan University, department of engineering college.

Also I wish to express my sincere thanks to staff of the Amarah Technical Institute laboratories especially Dr. Mohammed Salih (the Dean of Amarah Technical Institute)

.

Jassim kadhem Zamel

September 2020

Abstract

The main aim of study is to investigate the efficiency of considering in plane non-prismatic flanges on upgrading strength rating, flexural ductility, rotation capacity without significant effect upon ultimate load capacities, stiffness, and load deflection behavior. For this goal variables were chosen so that fit this idea, the main parameters experimented in this investigation were, 1- flange tapered thickness variation, 2- web thickness. Since the flexural strength is proportional to the distance from the middle of the beam, so the non prismatic flange was chased to this aim and the web to compared with rectangular and Tee beams.

The study includes twelve concrete beams with identical quantity and distribution both the longitudinal reinforcement and stirrups, the beams divided into four groups, each one consists of three beams, the first group with three specimens, the first is with prismatic rectangular section, while the other two specimens are T-beam section constant flange, one of them has 50mm flanges depth and the other 150mm flanges depth and the other groups were non prismatic flanged beam, the variables were thickness of web and consequently changed the thickness of flange in edge of beam equal 50mm and 150mm in midspan, in addition to that the geometrical shape of tapered flange had been changed in each group, the casting process and curing were conducted under the same conditions and according to the specification , to investigate the behavior of beams in the time of test was installed two dial gage and four strain gage are installed in various places. The results confirmed upgrading strength rating, flexural ductility, and rotation capacity without significant effect upon ultimate load capacities, stiffness, and load deflection behavior.

The ultimate load ratio for non prismatic flanged in respect to rectangular beam was greater than rectangular, large ratio indicated is 1.075, this study confirming that changing section maintains ultimate strength with slightly increment, the strength rating of non-prismatic flanged section developed higher strength rating, flexural ductility and plastic sustainability higher than corresponding with control rectangular and ordinary T- beams although all had constant steel ratio and same concrete grade, the deflection curve lines at ultimate loading level have significant different and flexural ductility increased in the three group of non prismatic flanged beam, this observation enhancing that non-prismatic flanged efficiency to upgrade ductility thorough out non-prismatic flanged flexural element length, the steel reinforcement yield and flexural bending maintained with gradually spreading of cracks companied with plastic behavior till failure occurring, plastic rotation capacity (θ) values have increased significantly for the non prismatic flanged beam compared with control beams. In investigation, the mode failure for control specimens initiated cracks limited in approximately middle point which is corresponding to maximum moment, while for developed section initiative cracks started within middle region which is corresponding to range of proportional moments, after that the cracks were increased in number and spread along the beam, then one or two cracks start to widen more than the others and rend upward to compression face.

CONTENTS

List of Tables

List of Figures

LIST OF FIGURE

LIST OF FIGURE

Nomenclature

Symbols	Description
A_S	Area of steel reinforcement, mm^2
h_f	Depth of flange, mm
f'_c	Stress of concrete to cylinder, MPa
fy	Yield stress of steel reinforcement
M_n	Nominal moment strength, MPa
ρ	Steel ratio
β	Coefficient related to kind the concrete
$\emptyset$	Curvature
θ	Angle of rotation
ε'_c	Strain capacity of concrete
lp	Length of Plastic hinge, mm
εp	Strain of plastic hinge
λ	Ratio(c/d)
f_{sp}	Splitting strength, MPa
fr	Modulus of rupture, MPa
E_c	Modulus elasticity of concrete, MPa
Rs	Strength rating
ψ	Ductility index
f_t	Concrete strength in tension, MPa
c	Depth of the compressive block, mm
ε_{cu}	Ultimate compressive strain of concrete

Chapter One

Introduction

Chapter one

Introduction

1.1 General

It is very important to develop and reduce weight of concrete beam sections as the design and analysis aim to develop sections of minimum cost with keeping of basic requirements.

The long-span concrete beams with flanged sections are often used to increase their structural efficiency. Developing of non-prismatic flanged section is to provide a close solution of rotations and ductility of the non- prismatic members and to do comparison with related T-beams and rectangular beams.

The characteristics of these members such as deformation and strength for both elastic and inelastic analysis will be determined in an experimental program. In this study, description of the experimental results is done for twelve reinforced concrete beams subject to load of three points, one rectangular prismatic section and two T- section of lower and upper flange thickness limit for considered non-prismatic flanged nine sections.

1.2 Non Prismatic Section

Sometimes, Non-prismatic beams are mentioned as beams of variable cross section or beams with non-constant cross section as can be seen in Figure (1-1).

This mode, sometimes has been used because the advantages of possibility of optimizing their geometry regarding to specific needs. In spite of there are advantages that the engineers can obtain from their use, non-slight difficulties occur in the modeling of non-prismatic beam often lead to inaccurate predictions that vanish the gain the process of optimization [1].

The cost of molds is nothing to mention for the prices of precast reinforced concrete there are many advantages to use and producing non-prismatic beams, for example reduced the dimensions of beams in the sections which are not critical consequently produced sections less weight and economical further increase the dimensions in the sections that subjected to high curvature to reduce it or increase the plastic moment. However, a consequence, an effective non-prismatic beam modeling still represents a branch of the structural mechanics where significant improvements are required. Since the mid-eighteenth century, the phenomenon of Elastic stability, or buckling, has given rise to extensive theoretical and experimental investigations.

The problem of an important stability which has not received a suitable research attention is that of non-prismatic flanged beam and here will be discussed type of non-prismatic beams have not been discussed before.

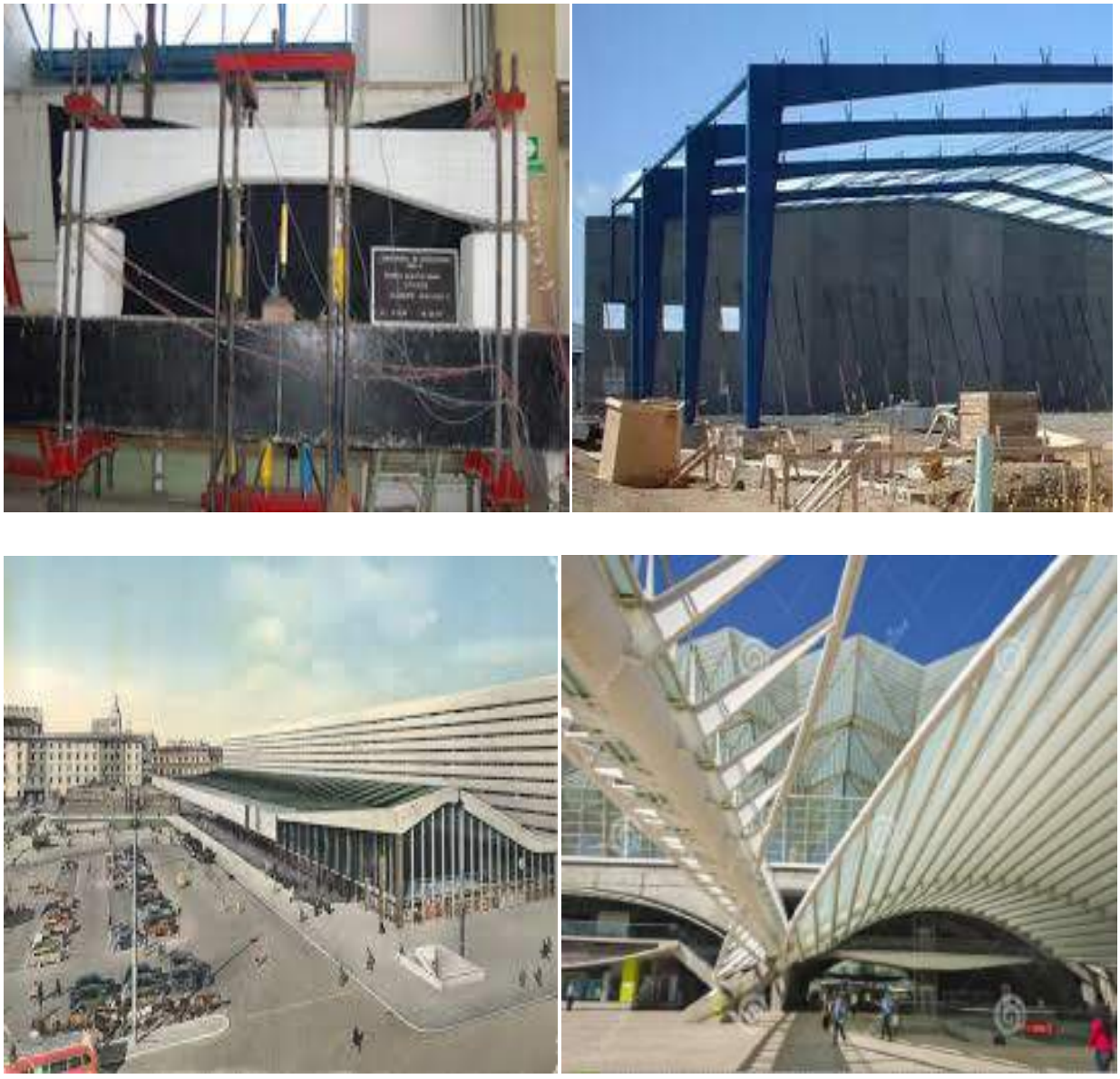

Figure (1-1) various application of no prismatic structural members [2]

1.3 Flanged Section; Description and Capacity

With the exception of precast systems, reinforced concrete floor, roofs, decks, etc., are almost monolithic. Forms are built for beam soffits, sides, the underside of slabs and the entire construction are cast at once, from the bottom of the deepest beam to the top of the slab. Beam stirrups and bent bars extend

up in to the slab. It is evident therefore that the part of the slab will act with the upper part of the beam to resist longitudinal compression. The resulting beam cross section is T-shaped Fig. (1-2) rather than rectangular. The slab forms beams flange while the part of the beam projecting below the slab forms is called web. Fig (1-3) and (1-4). The upper part of such T- beam is stressed laterally due to slab action in that direction, although transverse compression at the level of the bottom of the slab may increase the longitudinal compressive strength by as much as 25 percent this neither taken into account in the design[2].

Figure (1-2) T-Beam member[2]

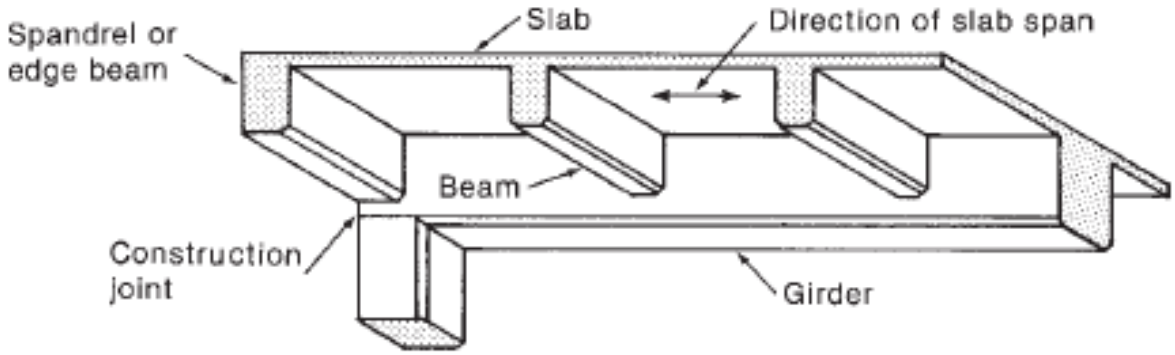

Figure (1-3) Details of the slab and location of T- beams[3]

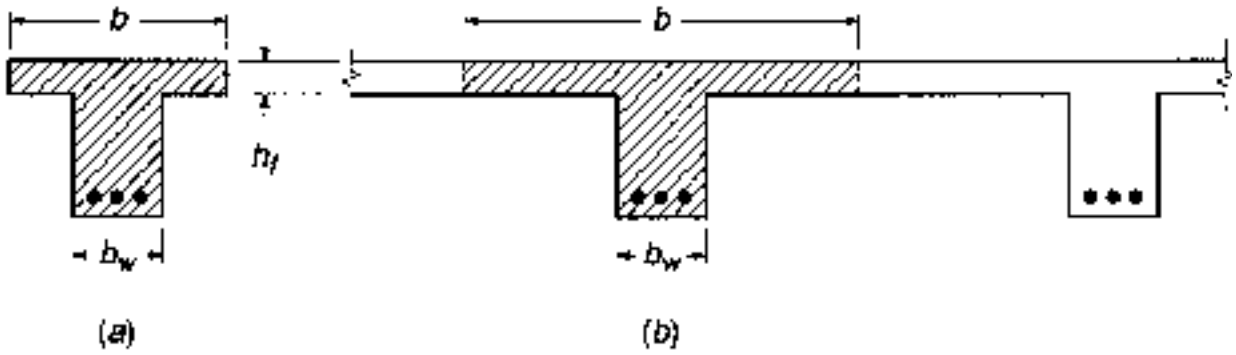

Figure (1-4) Details of flanged section beam[3]

The forces acting on the flange of a simply supported T-beam are illustrated in Fig. 1-5.At the support, there are no longitudinal compressive stresses in the flange, but at mid span, the full width is stressed in compression. The transition requires horizontal shear stresses on the web–flange interface as shown in Fig. 1-5. As a result there is a "shear-lag" effect and the portions of the flange closest to the web are more highly stressed than those portions farther away, the figure 1-5 shown the actual flow of forces on a flanged section while the figures 1-6 and 1-7 shown the effective width of Tee beam[3].

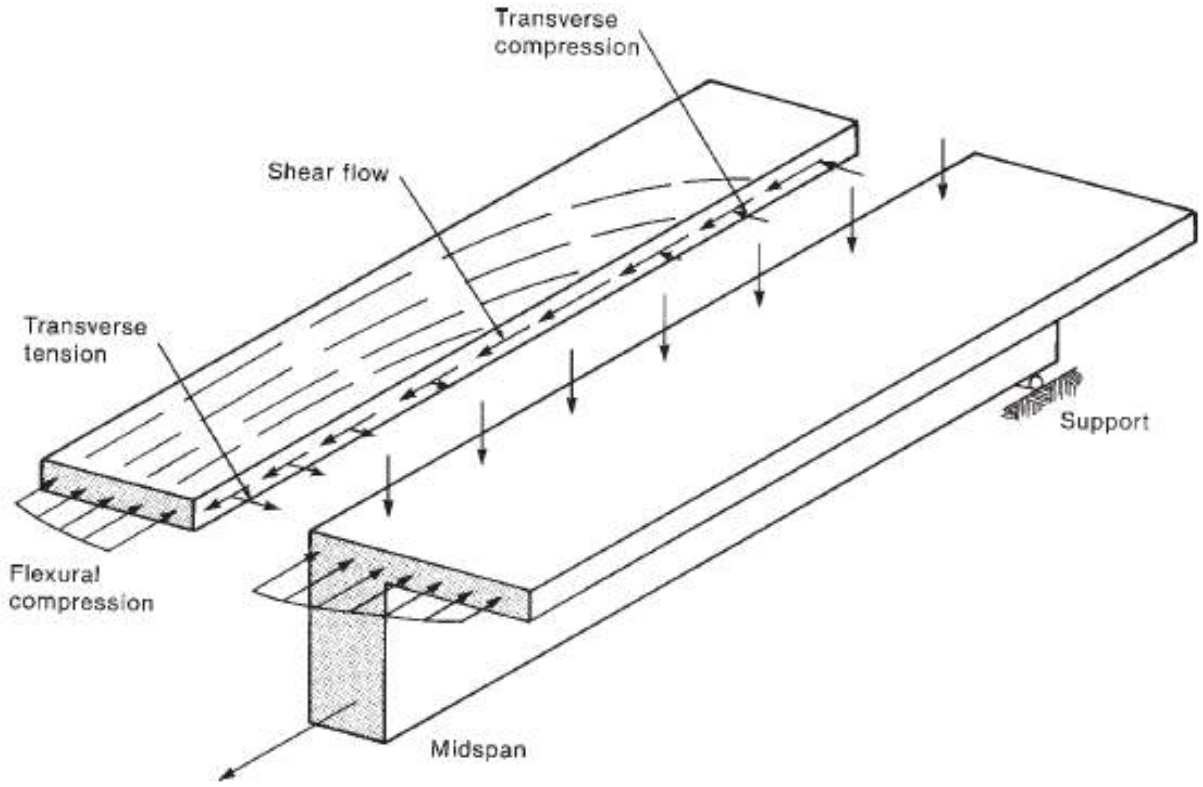

Figure (1-5) Actual flow of forces on a flanged beam[4]

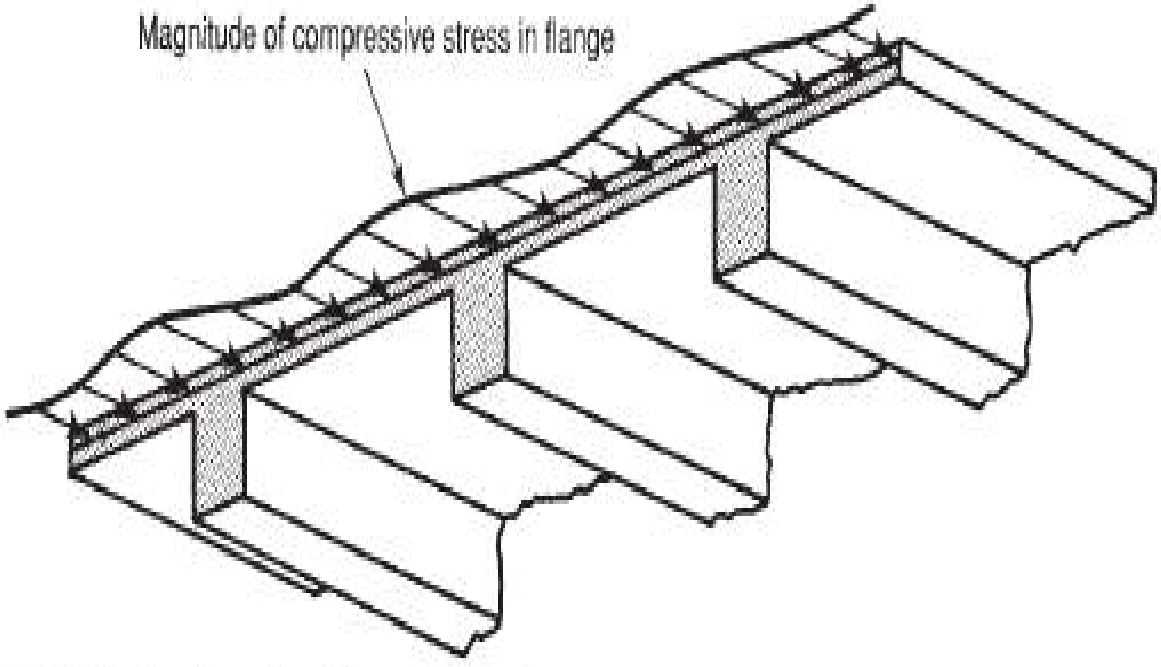

Figure (1-6) Distribution of maximum flexural compression stresses[4]

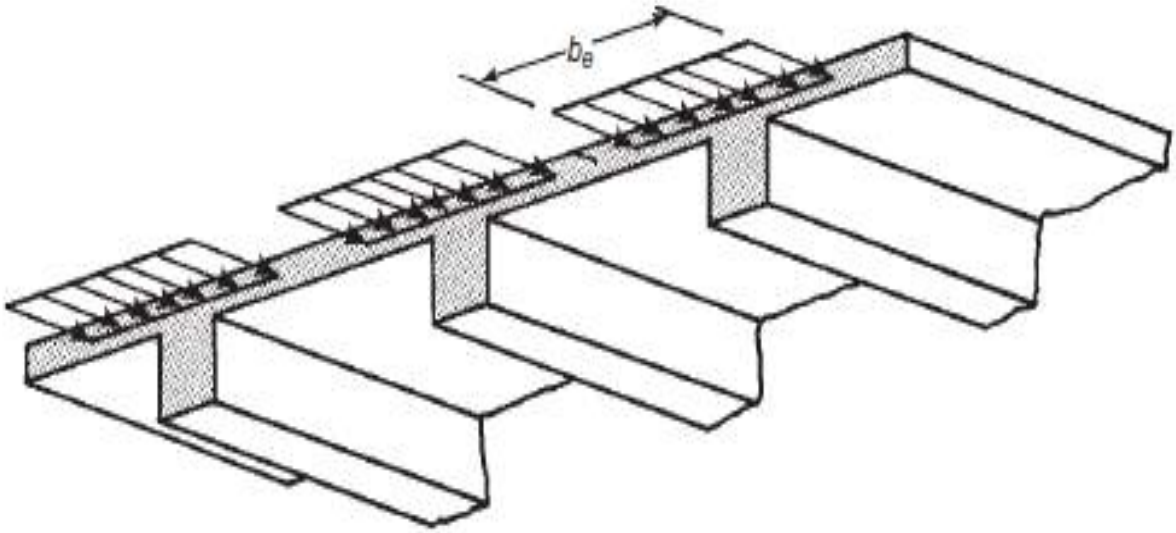

Figure (1-7) Flexural compressive stress distribution assumed in design [4]

For the sections with flanges in the compression zone, the procedure of analyzing the nominal moment strength, Mn can be divided into two general cases: For Case 1, the effective depth of Whitney's compressive stress block model equal to or less than the thickness of the compression flange hf, for normal reinforced concrete flanged section and this the case that usually governs analysis Mn. For Case 2, the depth of Whitney's compressive stress block a model is greater than the thickness of the flange [5].

1.4 Flexural Member Moment Capacity of Flanged Section

The most important single property for a structure is its strength because the strength of a member relates directly to its safety [6]. Sufficient strength for a pre-stressed member is not automatically insured by limiting stresses at service load. Significant changes in the behavior result from the cracking when the member be overloaded and because of one or both of the materials will be stressed into the

inelastic range before the failure. By calculating the member strength, the safety true factor can be established and with full recognition of these effects and comparison the load that will cause the member failure because the load that is actually expected to act.[7]

Neutral axis of T-beams may be either in the web or flange depending on cross section proportions, the strengths of the materials and the amount of tensile steel. If the calculated depth of the beam neutral axis equal to or less than the flange thickness hf, the beam can be analyzed as if it was a rectangular beam with width equal to effective flange width (b) as in fig. (1-8 a) which shows a T-beam with the neutral axis in the flange. The compressive area is indicated by the shaded portion of this figure. If the additional concrete casted in areas 1 and 2 with the beam, the physical cross section would have been rectangular with width b. No bending strength would have been not added because areas 1and 2 are entirely in the tension zone, and tension concrete is disregarded in flexural calculations. The rectangular beam and the original T-beam are equal in flexural strength and the analysis of the rectangular beam for flexure applies.

The preceding argument is no longer valid when the neutral axis is in the web as shown in Fig. (1-8 b). In this case, method should be developed to account for the actual compressive zone of T- shape.

It is appropriate treating T-beam to adopt the same equivalent stress distribution which is used for rectangular cross section beam. As shown in Fig. (1-9 c), the rectangular stress block having a uniform compressive –stress intensity $0.85\ f'c$.

Where $f'c$ is stress of cylinder concrete compressive strength (Mpa).

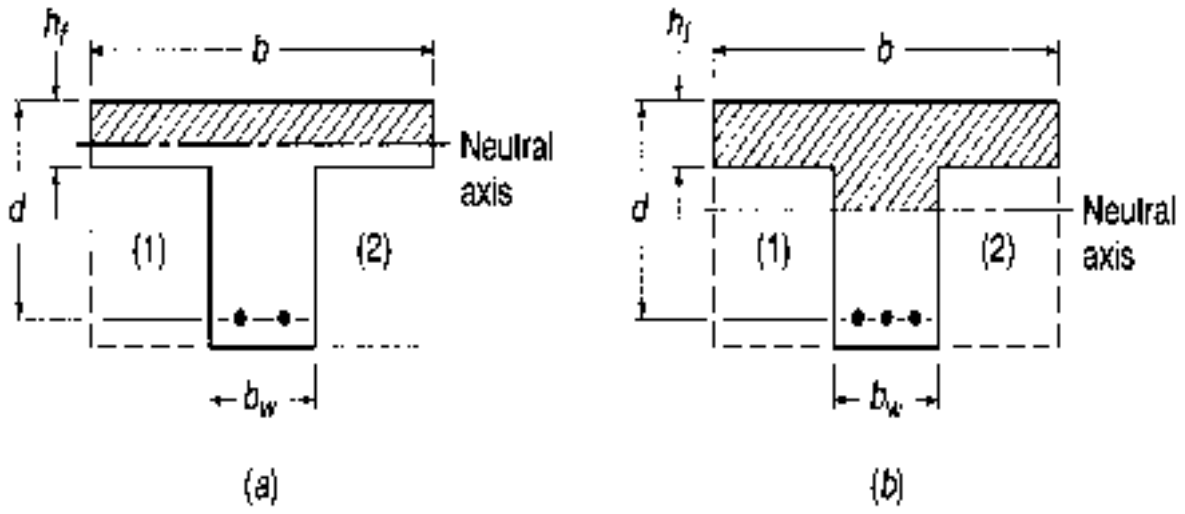

Figure (1-8) Location the neutral axis [3]

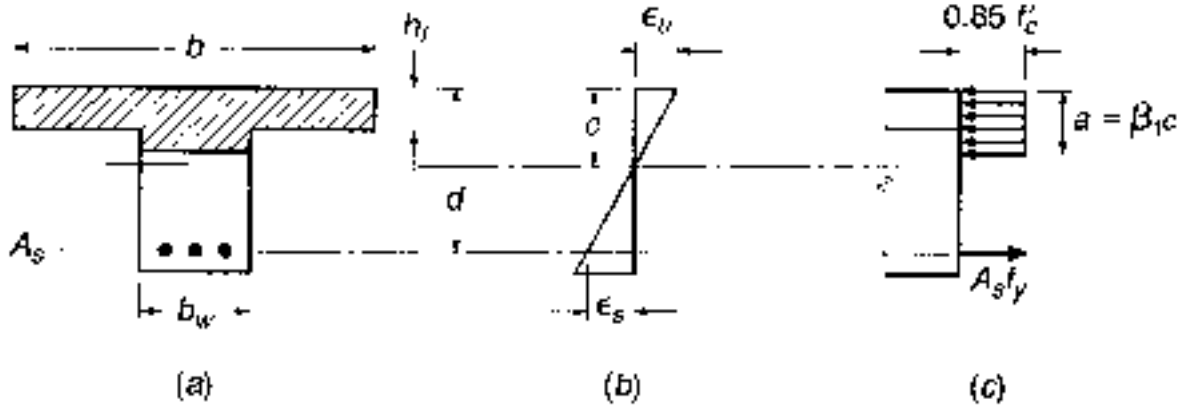

Figure (1-9) Whitney's compressive stress block and tensile reinforcement [7]

However, extensive calculations based on actual stress-strain curves.

Accordingly, Tee beam may be treated as rectangular beam if the depth of the equivalent is less than or equal to the flange thickness, Fig. (1-9 b) shows tensile reinforced T beam with effective flange width b, web width *bw,* effective depth to

the steel centroid d, and flange thickness hf. If (for trial purpose) the stress block is assumed to be completely within the flange

$$\boldsymbol{a} = \frac{A_s f_y}{0.85 f'_c} = \frac{\rho f_y d}{0.85 f'_c} \quad (1\text{-}1)$$

$$C = \frac{a}{\beta 1} \quad (1\text{-}2)$$

where $\rho = As/bd$.

A_s Steel reinforcement area (mm^2).

f_y Yield stress of steel reinforcement (Mpa).

$f'c$ cylinder concrete compressive strength (Mpa).

C Depth of the compressive block (mm).

b The flanges width (mm).

d Effective depth of steel reinforcement (mm).

If ($\boldsymbol{a}$) is equal to or less than the flange thickness hf, the member will treated as a rectangular beam of width b and depth d. If ($\boldsymbol{a}$) is greater than hf, the member will treated as Tee beam, the compressive force in the concrete is divided in this case into two forces, one represents the force in the rectangular flange and the second represents the forces in the parts of web over the neutral axis, as shown in Fig. (1-9)

In this study, ($\boldsymbol{a}$) is less than hf and the discussion will just focus on that situation in design and analysis. The extraction of suitable reinforcement for the beams was done according to the ACI equations and table.

1.5 Rotational Capacity

Typical tensile plastic rotational capacity at mid span sections of a frame are shown in Fig.(1-10).The rotation capacity depends mainly on the following[8]:

1. The ultimate strain capacity of concrete $\boldsymbol{\varepsilon'_c}$, which may be assumed to be 0.003 or 0.0035.
2. 2. The length of plastic hinge (lp), over which yielding occurs at the plastic hinge, which can be assumed to be approximately equal to the effective depth of the section where the plastic hinge developed (lp=d).
3. The depth of the compressive block, C in concrete failure at the section of the plastic hinge.

The angle of rotation θ, of a tensile plastic hinge could be estimated as follow (from Figs (1-10, 1-11) [8] :

$$\theta = \frac{\varepsilon p \; lp}{c} \qquad (1\text{-}3)$$

Where, ε_p is the increase in the strain in the concrete measured from the initial yielding of steel reinforcement in the section (see Fig. (1-11)):

$\varepsilon p = \varepsilon'_c - \varepsilon_{cy} = 0.0035 - \varepsilon_{cy}$

$\varepsilon p = d$ And the ratio c/d equals $\lambda \leq 0.5$

$$\theta = \frac{(0.0035 - \varepsilon_{cy})d}{\lambda d} = \frac{0.0035 - \varepsilon_{cy}}{\lambda} \qquad (1\text{-}4)$$

From strain triangles

$$\varepsilon_{cy} = \left(\frac{c}{d-c}\right) = \frac{fy}{Es}\left(\frac{\lambda\, d}{d-\lambda\, d}\right) = \frac{fy}{Es}\left(\frac{\lambda}{1-\lambda}\right) \qquad (1\text{-}5)$$

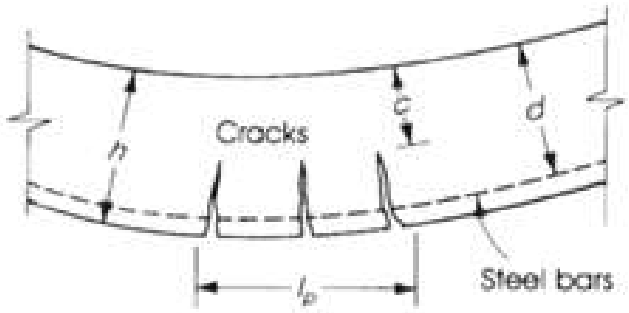

Figure (1-10) Mid span plastic rotation capacity[9]

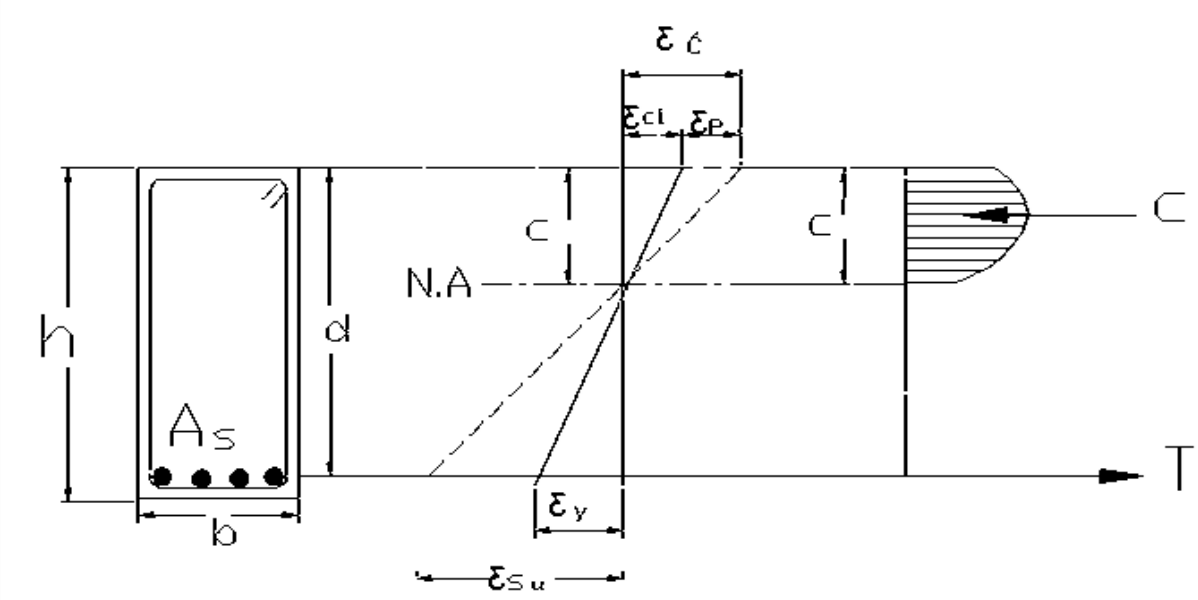

Figure (1-11) Strain distributions

The θ min calculated here is from one side only and the total permissible rotation at the plastic hinge equals 2θ.

The actual λ can be calculated as follows, given α =β1 c and β1= 0.85 for f'c ≤ 4ksi:

$$C=\frac{a}{0.85}=\frac{As\,fy}{(0.85)^2 f'c\,b} \quad (1\text{-}6)$$

$$\lambda=\frac{c}{d}=\frac{Asfy}{0.72\,f'c\,b}=\frac{\rho fy}{0.72f'c}\leq 0.5 \quad (1\text{-}7)$$

Table (1-1) Values of $\beta 1$ for equivalent rectangular Concrete stress distribution [(22-2.2.4.3) of ACI code]

$f'c$ Mpa	β1
17< $f'c$ <28	0.85
28< $f'c$ <55	0.85-0.05(f′c − 28)/7
$f'c$ >55	0.65

If the rotation provided is not enough, one can reduce the percentage of steel reinforcement or increase the section dimensions to obtain smaller values for c and λ and a greater value for θ, the proposed section could be introduced suitable technique to achieve that. The ultimate crushing strain in bound concrete may be as high as 0.012 if special binding or spirals are used [7].

1.6 Aim of study

The main aim of this study is to investigate the efficiency considering in plane of non-prismatic flanges on upgrading strength ratio, rotation capacity and flexural ductility without considerable effect upon ultimate load capacities, load deflection behavior and stiffness. For this aim, variables were selected to fit this idea and the main variables experimented in this study are flange tapered thickness variation

and web thickness. Since the flexural strength is proportional to the distance from the middle of the beam, so the non-prismatic flange was chased to this aim and the web to be compared with ordinary T-beams and rectangular beams.

1.7 Thesis layout

This thesis consists of five chapters:

Chapter one: presents a general introduction that deals with the behavior of non-prismatic flanged beams and describes the objectives and scope of the work, also describes the properties of flanged beam in addition the method of design and analysis that using in the research.

Chapter two: gives a review of previous work related to T-beams and non-prismatic flanged beams.

Chapter three: involves the tests carried out throughout the experimental work, the procedure adopted, the properties of the materials used and drawings and photos that illustrate the stages of working and process of testing.

Chapter four: discusses the results obtained from experimental work and the behavior of nine non-prismatic flanged concrete beams and compared it with two T-concrete beams and one rectangular concrete beam.

Chapter five: summarizes the conclusions drawn from the present study and the recommendations for the future studies.

Chapter Two

Literature Review

Chapter Two

Literature Review

2.1 General

Although there are no current researches similar or identical to this research, but there are researches in geometrical shape and it's influential on beam properties. Most of those researches focus on common shape as Timoshenko model, tapered and hunch beam to get an economic performs have the same work, but with less weight and cost. This chapter focuses on the previous researches that studied non prismatic beams, intersected and related to this research such as strength of concrete, flexural failure, cracking pattern, ductility, rotation capacity, length of plastic hinge...etc.

2.2 Reinforced concrete beam of non-prismatic Section

2.2.1 Analytical Studies

In 1992, Romano [38] studies the deflections in Timoshenko beam with varying cross-section. Solutions of closed form are presented for bending beams with linearly and (in the binomial form) parabolic ally varying depth and for bending beams with linearly varying width along the beam's length. These solutions are developed taking into consideration shear deformation in the beam, and they achieved, in an original manner, by changing the fourth order differential equations that have variable coefficients to fourth-order differential equations that have constant coefficients. Although these presented solutions refer to three recurrent variations in the shape of beam section, the summarized procedure can be applied into beams that have binomial variation (with any exponent) in the width or depth of the cross section. Furthermore, these solutions can be done for polynomial,

sinusoidal and exponential load conditions and they can be used to get the factors of stiffness and the beams flexibility coefficients in the frames analysis. The solutions of closed form for longitudinal displacement are also presented. For four recurrent beams which commonly used in civil engineering practice, the analytic solutions are applied and compared with a numerical procedure.

In 1995, exact deflection in non-prismatic members was studied by Baker[37]. closed form solution for the exact small deflections of a class of non-prismatic members was presented. Convergence and accuracy studies, carried out in conjunction with a finite element analysis, show the series solution to be rapidly convergent, stable and cost efficient. The solutions are also compared with plane stress finite element studies to assess the range of applicability of the Bernoulli Euler equations to tapered members. The analytic solution is a powerful tool in that it can be reduced for specific problems or used to form general exact stiffness relations for structural analysis, where one element only is required for each non-prismatic section. Both approaches are demonstrated with examples. The results are compared with cubic finite element studies and again show the accuracy and computational efficiency of the closed form solution.

In 2005 Mohammad and, Al-Sadder [39] studied the behavior of very large deflection for prismatic and non-prismatic cantilever beams that subject to different types of loadings. The formula relies on representing the beam rotation angle by a polynomial on the position variable along the deflected beam axis. The polynomial coefficients were obtained by decreasing the residual error integral of the governing differential equation and applying the conditions of beams boundary. Prismatic and non-prismatic cantilever beams were presented by several numerical examples and they subjected to uniform, non-uniform distributed loads and tip concentrated loadings in horizontal and vertical directions. In that study, the loads considered were restricted to non-follower type loads. Comparison was done

between different loadings and geometries with MSC/NASTRAN computer package. However, MSC/NASTRAN computer package failed for some cases of very large deflection to predict the shape of deflection because of divergence problems.

In 2012, Mehdi and Solmaz[40], studied Green's function for deflection non-prismatic simply supported beams by an analytical approach. The behavior of non-prismatic T-section beams on a 3D finite element investigation was the purpose of that study. According to the results of parametric studies, a practical and simple 2D beam model with a concept of an effective length is proposed for analytic non-prismatic members having T-section. The effective length of the 2D beam element in the proposed model representing the haunch evolves as 75% of its actual length. It was concluded that deviation in the results from the finite element analysis results was within 15%.Moreover, an investigation was achieved in different modeling scheme in the analysis of frames with the members of non-prismatic by using the proposed 2D beam representation.

In 2015 Balduzzi, et al[41], studied Non-prismatic beams: A simple and effective Timoshenko-like model. Simple compatibility, equilibrium and constitutive equations were discussed in that paper for a non-prismatic planer beams. The proposed model depends on standard Timoshenko kinematics (i.e.) planar cross-section remains planar as a result of deformation, but it can rotate regarding to beam Centre line. An initial discussion of a 2D elastic issue states that the boundary equilibrium highly influences on the distribution of the cross-section stress. All unknown fields were represented regarding to global Cartesian coordinates.

A model of simple beam (i.e. set of Ordinary Differential Equations (ODEs)) was derived to describe accurately non-prismatic geometry effects on the behavior of

the beam and to motivate equation's terms with both mathematical and physical arguments. Lastly, comparison is done between several numerical and analytical solutions with the results existing in previous studies. The main conclusions had been summed up as the following:

(i) The distribution of the stress within the section of beam is not slight as in the prismatic beams, particularly the distribution of the shear stress relies on the beam geometry and all generalized stresses

(ii) The simplified constitutive relations derivation state highly dependence on each generalized deformation on all the generalized stresses.

(iii) The problems of shear-bending and axial are strictly coupled.

(iv) The beam model can be naturally expressed as an explicit consists of six first order ODEs.

(v) The solution of ODEs can be calculated by the iterative integration of the right hand side term for each equation.

(vi) The proposed simple model foresees actual behavior for non-prismatic beam with a reasonable and good accuracy for the most of practical applications.

In 2015, elastic and inelastic analysis of non-prismatic members were studied by Demeter G, Fertis et al.[42], This study deals with the non-prismatic members static analysis for any arbitrary variation in its moment of inertia I_X, where there materials were stressed beyond the limits of their elastic causing the modulus of elasticity E_X to change along their length. The characteristics of the stress and deflection of such members for elastic and inelastic analyses will be determined by using the equivalent system method that plotted in figures. This method allows to replace the original member of variable stiffness member. A very accurate approximate and an exact solution is obtained and drastically minimizes the

mathematical complexity of the problem. In both elastic and inelastic range of failure, the member can be analyzed, thus permitting to observe the progressive deterioration of the ability of members for resisting stress, load and deformation to establish useful and critical limits regarding to these quantities.

In 2015, stiffness formulation for non-prismatic beam elements was studied by Tena-Colunga, et al.[18], In that study, a method is presented to define two and three dimensional (2D and 3D) for matrices of elastic stiffness of non-prismatic elements (hunched or tapered) according to theory of traditional beam and method of flexibility. The suggested formula includes the shape and deformations of the cross section, but the warping deformations are neglected in that formula. Though more strict formula for tapered elements have already been addressed, the suggested procedure is presented, so its direct Implementation or application computer programs for structural analysis are explicit. Comparison is done between the procedures with the design tables for Portland Association of Cement (PCA). It is proved that the PCA tables are outdated for today's state-of-the-knowledge for non-prismatic members as these tables can lead to considerable errors. For most common beams which are used in building structures, a new set of design aids have been developed to replace the handbook of PCA of frame constants. Closed form solutions are provided for elements of linearly tapered for square, rectangular and circular cross sections. Lastly, it is demonstrated that the factors of stiffness of non-prismatic elements rely on the span to the depth ratio of the element (L/h). To the knowledge of the writer, no one before has proved this fact.

The analytical derivation of a general 2D non-prismatic beam model was studied by Angela Beltempo et al.[11], in 2015 according to the Hellinger–Reissner principle and this study presents an analytical model to study two dimensions linear elastic of non-prismatic beams. The aim of the principle is to predict

accurately for both stresses and displacement by using a simple procedure and some unknown variables. For the model derivation, the approach adopted is the so-called reduction of dimensional starting from the Hellinger–Reissner functional which has stresses and displacements as independent variables. Moreover, the kinematic of the Timoshenko beam and suitable hypotheses on the field of stress are taken in consideration in order to enforce the boundary equilibrium. The usage of dimensional reduction permits the reduction of the integral over a 2D domain connected with the Hellinger– Reissner functional into an integral over a 1D domain (i.e., the so-called beam-axis).

Finally, the six ordinary differential equations which govern the behavior of the beam structural are derived through some mathematical manipulations. The solution of these six equations is obtained, to prove the capabilities of the proposed model, for beams of several non-prismatic with different constraints, geometries and load distributions. Then, the comparison is done between the solution and the results provided by an already existing, more expensive and the analysis of refined 2D finite element to show the proposed model efficiency to accurately predict for both stresses and displacement, at least for the cases of the practical interest.

2.2.2 Experimental Studies

In 1983, Stefanou[43], the work presented is concerned with the experimental investigation into the behavior of the shear of beams reinforced concrete for varying depth and the way in which they fail in shear compared to prismatic beams. Under the same conditions of loading, many beams were tested and the following parameters of controlling were varied: presence of stirrups, main longitudinal reinforcement, the beams slope and depth of beams at supports. The American A.C.I code, the application of the British Code of Practice, Code and the Russian Code of Practice were described in this paper to determinate the ultimate

shear strength for non-prismatic beams. The details of the beam and experimental data obtained during the tests are included (non-prismatic sections with shear resistance of reinforced concrete beams).

In 2004, ductility of R.C. Beams reinforced with FRC was studied by Rinaldi et al.[44], the aim was to evaluate the effectiveness of strengthening interventions with fiber reinforced concrete (FRC) with special reference to the behavior of the ductile. In fact, rehabilitation intervention with a material working in tension, but with the behavior of brittle, cannot be effective for the plastic capacity of the structure. In this frame, the concrete which has a high-performance fiber reinforced is defined and applied as thin layer to the elements of the beam. The composite schemes behavior is examined with numerical and analytical models and the FRC application effects on the global and local ductility are analyzed.

2.3 Flanged section

2.3.1 Analytical Studies

In 2003, Ferreira et al.[45], Executed conducted studies on the steel localization in a T-beam and the steel area optimization under bending. The expressions that give the equilibrium for a doubly or singly reinforced T-section in the different stages defined by the behavior of non-linear for concrete and steel are derived ones. The ultimate material behavior is defined according to the codes of design such as model code 1990 and EC2.The obtaining of analytical optimal design of the reinforcement of a T-section was the purpose of this work in terms of the ultimate design. In the last section, design abacus is delivered and the expressions that developed are applied to examples. A comparison is done with current practice method as clarified in CEB.

In 2004 kwan and AU[36], studied the performance of the flexural strength–ductility for flanged beam sections cast of concrete high-strength. Flanged sections are oftentimes used for beams of long-span concrete to maximize their structural efficiency. Although, for the sectional area, a flanged section could lead to a higher flexural strength, it would also render a lower flexural ductility, particularly when they are heavily reinforced. Thus, both the ductility and flexural strength should be considered when evaluating a beam section flexural performance. In this study, the flexural behavior of the post-peak for flanged sections is evaluated by an analytical method which uses the curves of the actual stress strain of the materials and taken in consideration strain reversal of the tension reinforcement. From the numerical results, the performance of the flexural strength–ductility of flanged section is examined by plotting the ductility and strength that can be simultaneously done in the form of design graphs. It is found that (1) a flanged sections has lower flexural ductility than a rectangular sections at the same amount of reinforcement provided and the same overall dimensions, (2)A flanged section has inferior performance of strength-ductility compared with rectangular section at the same overall dimensions and (3) A flanged section has a better performance of strength–ductility compared with a rectangular section at the same sectional area.

Optimal Design of Reinforced Concrete T-Beams under Ultimate Loads was studied in 2010 by Tliouine and Fedghouche[29]. This study deals with the optimization of the structural design under ultimate design loads for reinforced concrete T-beams. An analytical approach is developed for the problem according to a reduced number of design variables and a minimum cost design criterion. It is clear among other things that the formulation of the problem can be casted into a format of a non-linear mathematical programming.

Illustratio of the formulation applicability presented by typical examples according to the current French design code BAEL-99. The results are confronted to design solutions of reinforced concrete tee beam derived from current design practice. The significant savings can be seen through the optimal solutions in the predicted amounts and thus in the absolute costs of the used construction materials.

In 2017, regarding advantages and disadvantages of T-beam, Ayres[46], posted on the site of Kuora replying to questions of some subscribers of the site. It's simply a rectangular beam cast monolithically with the slab shaped as Tee. The various T-beam's advantages and disadvantages are as the following:

Advantages:

1. The flange takes up the compressive stresses because the beam is cast monolithically with the slab and that means the flange will be more effective to resist the sagging moment acting on the beam.
2. The direct outcome of the first point is better head room since the beam's depth can be significantly reduced.
3. For larger spans, T-beams are usually preferred rather than rectangular beam because the deflection is decreased to a good extent

Disadvantages:

1. There is a considerable increase in the shear stress at the junction of the flange and the web of the beam due to the change in cross section. So casting should be done very carefully to ensure both are bonded well.

2. The beam slab becomes very weak to resist forces of lateral shear since it is monolithic (rigid), (Cracks develops quickly). Usually in the zones of

earthquakes, the T-beams for high height buildings is reinforced with mechanical stiffeners in the junction.

3. There will be small savings in steel too (not a significant amount though).

2.3.2 Experimental Studies

In 1976, analytical and experimental studies on the Hysteretic Behavior for both T-beams and reinforced concrete rectangular were investigated by Shao-Yeh M. Ma[47], This study describes an experimental and analytical study program carried out for

investigation the inelastic behavior of critical regions that may develop in a beam near its connection with the column of a reinforced concrete ductile moment resisting space frame when subjected to severe earthquake excitations.

In the experimental program, a series of nine cantilever beams, ductile moment-resisting reinforced concrete office building, was designed according to present seismic codes. These beams were designed in order to study the effects of (1) the slab by testing T-beams with a top slab width equal to the effective width specified by the ACI (318-71) Code; (2) relative amounts of top and bottom reinforcement by varying the amounts of bottom reinforcement; (3) supplementary ties by providing hairpin ties around main bars not restrained by the corners of stirrup ties; (4) the high shear force by varying the shear-span ratio; and (5) loading histories by testing some beams under loading reversals inducing a gradually increased deformation l and others l under monotonic loadings to large deformations in one direction. Detailed descriptions of the specimens, testing procedures, experimental data, and results obtained are presented. The significance of the experimental results in relation to the seismic design of the reinforced concrete critical region is also discussed. The results showed that the main effect of the slab in T-beams was

an increase in the moment capacity of the beam in one direction due to the slab reinforcement at the top. By increasing the bottom steel area up to the same amount as that of the top s tee1 area, the energy dissipation capacity of the beam increased between 27 and 54 percent; by providing supplementary ties for supporting main compression bars not restrained by the corner of ties, the energy dissipation capacity increased about 74 percent. The development of a maximum nominal shear stress, v_{max}, of $5.3\sqrt{f'c}$ in the shortest beam reduces tile energy dissipation by one half when compared with a similar, but longer, beam with a v_{max} of $3.5\sqrt{f'c}$. Greater amounts of energy can be dissipated by subjecting the beam to loading reversals of gradually increasing amplitude than by subjecting it directly to loading reversals of large amplitude. The inelastic rotations obtained from the test beams reached peak values in each sense ranging from 0.026 rad. to 0.058 rad. These values are considered to be adequate for the efficient design of a ductile moment-resistin9 frame member. Photogrammetric measurements proved to be useful for studying the deformation patterns of the beam critical region subjected to reversed loadings. These measurements were especially useful for detecting shear deformation occurring along large cracks that were forming across the entire beam section. Analytical studies were carried out to gain a better understanding of the flexure, shear, and bond resisting mechanisms in the reinforced concrete critical regions subjected to inelastic load reversals. The analytical studies include: (1) a moment-curvature analysis. based on a hysteretic stress-strain model of reinforcing steel developed from tests on machined main reinforcing bars; (2) a finite element analysis of stress transfer [bond) between concrete and anchored main bars; and (3) an analysis of the shear force-shear deformation hysteretic relationship of reinforced concrete beams considering aggregate interlocking,

stirrup-tie resistance, dowel action of main bars, and shear resistance offered by un cracked concrete. The significance of these studies is discussed and summarized.

In 2002, Wickline [48], studied the effective moment of inertia models for Tee-beam of full scale reinforced T-concrete which subjects to configuration of a tandem-axle load. This study is a product of the U.S. Army Corp of Engineer's desire to develop a more accurate procedure for estimating the load capacity of an in-service T-beam bridge. A bridge type that is a stumbling block for U.S. Army field engineers due to the unknown amount and placement of the flexural reinforcement in the T-beam girder cross-sections. Personnel from the U.S. Army Corp of Engineer's Waterways Experiment Station in cooperation with personnel from Virginia Tech conceived a procedure that is potentially more accurate, can be quickly executed in the field, and is relatively easy to use by field engineers. In general, the procedure provides a method for transition between the quantity of flexural reinforcement in a reinforced concrete T-beam and the member's actual moment of inertia. Specifically, the goal of this thesis is to evaluate the accuracy of selected, effective moment of inertia models as a component in the proposed analysis procedure. The accuracy of the selected models is evaluated with test data generated from a testing program detailed herein, which load tested full-scale reinforced concrete T-beams. The test specimens were subjected to a closely-spaced, tandem-axle load configuration, a load configuration typical of military equipment.

In 2013, both A. Deifalla and A. Ghobarah[49], searched the analysis and behavior inverted T-shaped RC beams under the torsion and shear. The 1998 ASCE-ACI Committee 445 on torsion and shear identified researching combined

torsion and shear as well as giving physical importance for the design of the torsion as an upcoming challenge (ASCE-ACI Committee 445 on torsion and shear, 1998).Most of the previous experimental researches and studies focused on reinforced (RC) beams under the torsion, shear and flexure. The behavior of the beams of inverted T-shaped are not fully explored in both flange closed stirrups and web. In this study paper, an innovative test setup was implemented and developed and it has the ability to simulate the behavior of beams of inverted T-shaped under combined torsion and shear. Under different ratios values of the applied torque to the applied shear force, the behavior of three inverted T-shaped beams was discussed. The value of the torque to the shear ratio considerably affects the inverted T-shaped beams behavior in terms of failure mode, cracking pattern, cracking and ultimate torque;, strut angle of inclination, cracking and ultimate shear, post-cracking torsional rigidity, web stirrup strain and web. The flange stirrup is more efficient in resisting torsion moment over shear forces. A model was developed and implemented and it is capable of predicting the flanged beams behavior under combined actions. From three different experimental studies, the model showed good agreement with the experimental results.

The flexural Behavior of reactive powder concrete (RPC) T-beams was investigated by Murtada Ameer Ismael et al. In 2014[50], The influence of three ratios of steel fibers (0, 1 and 2%) and three ratios of silica fume (15, 20 and 25%) on flexural behavior of RPC T- beams was presented in that research. From the experimental results, the volumetric ratio of steel fibers considers important parameter to enhance flexural behavior of T-beams. However, as the volumetric ratio of steel fibers increased from 0 to 2% the first crack load, ultimate deflection and ultimate flexural load increased with 55.56%, 57.32%, and 57.88% respectively. The results also showed that the influence of silica fume ratio was less significant when its range of 15 to 25%.

In 2015, flexural behavior of hybrid T-beams (Containing normal strength concrete reactive powder concrete and normal strength concrete) was investigated by Murtada Ameer Ismael et al[51]. In this research reactive powder concrete has superior structural and mechanical properties, but the high cost of that new construction martial was the major drawback. Also, this research investigated the ability of using normal strength concrete together with RPC as well as flexural behavior of hybrid T- beams as experimental study in the same section to take advantage in optimal way of these two materials. The experimental results showed that using normal strength concrete in the flange and RPC in the web effectively enhances the performance of hybrid T-beams compared with T-beam of normal strength concrete. However, the increases in ultimate deflection, ultimate flexural load and the first crack load were 29.19%, 60%, and 86.67% respectively, while, the increases in the case of using normal strength concrete in the web and RPC in the flange were 20%, 34.28% and 14.97 respectively compared with T-beam of

2.4 Rotational Capacity and Plastic Hinge of RC Members

2.4.1 Analytic studies

Hillerborg in 1990 [32], presented theoretical study to determine stress-strain strain relation in the compression zone of concrete beam using approximate model with localization and strain softening, i.e. with the descending branch described as a relation of stress-deformation instead stress-strain relation. This results of stress-strain relation for the compression zone which was strongly dependent on the compression zone depth. This was in contradiction with the existing design rules which assumes that no such size dependence exists. Confirmation of the theoretical results was done by doing comparison with the test results and rotational capacities.

Kwan et al in 2002[30].predicted the relationship between the flexural strength and flexural ductility, the interrelation between them was achieved by a beam section has been evaluated and plotted for concrete with different grades and steel ratios in the form of charts. From these charts it can be observed that the use of a higher grade concrete could increase the flexural ductility at the same flexural strength, or increase both flexural strength and ductility. The addition of compression steel without increasing the tension steel could produce significant increase in flexural ductility with little increase in flexural strength. On the other hand, the addition of steel reinforcement in both tension and compression together lead to increase in both the flexural strength and ductility.

In 2003, theoretical model to determine the plastic rotation capacity in the of reinforced concrete beams was studied by Carmo. et al[52]. The evaluation the ductility of reinforced concrete beam was essential to avoid a fragile collapse of the structure by assuring a suitable deformation at ultimate load. A theoretical model for the calculation of plastic rotation was presented in this study. Comparison was done between the results obtained from experimental with those obtained from model. A good agreement between the experimental and theoretical results was achieved. The proposed theoretical model takes in consideration the influence of some factors such as concrete strength, steel properties, the effect of tension stiffening and section depth. The strength of the concrete, particularly, is an interesting parameter since for high strength, the ultimate concrete strain, ε_{cu}, decreases as the concrete strength increases.

In 2004, the effects of concrete grade and yield strength of steel on flexural ductility of (RC) beams were studied by Kwan, et al[31]. According to established theoretical equation correlating the flexural ductility of a reinforced concrete beam section to the steel ratios and the strength of the concrete has been extended to

account for the tension and compression steel yield strengths effects by means of a parametric study. In this study, it was detected that at a fixed degree of the beam section being under-or over-reinforced, the flexural ductility decrease slightly with the tension steel yield strength as well as the concrete strength but increase slightly with the compression steel yield strength slightly. From the charts plotting the flexural ductility and flexural strength that could be together achieved by a beam section, it was clear that the using of a higher concrete strength could increase either the flexural ductility or flexural strength or both. On the other hand, at a given flexural strength, a higher compression steel yield strength would lead to higher flexural ductility while a higher tension steel yield strength would lead to lower flexural ductility. Lastly, to meet any specified requirements of flexural ductility, a simple method of designing beam sections has been proposed.

Carpinteri and Corrado in 2010[53], presented dimensional analysis approach for determine plastic rotation capacity of flexural RC beams with over reinforced ratio. The flexural behavior was governing by combination of mechanical and geometrical parameters (NP and NC), (NC is brittleness number in compression and NP is reinforcement brittleness number). It can be also evidenced that the normalized rotation was a decreasing function of NP, NC being kept constant.

In 2011, Zhao et al [9]. Studied the length of plastic hinge in the members of reinforced concrete flexural. The plastic deformation for the members of reinforced concrete flexural was localized in a small zone after the yielding of the member and the zone namely the plastic hinge zone. The performance of this zones critical for flexural members as it governs the members' deformation capacities and load carrying. Therefore, for decades, this zone has a great interest to structural researchers and designer. The plastic hinge zone length has a significant design parameter where intense confinement must be provided to increase member

ductility to survive from extreme events such as earthquakes. The plastic hinges behavior is very complex because of the strain localization, high nonlinearity of the materials and relative movement and the interaction between the constituent materials. As a result of these experimental testing, most researchers investigated the problems. Restricted by the cost and time involved in large tests, very limited knowledge was obtained yet. This work attempt to explore the problem analytically with Finite Element Method (FEM) by using the computational software Diana. By using existing experimental data including rotational capacity, response of load deflection, stress and strain distributions of reinforcement, a computational model is built and verified. Also by using calibrated FEM model, concrete crush zone, the extent of the rebar yielding zone, the length of real plastic hinge and curvature localization zone are studied. Parametric studies are later used investigate the plastic hinge length in terms of material properties of rebar and concrete, dimensions of the member, and reinforcement ratio.

2.4.2 Experimental Studies

In 2001, Ko. M. Y. et al[33]. Conducted an experimental study on the plastic rotation capacity of reinforced high strength concrete beams. Thirty six beams have different compressive strengths of concrete, compressive reinforcement ratios, tensile reinforcement ratios and loading patterns (1 point loading and 2-point loading) were examined to evaluate the capacity of plastic rotation, extreme fiber concrete compressive strain and the length of equivalent plastic hinge. Also numerical analysis was conducted and compared with the experimental data. Based on the experimental results, for ultimate curvatures were significantly larger than those of theoretical approach. Based on these observations, a new formula was proposed for ultimate strain for the beams of high concrete compressive strength. Also, the results of the test for capacity of plastic rotation were closer to the results

obtained by using the moment-curvature relationship considering concrete tension stiffening of concrete and shear effect than results obtained by using equivalent plastic hinge length. This a proof that for accurate evaluation of the capacity for plastic rotation the consideration of shear effect and concrete tension stiffening were most important.

In 2003, Lee and F. Watanabe [35], studied the effect of longitudinal axial strain in the regions of plastic hinge of RC beams subjected to reversed cyclic loading. The longitudinal axial strain in the regions of plastic hinge for RC structures has considerable effect on the behavior of these structures subjected to reversed cyclic loading. This strain affects the dissipation of the energy in the hysteretic response by causing the sliding along interconnecting wide flexural cracks. Furthermore, this strain decreases the effective compressive strength of cracked concrete of the RC members, such as coupling beams, dominated by shear action. The study reported in that study was suggested a model to predict the axial strain in the regions of the plastic hinge for RC beams. The suggested model involves four path types:

Path 1: Unloading region or pre-flexural yielding, Path 2: post-flexural yielding region, Path 3: slip region, and Path 4: repeated loading region. In addition, this study provides an equation for predicting the longitudinal axial strain in the regions of the plastic hinge subjected to reversed cyclic loading for different patterns. To verify the longitudinal strain in the region of plastic hinge by the suggested method, twelve RC beams were tested under reversed cyclic loading. The observed longitudinal strains in the regions of the plastic hinge for the tested beams agreed with the calculated longitudinal strains.

In 2007, the capacity of the plastic hinge rotation of reinforced concrete beams was studied by Kheyroddin and Naderpour [34]. A parametric study was performed to evaluate the influence of the index of tension reinforcement, ($\omega = \rho$ fy /f′c), and the distribution of the bending moment (loading type) on the ultimate deformation characteristics of reinforced concrete beams. The analytical results of 15 beams that simply supported with various amount of tension reinforcement ratio under three different loading conditions were offered and compared with the predictions of the different experimental data and formulations, where available. The capacity of plastic hinge rotation increases as the loading changes from the concentrated load at the middle to the third-point loading, and it was a maximum for the case of uniformly distributed load. The influence of the loading type on the capacity of the plastic rotation for the beams of heavily reinforced was not as significant as that for beams of little reinforced. According to analytical results obtained using nonlinear finite element method, new simple equations as a function of the tension reinforcement index, ω, and the loading type were proposed. The suggested equations can be used for analyzing the ultimate capacity and the associated deformations of RC beams with sufficient accuracy.

2.5 Concluding Remaking

The following points could be withdrawing from previous studies related to non prismatic and flanged sections or those relate to rotation capacity studies of reinforced beams.

1- All studies related to non prismatic section considered entire section to be variable and there is no study relate to developing member with concerned part to be non prismatic.

2- Strength, ductility, and member weight are important issues in design requirements and should be consider and investigate in current developed section.

3- The rotation capacity investigation is an important issue for enhancing ductility requirements and should be consider in any developing section.

Chapter Three

Experimental Work

Chapter Three

Experimental Work

3.1 General

The main purpose of the experimental work is to investigate experimentally the cracks pattern, ductility, rotation capacity, strength ratio and deflection in structural simply supported reinforced concrete beams with non-prismatic flanged members. This chapter includes the details of materials used, the details and sketches of twelve beams includes shapes, dimensions and sections as well as steel reinforcement, description of the characteristics of the materials, testing of aggregate properties, testing fresh and hardened concrete, fabrication the forms of concrete casting, casting the beams and explained the all testing of stages of work enhanced with definition graphics and realistic images.

3.2 Material Properties

This section presents details of the constituent's material properties required in the experimental work and describing the process of working which are described below and included the process of testing that relating of them.

3.2.1 Cement

Ordinary Portland cement type cresta was used, which is available in the local market satisfying requirements of IQS No.45-1984[10].Throughout the investigation the whole quantity required was brought to the laboratory before one day from the casting, it was stored in laboratory in a dry place in it before but performs the test before brought it. The chemical and physical properties of the used cement are presented in the Tables No. (3-1) and (3-2).

Table (3-1) Physical Properties of Cement

Physical properties	Test results	ASTM C150
Fineness using Blain air permeability apparatus (m^2/kg)	380	280**
Setting time using Vicat's instrument Initial (min.) Final (hr.)	 110 4.0	 45** 10*
Smoothness %	0.02	5* %
Compressive strength at: 3days (M_P) 7days (M_P)	 16.5 22.9	 12** 19**

* Maximum limit. ** Minimum limit

Table (3-2) Chemical composition of cement

No.	Compound composition	Chemical composition	Content (%)	ASTM C150
1	Lime	CaO	60.4	------
2	Alumina	Al_2O_3	5.32	------
3	Iron oxide	Fe_2O_3	5.5	------
4	Sulphate	SO_3	2.5	2.5*
5	Loss on ignition	-------	1.6	4.0*
6	Lime saturation factor	L.S.F	0.68904	(0.66-1.022)%
7	Tricalcium aluminates	C_3A	7.60	-------
8	Silkone oxide	SIO_2	27.21	-------

* Maximum limit

3.2.2 Silica Fume

The silica fume used in this study is SikaFume MegaAdd MS (D), which is a concrete additive of a new generation in gray powder form ready to use, MegaAdd MS (D) is a very fine pozzolanic, ready to use as high performance mineral additive to concrete. It acts physically to optimize particle packing of the concrete or mortar mixture and chemically as a highly reactive pozzolan. MegaAdd MS (D) in contact with water goes into solution within an hour. The silica in solution forms an amorphous silica rich, calcium poor gel on the surface of the silica fume particles and agglomerates. After time the silica rich calcium poor coating dissolves and the agglomerates of silica fume react with free lime (CaOH) to form 2 calcium silicate hydrates (CSH). This is the pozzolanic reaction in cementitious system. MegaAdd MS (D) can be used in a variety of applications such as concrete, grouts, mortars, fiber cement products, refractory, oil/gas well cements, ceramics, elastomeric, polymer applications and all cement related products. It is generally used in the range 5 to 12% by mass of cementations materials as a partial replacement for concrete structure that need high strength or significantly reduced permeability to water [40]. The silica fume used in this work meet with typical properties requirements of standards ASTM C1240 as shown in Tables (3-3).

Table (3-3) typical properties at 25°C of SikaFume MegaAdd MS (D) [11]

property	value
State	Sub-micron powder
Colour	Grey to medium grey powder
Specific Gravity	2.10 to 2.40
Bulk Density	500 to 700 kg/m

Chemical Requirements	
Silicon Dioxide (SiO_2)	Minimum 85%
Moisture Content (H_2O)	Maximum 3%
Loss on Ignition (LOl)	Maximum 6%
Physical Requirements	
Specific Surface Area	Minimum 15 m /g
Pozzolanic Activity Index, 7 days	Maximum 105% of control
Over size particles retained on 45 micron sieve	Maximum 10%

3.2.3 Aggregate

3.2.3.1 Fine Aggregate

Natural silica sand brought from Jabil Sinam area was used as fine aggregate. The grading of the fine aggregates are shown in Tables (3-4) and (3-5). The obtained results indicated that the fine aggregates grading were within the limits of Iraqi specification No. 45/1984[10], ASTM C33-03[12] and B.S. 882:1992[13]. Tables (3-4) and (3-5) showed the specific gravity, sulphate content and absorption of the fine aggregates.

Table (3-4) Grading of fine aggregate

No.	Sieve size	Passing (%)			
		Test results of passing	Iraqi specification No. 45/1984[10]	ASTM C33-03[12]	B.S. 882:1992 Overall grading[13]
1	4.75 mm	95	90-100	95-100	89-100
2	2.36 mm	82	75-100	80-100	60-100
3	1.18 mm	62	55-90	50-85	30-100
4	600 mm	39	35-59	25-60	15-100
5	300 mm	17	8-30	5-30	5-70
6	150 mm	2.5	0-10	0-10	0-15
7	pan	0	-----	-----	----

Table (3-5) Properties of fine aggregate

Physical properties	Test results	Iraqi specification No. 45/1984[10]
Specific gravity	2.64	---------
Sulfate content (SO_3)	0.41 %	≤ 0.5 %
Chloride content (Cl)	0.073 %	≤ 0.1 %
Absorption	1.70 %	---------

3.2.3.2 Coarse Aggregate

Coarse aggregate was used is natural gravel brought from Ali algarby area. After the testing in laboratory of Amarh institute was found its grading satisfies the limits of Iraqi Standard 45/1984[10] for graded gravel with maximum size of 13.2mm and smooth surface. Properties of the used aggregate are presented in Table (3-6) and (3-7).

Table (3-6) Grading of Coarse Aggregate

No.	Sieve size	Passing (%)			
		Coarse Aggregate	Iraqi specification No. 45/1984[10]	ASTM C33-03[12]	B.S. 882:1992 Graded aggregates[13]
2	19 mm	100	100	100	100
3	13.2 mm	96	90-100	90-100	90 - 100
4	9.5mm	56	50-85	20-55	30 - 60
5	4.75 mm	2.1	0 - 10	0 - 10	0 - 10
6	pan	0	----	0 - 5	-----

Table (3-7) Properties of coarse aggregate

Physical properties	Test results	Iraqi specification No. 45/1984[10]
Specific gravity	2.67	---------
Sulfate content (SO_3)	0.098 %	≤ 0.1 %
Chloride content (Cl)	0.091 %	≤ 0.1 %
Absorption	1.1 %	---------

3.2.4 Water

Reverse osmoses (R.O.) water was used for mixing and washing aggregate before casting to remove mud, dust salts and foreign matter suspended, free from harmful materials and according to Iraqi standard 1703/1992 [14]. As shown in Table (3.8).

Table (3.8) Chemical test of water

Tested	Standard (mg/L)	Tested sample
SO3	1000	280
Carbonate and bicarbonate	1000	Non
Chloride	500	210
Non Organic	Sum. of ions<3000	321
Organic	Tested if there color or test	Non

3.2.5 Superplasticizer

The superplasticizer used in this study was Sika®viscoCrete5930 which is ready to use, dual action liquid admixture for high performance concrete, which is specially modified super plasticizer to control the water addition giving high workability with excellent slump to produce high strength concrete.

Superplasticizer can be used for all types of Portland cement, and it is a third generation superplasticizer for concrete and mortar. It meets the requirements for superplasticizer according to ASTM-C494/C494M-1999[15] Types G and F and BS EN 934 part 2: 2001.The typical properties of Sika®viscoCrete5930 are shown in Table (3-9).

Table (3-9) typical properties of Superplasticizer

Appearance	Turbid liquid
Density	1.095 kg/It
Chloride content	NIL
Colour	Turbid
Basis	Aqueous solution of modified Polycarboxylate

3.2.6 Steel Reinforcement bars

Ukraine manufactured deformed bars of (10 mm) diameter are used for the longitudinal reinforcement and Turkish deformed bars of (8 mm) diameter were used for stirrups. The steel reinforcement distribution and fabricated are shown in Fig. (3-2). several tensile specimens of each size of bars are presented in Fig. (3-3). The properties of the two bars was tested is presented in Table (3-10). The test was conducted according to ASTM A615/A615M-04b [16]**.** And the stress-strain curves were drawn in Figure (3-1) a and b.

Table (3-10) Results and specification limits of reinforcing bars [16]

Test Results			ASTM A615/A615M-04B limits			
Bar Size (mm)	Yield strength (N/mm^2)	Ultimate Strength (N/mm^2)	Elongation (%)	Yield strength Min.(N/mm^2)	Ultimate Strength Min.(N/mm^2)	Elongation .(%)
8	421	523	30.6	419	525	29.8
10	488	598.6	24.90	492	621.40	21.40

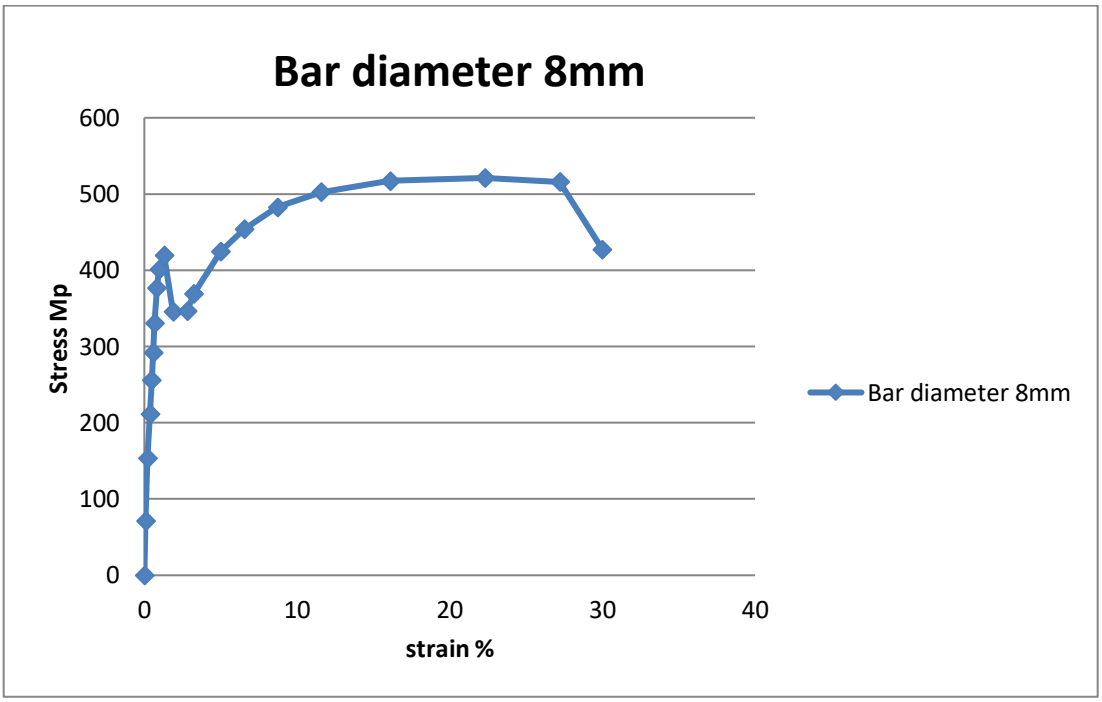

Figure (3-1a) stress-strain diagram of steel bar 8mm diameter

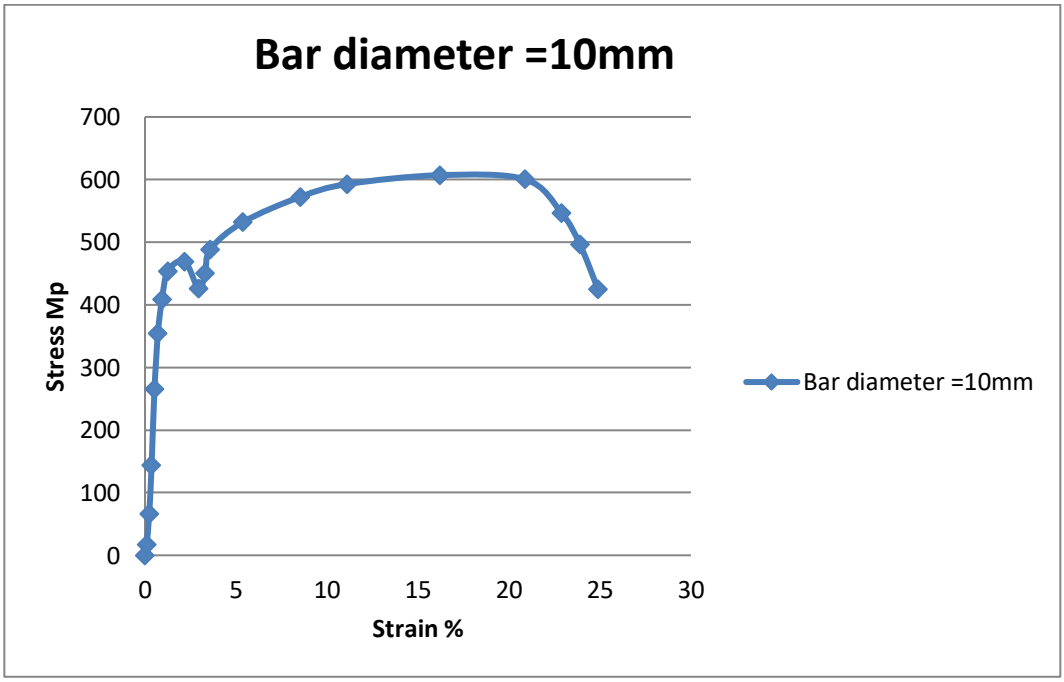

Figure (3-1b) stress-strain diagram of steel bar 10mm diameter

3-3 Trial Mixes of Concrete

Three experimental mixtures were made to reach the required strength with good workability. The third mixture was chosen in this work. Workability was investigated by slump test, the test was carried out three times for each mix according to ASTM C 143M-03[17]. Mixes were made to achieve slump about 50 mm for Approved Mix. Table (3-11) shows the quantities of trial mixes

Table (3-11) Quantities of materials for trial mixes

Material	**Trails Mix 1**	**Trails Mix 2**	**Trails Mix 3**
Cement kg/m³	461.6	461.6	461.6
Silica fume kg/m³	23.1	23.1	23.1
Fine Sand kg/m³	646.25	646.25	646.25
Coarse aggregate kg/m³	791.3	791.3	791.3
Water l/m³	166.2	175.5	184.6
super plasticizer l/m³	2.8	2.9	2.5
Ratio of mixing materials			
Cement	1	1	1
silica fume	0.05	0.05	0.05
sand	1.4	1.4	1.4
aggregate	1.7	1.7	1.7
water	0.343	0.362	0.38
super plasticizer	0.005	0.006	0.005

3.4 Design of T- Beams

Though T-beams are simple in design but contains multiple design elements of interest. Unlike an I-beam, a T-beam lacks a bottom flange, which carries savings in terms of materials, but it is weak in resisting tensile forces, this lack of a bottom flange on a T-beam serves as an advantage in that the stem rests on edge making the flange the upper deck. T- Beam designs come in many sizes, lengths and widths depending on what the structure is and its compression tension needs. However, the simplicity of the T-beam is in question by some who would rightly test more than one complex structure; for example, a group of researchers tested pretension inverted T-beams with circular web openings, with mixed but generally favorable results. Thus, in some cases, the extra time and effort invested in creating a more complex structure proves worthwhile. A simpler matter to consider is that of which material or materials make up the construction of T-beams. Concrete alone is brittle and thus overly subject to the shear stresses a T-beam faces where the web and flange meet. This is the reason that steel is combined with concrete in

T-beams. A problem of shear stress can lead to failures of flanges detaching from webs when under load. This could prove catastrophic if allowed to occur in real life; hence, the very real need to mitigate that possibility with reinforcement for concrete T-beams. In such composite structures, many questions arise as to the particulars of the design, including what the ideal distribution of concrete and steel might be: "To evaluate an objective function, a ratio of steel to concrete costs is necessary". This demonstrates that for all aspects of the design of composite T-beams, equations are made only if one has adequate information. Still, there are aspects of design that some may not even have considered, such as the possibility of using external fabric-based reinforcement, "All the beams failed in shear and those with composite reinforcement displayed excellent bond characteristics. For the beams with external reinforcement, increases in ultimate strength of 60 to 150 percent were achieved" [18]. When it comes to resistance to shear forces, external reinforcement is a valid option to consider. Thus, overall, the multiple important aspects of T-beam design impress themselves upon the student of engineering.

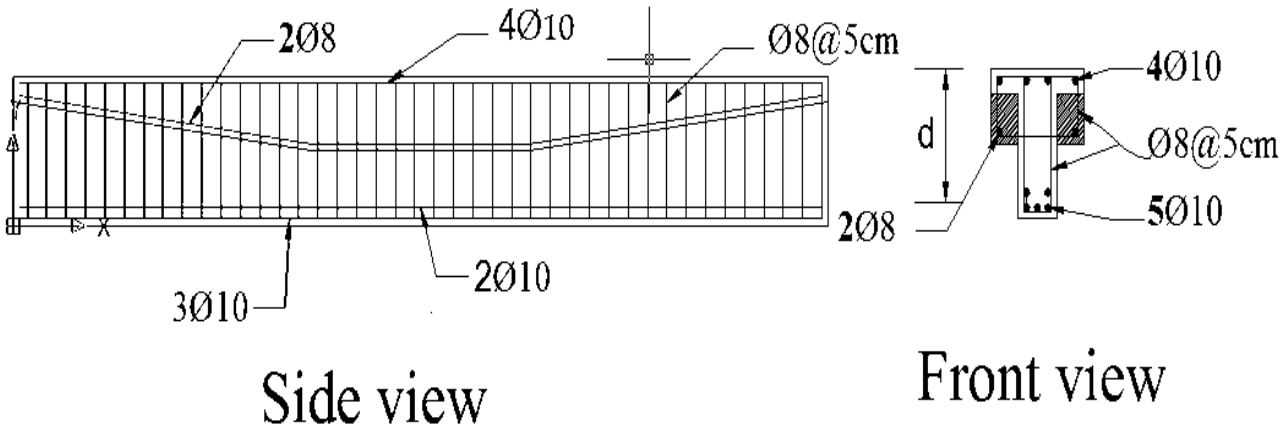

Figure (3-2) distribution of steel reinforcement in beams

Table (3-12) Mechanical properties of used steel reinforcement

No.	Diameter, mm	fy, MP	fu	εu %	εy %	E
1	8	420	524	30.2	0.21	200000
2	10	490	610	23.2	0.24	204166.7

Figure (3-3) Stress-Strain relationship for steel

3.5 Hard Concrete Strength

3.5.1Compressive Strength

The compressive strength test of concrete was carried out in accordance with ASTM C39-03[19], using three (150×300 mm) cylinders at age 28 days loaded uniaxially, also the average of three(150×150×150 mm) cubes were used to estimate the compressive strength according to BS1881 116-83[20].

Figure (3-4) Compressive strength test

3.5.2 Splitting Strength

Splitting tensile strength was carried out in accordance with ASTM C496-04[21]. The splitting tensile strength tests are made on (150×300 mm) concrete cylinder specimens loaded as shown in Fig. (3-5). The splitting tensile strength was determined according with equation below and was took the average of values of three cylinder results :

$$f_{sp} = \frac{2P}{\pi dL} \qquad \text{(ASTM C496-04)[21]} \qquad \ldots\ldots\ldots\ldots\ldots\ldots(3\text{-}1)$$

where:

f_{sp} = Splitting strength(Mp)

P: maximum applied load (failure load) (N)

L: height of cylinder (mm), (L=300 mm)
d : diameter of cylinder (mm)

Figure (3-5) Splitting tensile strength

3.5.3Flexural Strength

The ASTM-C78 [22] was adopted to examine the flexural strength of concrete using prism (150*150*500)mm specimens for testing. This test was done in Technical Institute of Amarh laboratory by using machine with a capacity 100 ton as shown in Fig. (3-6).

The following equation is utilized to calculate the flexural strength:

$$fr = \frac{3pl}{2bd^2} \qquad \text{.....(3-2)}$$

where

fr : modulus of rupture (Mp)

P : maximum applied load(failure load) (N)

L : span length (mm), (L=500 mm)

b: width of the specimen (mm)

d: depth of the specimen (mm)

Figure (3-6) Flexural strength test

3.5.4 Modulus of Elasticity Tests (E_c)

Modulus elasticity of concrete tests was carried out in accordance with ASTM C469-02[23], using (150×300 mm) concrete cylinders, the instrument as shown in Fig. (3-7). Modulus of Elasticity was determined as follows:

$$E_c = \frac{S2-S1}{\varepsilon 2-\varepsilon 1} \quad \text{(ASTM C469-02) [23]} \quad \text{……..(3-3)}$$

Or

$$E_c = 4700\sqrt{f'c} \quad \text{(ACI Code 318-14)[24]} \quad \text{……..(3-4)}$$

Where:

E_c **:** modulus of elasticity for concrete (Mp)

S_2 : stress corresponding to 40 % of ultimate load (Mp)

S_1 : stress corresponding to a longitudinal strain(Mp), $\varepsilon_1 = 0.00005$

ε_2 : longitudinal strain produced by stress S_2

f'c : Stress of concrete to cylinder,(Mp)

Figure (3-7) Modulus of Elasticity Tests (E_c)

Table (3-13) Hard concrete properties at 28 days

f'c,(Mp)	fr,(Mp)	ft, (Mp)	Ec, (Mp)	Slump, (mm)	Unit weight, kg/m^3
35	3.67	5.92	27806	50 mm	2235

Figure (3-8) Casting Processes Samples and slump test

3.6 Specimens Description and Details

The typical dimensional configuration of used specimens is illustrated in Fig. (3-9). The length of considered samples is 2100 mm while the clear span is 2000 mm. Table(3-14) summarized description of all specimens while Photo depicts all prepared sample.

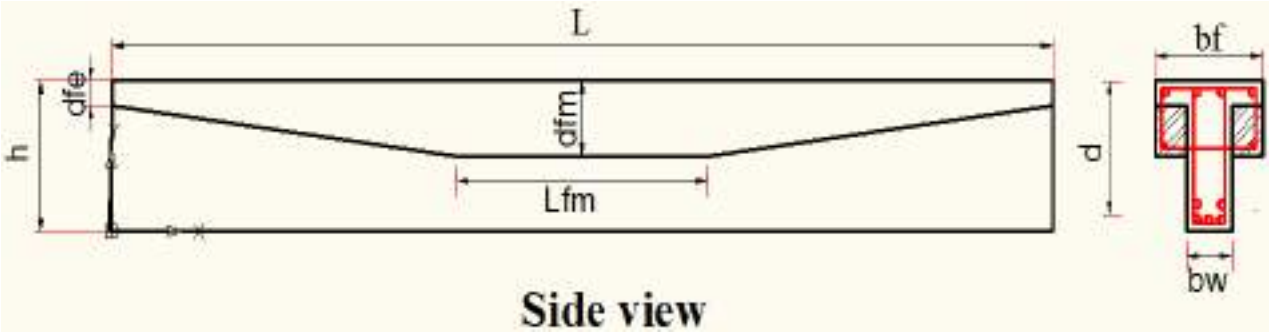

Figure (3-9) Typical drawing dimension

Table (3-14) Dimension of Beams

No	Code	AS	Description	Geometry details								
				bf cm	bw cm	dfe cm	dfm cm	Lfm cm	L cm	d cm	h cm	symbol of figure
1	B1	5¬10	Rectangular section Beam	24	24	30	30	210	210	26	30	(a)
2	B2	5¬10	T- BEAM	24	10	15	15	210	210	26	30	(b)
3	B3	5¬10	T-BEAM	24	10	5	5	210	210	26	30	(c)
4	B4	5¬10	Non-prismatic flange section	24	10	5	15	0	210	26	30	(d)
5	B5	5¬10	Non-prismatic flange section	24	14	5	15	0	210	26	30	(e)
6	B6	5¬10	Non-prismatic flange section	24	18	5	15	0	210	26	30	(f)
7	B7	5¬10	Non-prismatic flange section	24	10	5	15	26	210	26	30	(g)
8	B8	5¬10	Non-prismatic flange section	24	14	5	15	26	210	26	30	(h)
9	B9	5¬10	Non-prismatic flange section	24	18	5	15	26	210	26	30	(i)
10	B10	5¬10	Non-prismatic flange section	24	10	5	15	52	210	26	30	(j)
11	B11	5¬10	Non-prismatic flange section	24	14	5	15	52	210	26	30	(k)
12	B12	5¬10	Non-prismatic flange section	24	18	5	15	52	210	26	30	(L)

bf: flange width(cm)

bw: web width(cm)

dfm: depth flange at midspan(cm)

dfe: depth flange at edge(cm)

Lfm: length of horizontal part of flange(cm)

d: effective depth of steel reinforcement(cm)

h: depth of beam(cm)

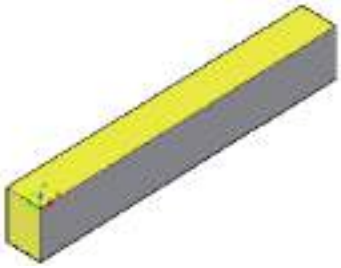

Side view

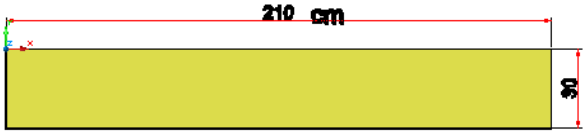

Front view

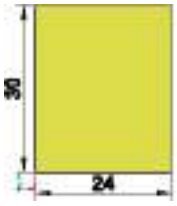

Bottom view

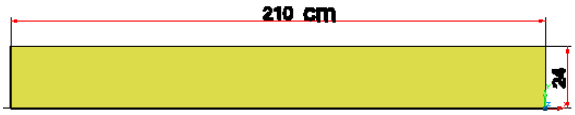

Details (B1)

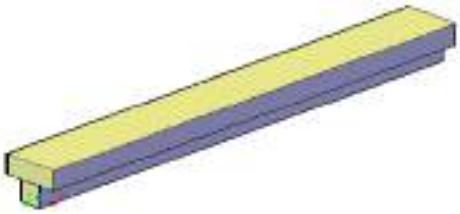

Side view

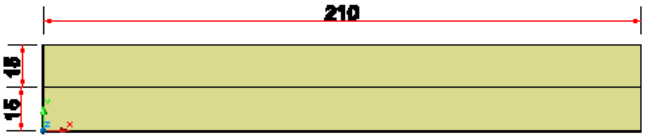

Front view

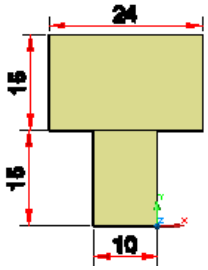

Bottom view

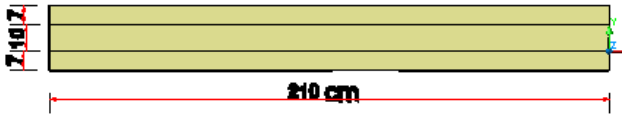

Details (B2)

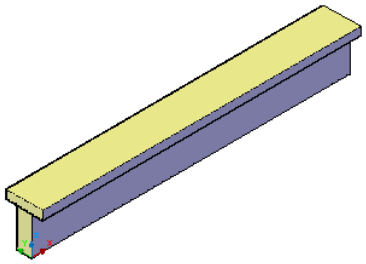

Side view

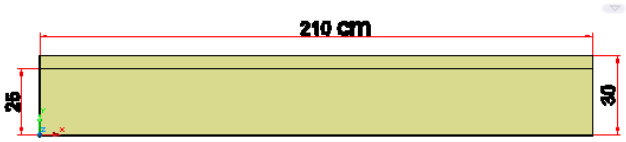

Front view

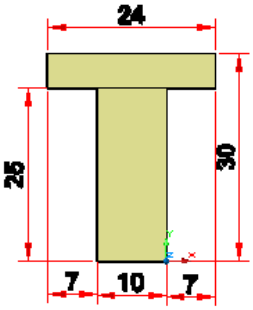

Bottom view

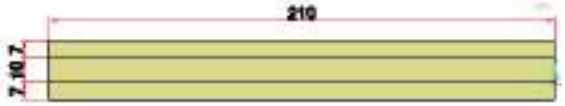

Details (B3)

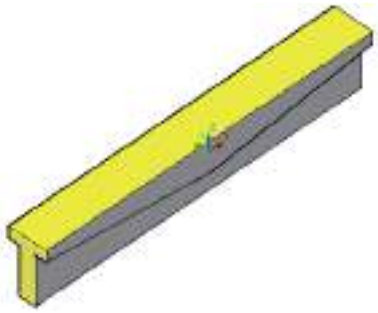

Side view

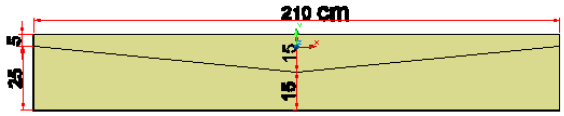

Front view

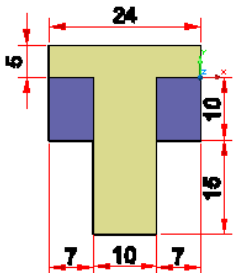

Bottom view

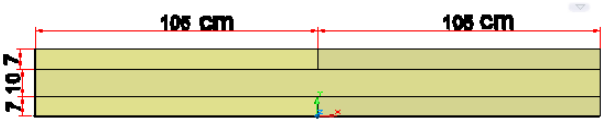

Details (B4)

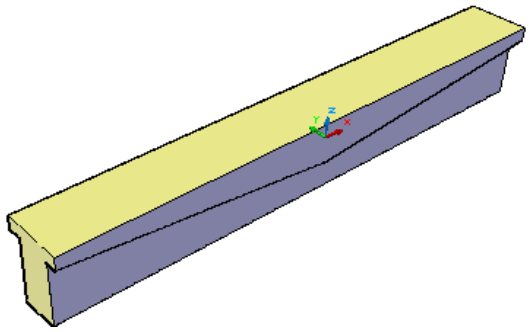

Side view

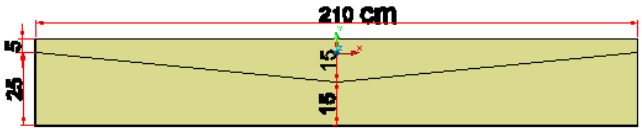

Front view

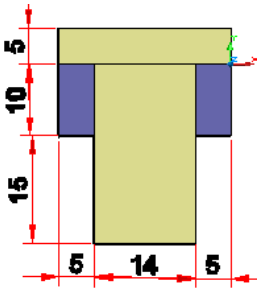

Details (B5)

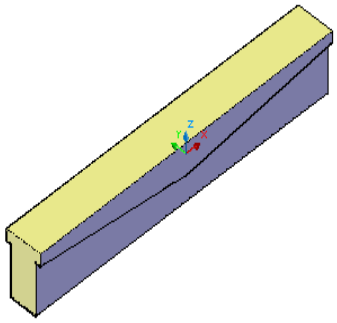

Side view

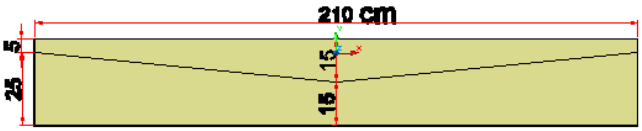

Front view

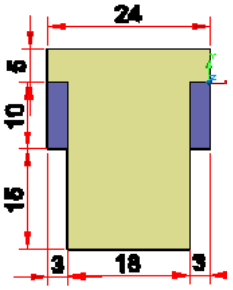

Bottom view

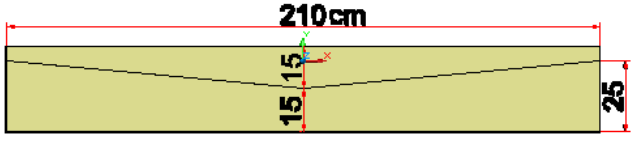

Details (B6)

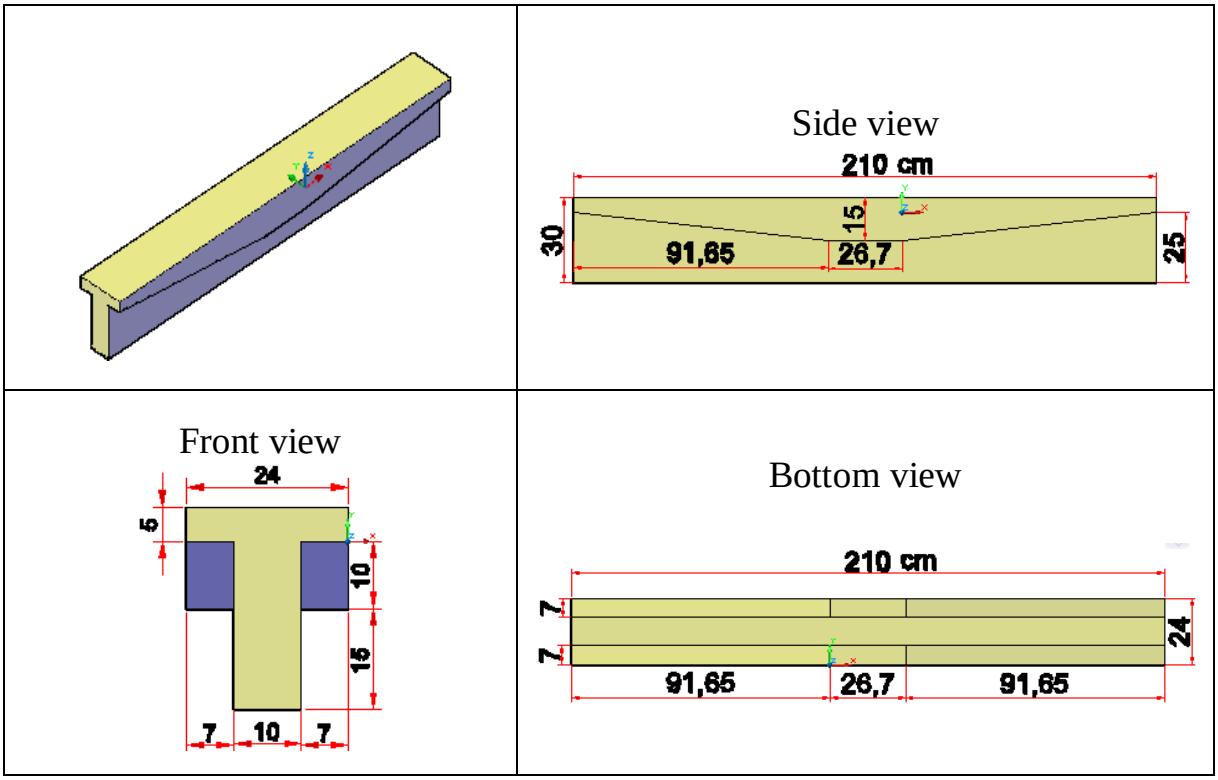

Details (B7)

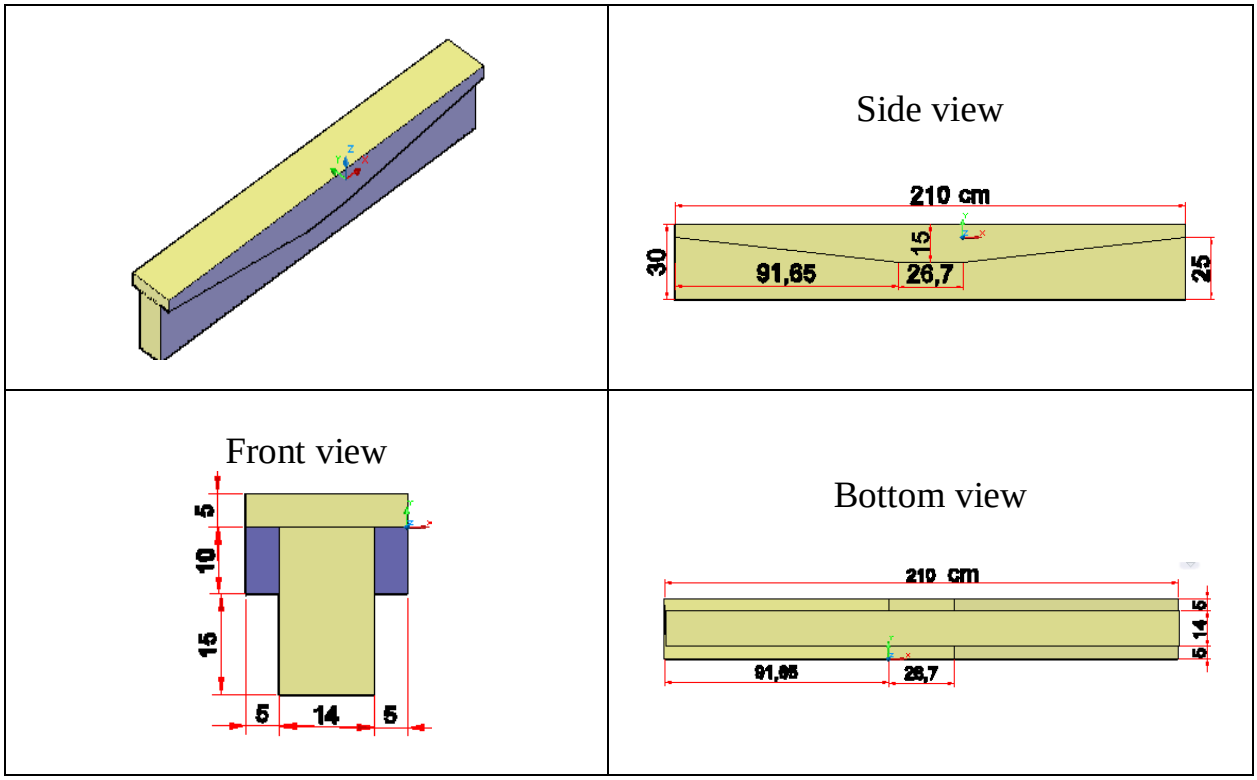

Details (B8)

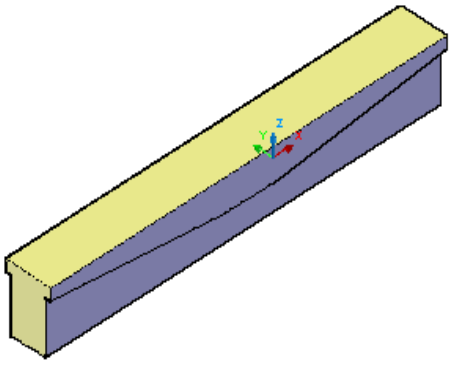

Side view

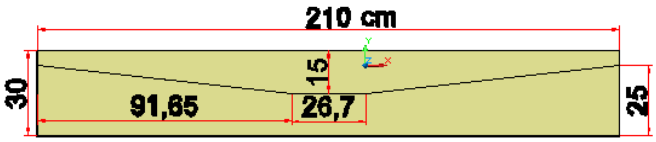

Front view

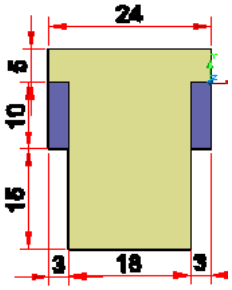

Bottom view

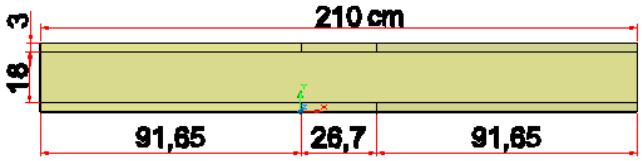

Details (B9)

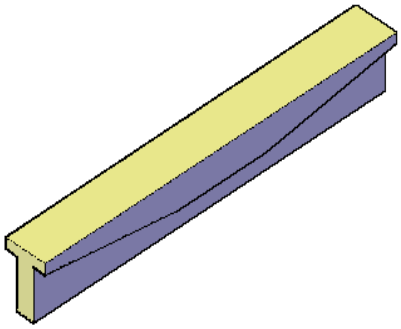

Side view

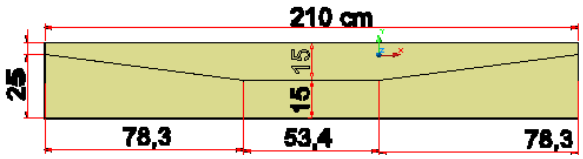

Front view

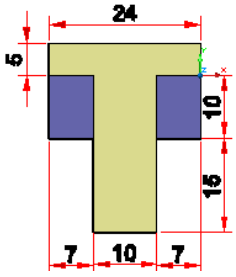

Bottom view

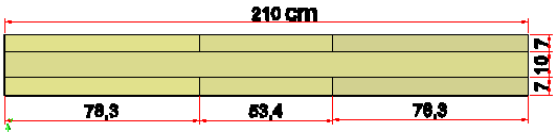

Details (B10)

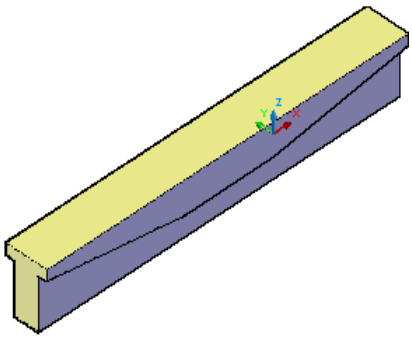

Side view

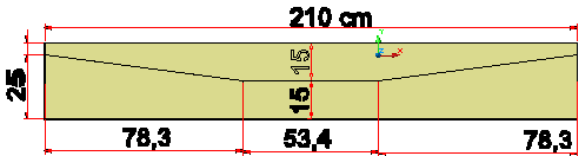

Front view

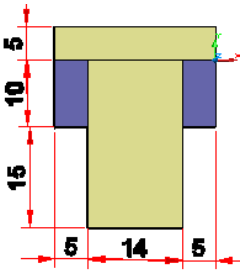

Bottom view

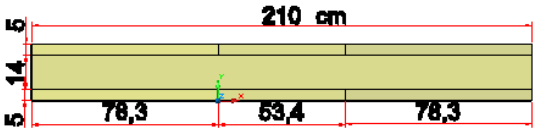

Details (B11)

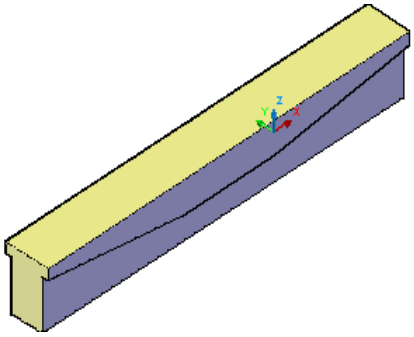

Side view

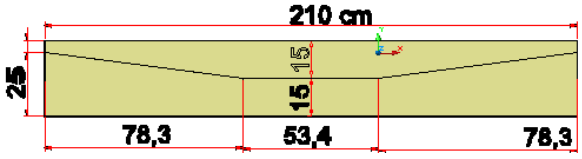

Front view

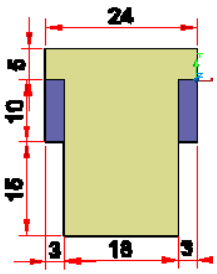

Bottom view

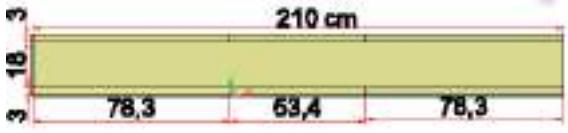

Details (B12)

Figure (3-10) detail of beams

3.6.1 Mould Fabrication

Since the templates are special shapes except rectangular and T-beams they were made from iron sheets gage 3mm also strengthened from the sides with square tubs steel shape 3 cm * 3 cm according to measurements and controlled by screws so as not to change dimensions when casting and the interior faces was painted with oil before placing the reinforcing steel inside the templates to ensure that the concrete does not stick to the template when it is hardening after

Figure (3- 11) Mould fabrication

3.6.2 Fabrication of steel reinforcement

The steel reinforcement fabricated at laboratory of Amarh technical institute. Five steel bars 10 mm diameter have put in two layers in bottom of the web and four bars in the flange, two with 10mm diameter in top and two of 8 mm diameter in the bottom of flange. The covers are 15 mm from all direction, the longitudinal steel tied up by stirrups every five centimetres in the web and one in the flange every 20 cm, the work was done by two technicians men according to the specifications. Fig.(3-12) shown steel reinforcement fabrication.

Figure (3-12) Steel reinforcement fabrication

3.6.3 Specimens Preparing and Casting

After prepared the moulds spacers were put under and around the moulds to controlled the covers then fabricated reinforcement have putted in the moulds.

All specimens were casted at the same conditions, steel reinforcement distributed accordion to ACI 318-14[25].

Drum mixer are use during concrete pouring while portable vibration device used throughout casting process according to ACI 318[26]. The prepared specimens were cured by covering them with canvas and watered twice with water over 28 days. Fig. (3-13) shown Specimens Preparing.

Figure (3-13) Specimens Preparing

3.6.4 Casting procedure

To maintain a single mixing uniform covering all the amount of casting without falling into personal errors can be caused a discrepancy in the specifications between mixing and the other has been hired drum mixer brought to the site and mixing the components of concrete in the work site, In the beginning, the internal surface of the mixer was cleaned by adding gravel and leaving the mixer rotated for five minutes after that the remaining aggregate were then added and leave the mixer three minute rolling around then wet by twenty litter of water, These operations took approximately quarter of an hour, after that the amount Main components was added as following, the sand was throw in mixer after one minute from mixing, the half of amount of cement with half amount of silica fume have been added then half of water was added that the half without superplasticizer, then the remaining of cement and silica fume had been added, the remaining of half of water that mixing with the amount of super plasticizer after eight minutes from the mixing were added, the components of concrete was obtained the homogenous and good workability of wet concrete and was started the casting of concrete. In casting, the speed factor in the achievement was achieved by providing sufficient number of workers and technicians in addition to the availability of the fully equipped. after this process the casting have been started by Filling the molds with soft concrete via the channel of mixer, this process was done in three layers to fill each mold, each layer was compacted by electrical vibration with Beating on the sides of moulds by a hammer to avoid caries After finishing the molds with soft concrete, the surface was smoothed and polished well.

Figure (3-14)
casing of concrete

Figure (3-15)
Compaction process

Figure(3-16) Finishing

3.6.5 Curing

The casting and processing of curing were done in the laboratory in the shade place, after twenty four hours from the casting the moulds of concrete is removed and the concrete beams were covered with canvas clothes and the process of curing was started by poured R.O water for 28 days At a rate of two watering per day until testing, the curing process shown in Fig. (3-18).

Figure (3-18) The process of curing

3.6.6 Preamble the Sample of Beams

After The expiration of the curing period the samples of concrete beams were prepared for test by painting beams in two different colors one for flanges and the other for the webs as shown in Fig. (3-19) after that the induction plates were then pasted on to the beams.

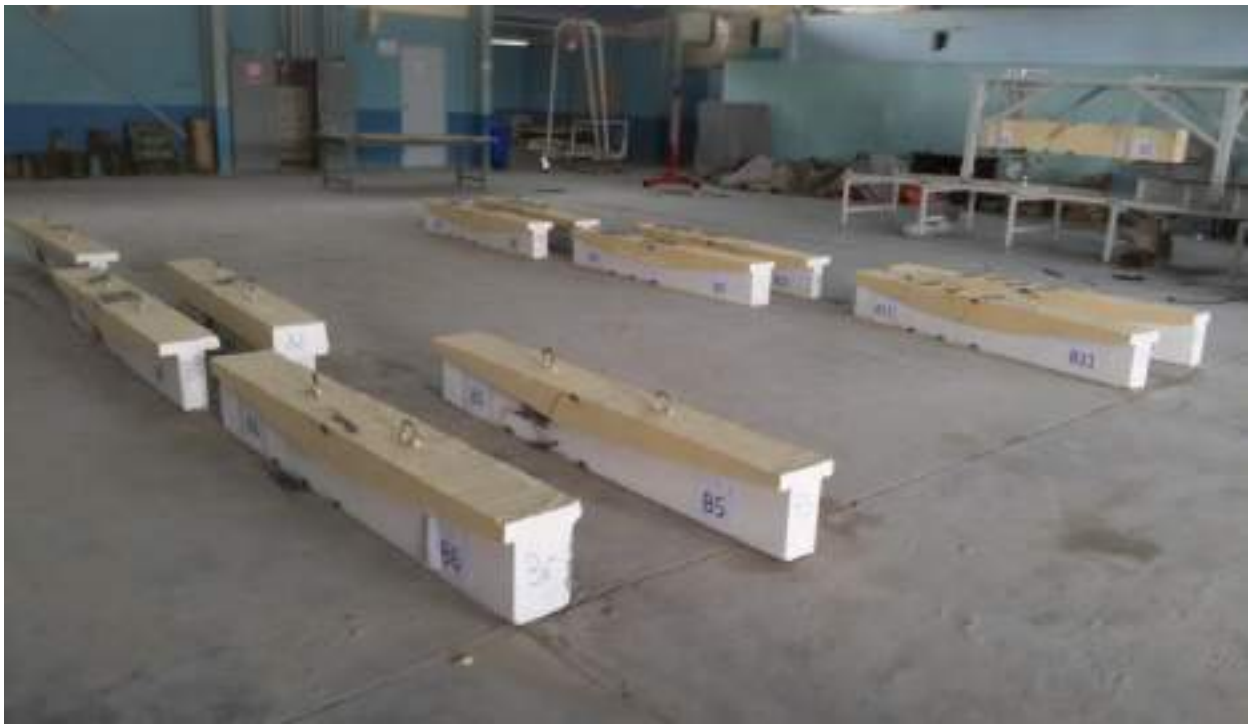

Figure (3-19) Prepare samples for test

3.6.7 Test Setting and Arrangement

Two dial gages fixed to the bottom of beam specimens to measure the deflections one at midspan of beam and the other at distance d (effective distance of steel reinforcement) (the dial gage has been used in middle of beam has accuracy 0.02 mm and maximum measure was 10 cm and the dial gage at 2d from middle of beam, the accuracy was 0.01 and maximum measure was 5cm). Four strain gages type(PLF-30-11-3LJC-F) and has transverse sensitivity -0.1% pasted on the edges of beam specimens, Strain gage (A) at top middle edge, strain gage (B) in bottom middle edge, strain gage (C) at (d) distance from middle of beam at bottom edge and strain gage (D) at (2d) distance from middle of beam at bottom edge to read the strain, the distance between two supported was two meter and the load applied at center of beam as shown in Fig. (3-20).

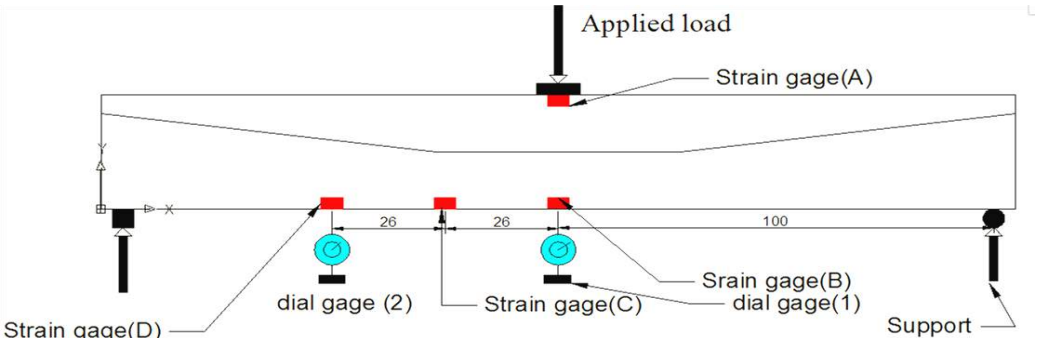

Figure (3-20) Test setting

Data loger

Figure (3-21) Test process

Figure (3-21) Test process

Chapter Four

Results and Discussion

Chapter Four

Results and Discussion

4.1 General

This chapter describes the experimental results of twelve reinforced concrete beams subjected to three points load. One of them is rectangular prismatic section, two beams is flanged section was constant flanges depth (5cm and 15cm), and nine beams is non-prismatic flange changes linearly from 5 cm at the edges to 15 cm at the mid span. The structural performance is discussed by studying ultimate load capacities, load deflection behavior, strength ratio, flexural ductility, plastic rotation capacity and crack patterns. The main parameters examined in this investigation are flange tapered thickness variation and web thickness and the effect of these variables on efficiency the non prismatic beams.

4.2 Ultimate Loads

Ultimate Load is the maximum ability induced in a structural element when an external force is applied to the structural member causing the element to bend and it is refers to maximum section withstanding of applied loads to be limit consider in design as dominated principle[27]. The assigned ultimate capacity of non-prismatic section exhibited efficiency of this sections additional there is slightly increment of ultimate load in spite of they have the same middle cross section, the large of ultimate load ratio in respect to control beam (B1) was1.075.This observations in the minimum limit confirming that changing section maintains ultimate strength with slightly increment. This efficiency could be related to proportionality the changing of non prismatic flange thickness with conjugated variable bending moment along the beam. Fig. (4-1), Clearly illustrated ultimate

strength of tested beams which included non-prismatic sections and controlled beams of rectangular (B1) and T-sections (B2, B3).

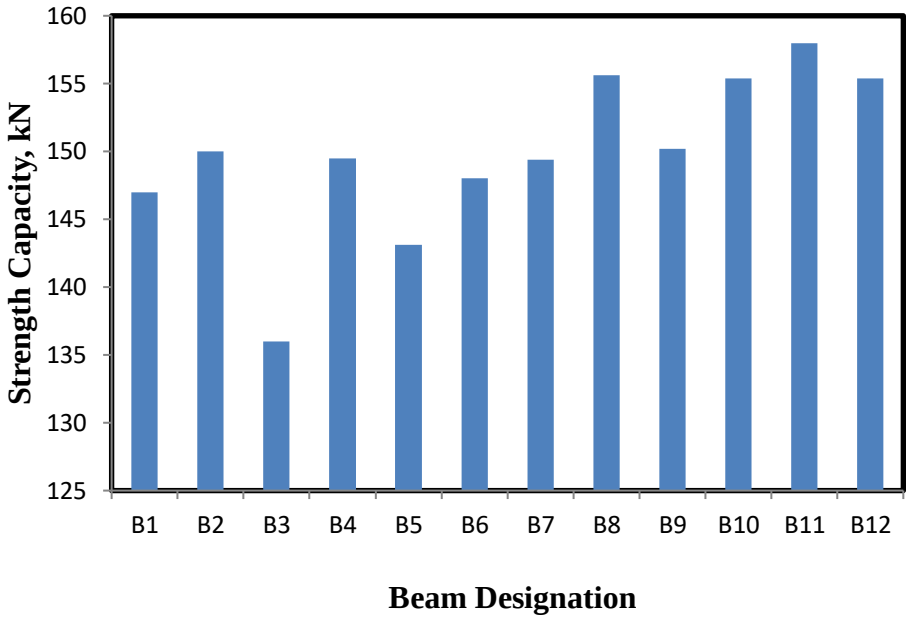

Figure (4-1) histogram of ultimate load

4.3 Flexural Stiffness

Flexural stiffness is defined as the force couple required to bend a flexible structure in one unit of curvature or it can be defined as the resistance offered by a structure while undergoing bending [34] and it's an index for measuring deformability. The flexural stiffness of a structure is a function based upon two essential properties: the elastic modulus (stress per unit strain) of the material that composes it, and the moment of inertia, which is a function of the cross-sectional geometry [28].

Flexural stiffness could be detected from load deflection curve by slope of linear part, Fig. (4-2), clearly indicated that all tested beams have closed stiffness in spite of cross section changing, this could be relate to the middle region still dominated as moment of inertia is the same for all member.

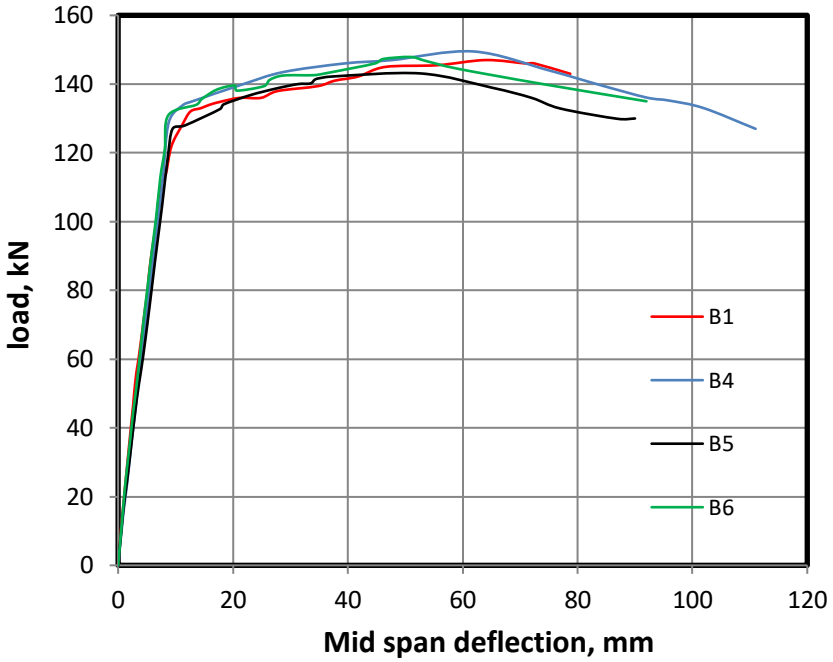

Load –deflection for B1, B4, B5and B6

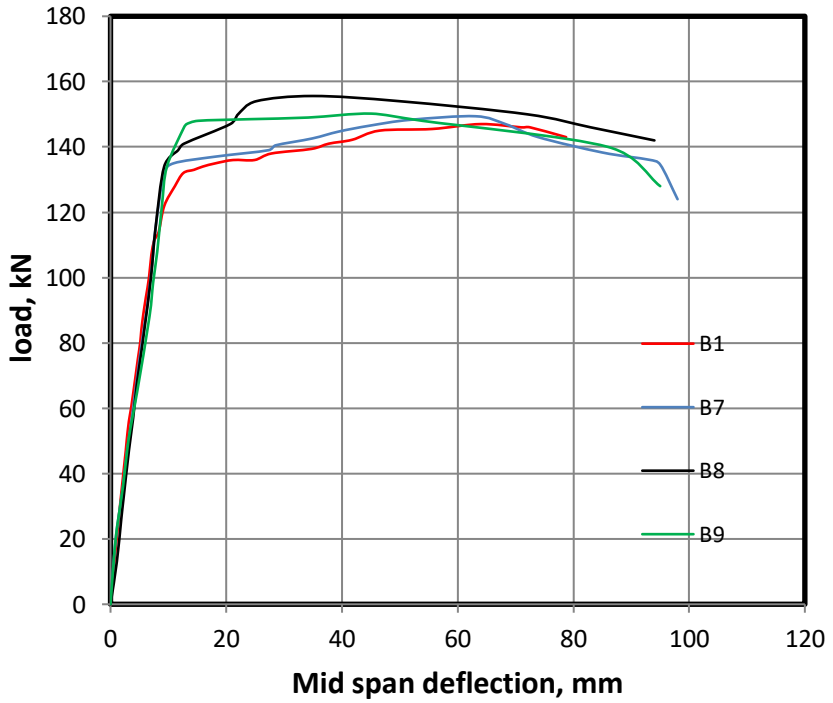

Load –deflection for B1, B7, B8 and

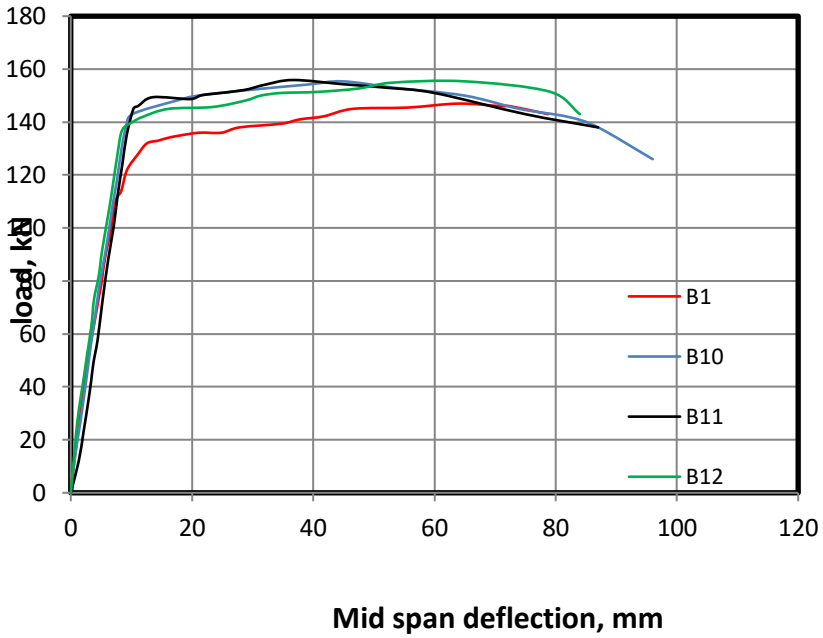

Load –deflection for B1, B10, B11 and B12

Figure (4-2) Comparison of load deflection response of tested specimens in scope of beam B1

4.4 Strength rating

One of most important issue in concrete design philosophy is to produce light structural element as much as possible without effect on intended strength. Strength rating which could defines as the ratio of ultimate strength to overall beam weight where it is introduced as reference function to measure element efficient in scope of economical provision relate to beam weight and so dead load[29]. Mathematical defining of strength ratio consider as:

$$Rs = Pu/Wb \qquad \text{…….. (4-1)}$$

Where: Rs is strength rating, Pu is ultimate strength and Wb is overall beam weight Table (4-1) illustrates significant beam geometry changing relate to volume and weight reduction ratios due to considering in plane non-prismatic flanges sections

in addition to ultimate load and related strength rating. All developed non-prismatic flanged section developed higher strength rating in comparison with control section B1.Table (4-1). Shows that strength rating and for all four considered groups that behavior trend to change in the same response of weight reduction and Fig.(4-3) shown the strength rating for all the beams.

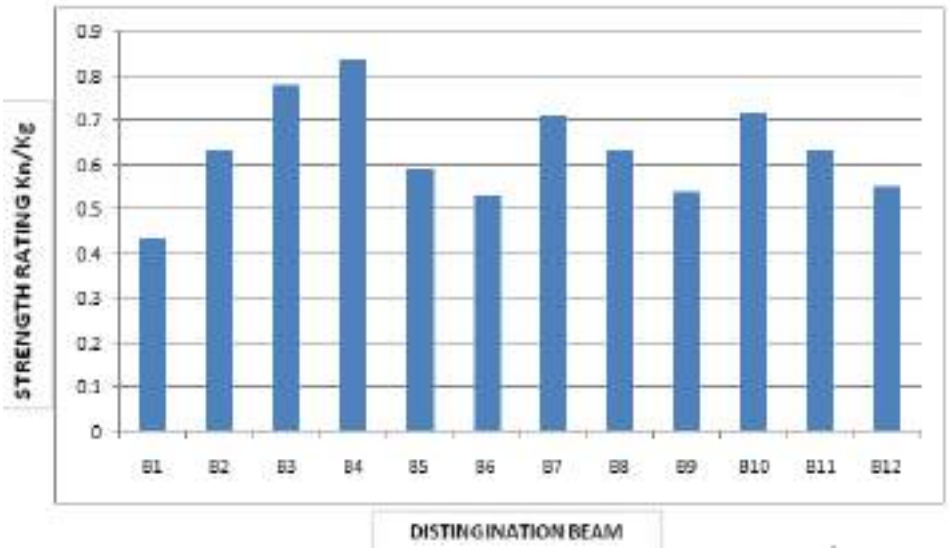

Figure (4-3) Strength rating diagram.

Table (4-1) Strength Rating Results Brevity

No.	Group	Code	Description	Ultimate load Pi, kN	Volume ,m3	Volume reduction ratio	Over all beam weight, kg	Weight reduction ratio	Strength rating*
1	G1	B1	Rectangular section	147	0.1512	0.0	337.9	0.00	0.44
2		B2	T-Section of prismatic flanges (upper limit)	150	0.1071	0.29	239.4	0.29	0.63
3		B3	T-Section of prismatic flanges (lower limit)	136	0.0777	0.48	173.7	0.49	0.78

continued

No.	Group	Code	Description	Ultimate load Pi, kN	Volume,m3	Volume reduction ratio	Over all beam weight, kg	Weight reduction ratio	Strength rating*
4	G2	B4	T-section of Non prismatic flanges	149.5	0.0924	0.47	206.5	0.47	0.84
5		B5	T-section of Non prismatic flanges	143.1	0.1092	0.27	244.06	0.28	0.59
6		B6	T-section of Non prismatic flanges	148	0.129	0.16	281.6	0.17	0.53
7	G3	B7	T-section of Non prismatic flanges	149.4	0.0948	0.52	210.6	0.53	0.71
8		B8	T-section of Non prismatic flanges	155.6	0.1105	0.26	247	0.27	0.63
9		B9	T-section of Non prismatic flanges	150.2	0.1268	0.15	283.4	0.16	0.54
10	G4	B10	T-section of Non prismatic flanges	155.4	0.096	0.36	214.6	0.36	0.72
11		B11	T-section of Non prismatic flanges	158	0.1118	0.25	249.9	0.26	0.63
12		B12	T-section of Non prismatic flanges	155.4	0.1276	0.15	285.1	0.16	0.55

4.5 Flexural Ductility

Evaluating the ductility of reinforced concrete beams is essential in order to avoid a fragile collapse of the structure by ensuring an adequate deformation at ultimate

load [27]. In reinforced concrete beam design, both the flexural strength and flexural ductility must be considered. Although the main concern is usually directed to flexural strength" and only a simple check is done to ensure a satisfied level of section flexural ductility is provided by maintaining the section under reinforced, this does not mean that the flexural ductility is not urgent[30]. From the overall safety view point, flexural ductility is at least as urgent as strength importance [31]. A better attending of ductility could provide the reinforced concrete beam with a better survival chance in case of overloaded, subjected to accidental impact or attacked by a severe earthquake [7].

The flexural ductility is measured in terms of a ductility index, given by:

$$\psi = \Delta u/\Delta y \qquad \ldots\ldots\ldots\ldots\ldots\ldots (4\text{-}2)$$

where:

ψ ductility index, unit less

Δu Maximum deflection corresponding to maximum strength, mm

Δy Deflection corresponding to elastic or yield behavior limit, mm

Table (4-2) exhibits deformation data relate to tested beams, generally all tested specimens of non-prismatic flanged exhibited higher plastic sustainability and more than corresponding control beams B1, B2 and B3. It is seen that at a given constant steel ratio, concrete grade, the ductility index increase for all developed non prismatic flanged beams with respect to control rectangular section B1 of 8.47 ductility index and so with respect to control T-section B2, B3 of considered flange thickness which are of 7.7and 6.31 ductility indexes, while positive measured ductility indexes ranged between 9.08 and 12.56,. For groups2, 3 and 4, assigned ratios ranged between (9.49 -12.56), (9.08-10.59), and (9.44-10.56) , respectively. the same observation depicted in term of plastic deformation upgrading ratio

$\Delta u_i/\Delta u_1$ (i is number of beam)where control rectangular section consider as referred section of the same middle cross section. For 2,3 and 4 groups, assigned ratios ranged between (1.410-1.168), (1.194-1.245), and (1.067-1.219) , respectively; where the minimum upgrading assigned for B12 which is of less volume reduction (15%)and the maximum upgrading assigned for B4 which is of maximum volume reduction (47%) and maximum observed defection, 111 mm.

Fig. (4-4) and (4-5) clearly shows ductility index and plastic upgrading ratio variation of no prismatic flanged beams in comparison of controlled beams B1, B2, and B3.

Table(4-2) Flexural Ductility Results

No.	Group	Code	Description	Ultimate load Pi, kN	Pi/P1	Deflection at elastic level end (Δy) mm	Maximum deflection (Δu) mm	Ductility Index	Δi/Δ1	Failure Mode
1	G1	B1	Rectangular section	147	1.000	9.30	78.74	8.47	1.000	Flexural Mode-Tension failure
2		B2	T-Section of prismatic flanges (upper limit)	150	1.020	10.26	79.00	7.70	1.003	Flexural Mode-Tension failure
3		B3	T-Section of prismatic flanges (lower limit)	136	0.925	8.56	54.00	6.31	0.686	Flexural Mode-Compression failure
4	G2	B4	T-section of Non prismatic flanges	149.5	1.017	8.84	111.00	12.56	1.410	Flexural Mode-Tension failure
5		B5	T-section of Non prismatic flanges	143.1	0.973	9.48	90.00	9.49	1.143	Flexural Mode-Tension failure
6		B6	T-section of Non prismatic flanges	148	1.007	8.76	92.00	10.50	1.168	Flexural Mode-Tension failure

continued

No.	Group	Code	Description	Ultimate load Pi, Kn	Pi/P1	Deflection at elastic level end mm	Maximum deflection mm	Ductility Index	Δi/Δ1	Failure Mode
7	G3	B7	T-section of Non prismatic flanges	149.4	1.016	9.25	98.00	10.59	1.245	Flexural Mode-Tension failure
8		B8	T-section of Non prismatic flanges	155.6	1.059	9.27	94.00	10.14	1.194	Flexural Mode-Tension failure
9		B9	T-section of Non prismatic flanges	150.2	1.022	10.46	95.00	9.08	1.207	Flexural Mode-Tension failure
10	G4	B10	T-section of Non prismatic flanges	155.4	1.057	9.09	96.00	10.56	1.219	Flexural Mode-Tension failure
11		B11	T-section of Non prismatic flanges	158	1.075	9.22	87.00	9.44	1.105	Flexural Mode-Tension failure
12		B12	T-section of Non prismatic flanges	155.4	1.057	8.48	84.00	9.91	1.067	Flexural Mode-Tension failure

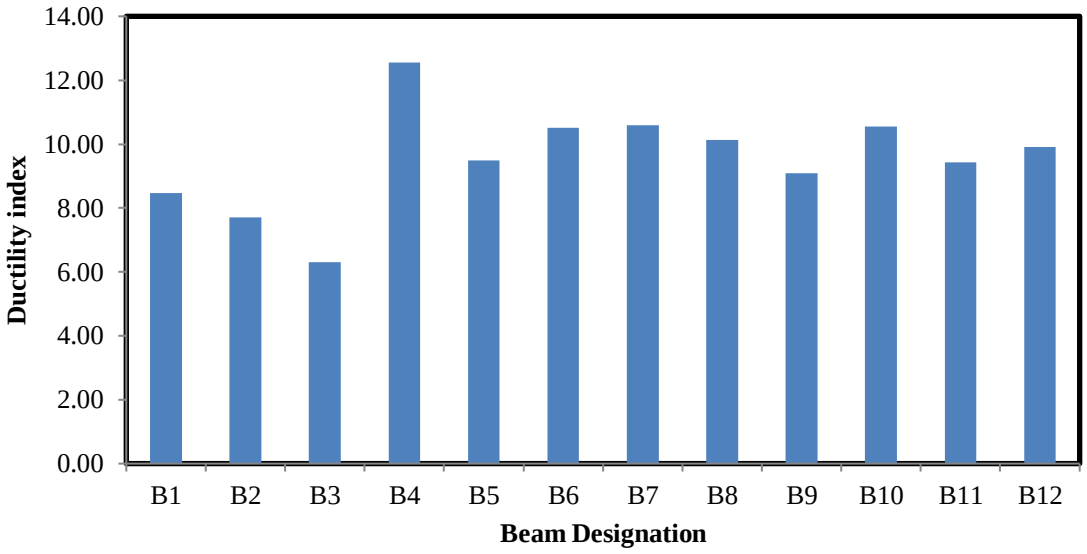

Figure (4-4).Ductility index variation of no prismatic flanged beams in comparison of controlled beams B1, B2, and B3.

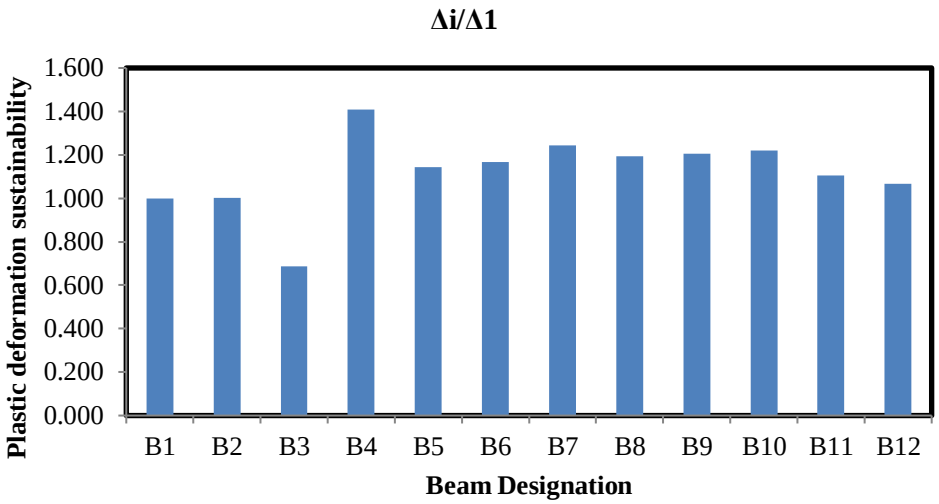

Figure (4-5) plastic upgrading ratio variation of no prismatic flanged beams in comparison of controlled beams B1, B2, and B3.

4.6 Load – Deflection response

During test process, deflection measured in two points along span, the first one is located at mid span length while the second point at 2d distance from mid span. Dial gauges are used to assign corresponding deflections of the beams at different loading stages.

Figs. (4.6) and (4-7) show the load-deflection curves for all tested beams in both locations. Curves clearly depicted that specimen's behavior that is distinguished by three significant portions. The first straight portion exhibits specimens response in elastic range which is of almost identical slope and so identical stiffness for all beams which failed in flexural as tension mode. The second portion represents plastic response that corresponding to strain hardening of providing steel reinforcement and extent to ultimate strength and it is similar trend and different in corresponding load level. The last region is depicted strength sudden dropping after ultimate strength where the section tend to collapse, the last portion obtain as

loading setting turn to displacement control. Figs. (4-6 c) and (4-7 c) assigned load deflection response of B3 which have different behavior where the failure characteristic was compression failure.

Figs. (4-8a and b) illustrates deflection curve at elastic region and at ultimate strength of tested beams along the length of specimens. The figures indicated that elastic curve are identical in spite of different section geometry while the deflection curve at ultimate loading level have significant different, the curves tend to be more smooth and gradual along beam span, that produce the increase of flexural ductility, this observation could be noticed in each group by carry out comparison among (B4, B5, and B6), (B7, B8, and B9), and (B10, B11, and B12) in addition to comparison of all non-prismatic flanged beam curve with respect to these of control group, this observation enhancing that non-prismatic flanged efficiency to upgrade ductility thorough out all flexural beam length.

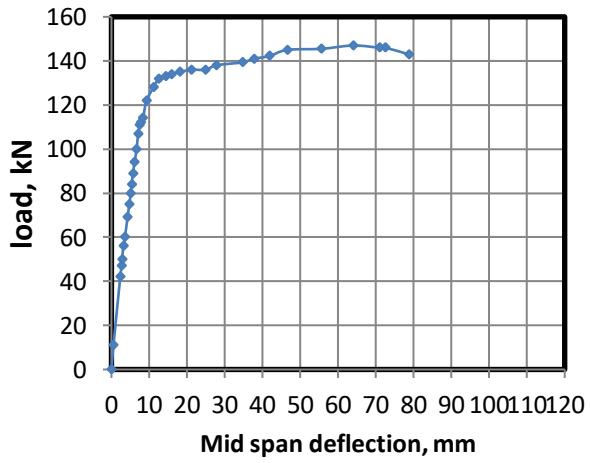

B1

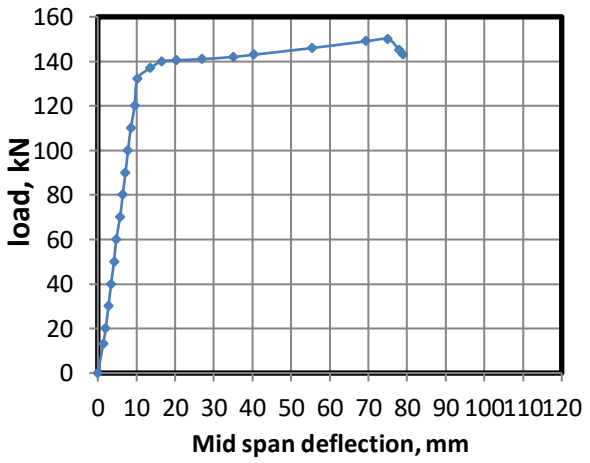

B2

Load –Mid span deflection relationship

continued

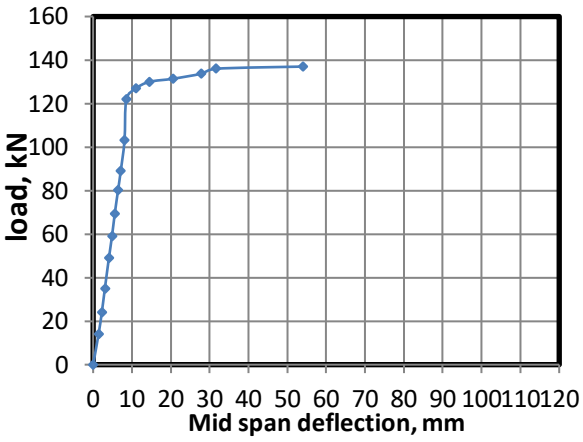

B3

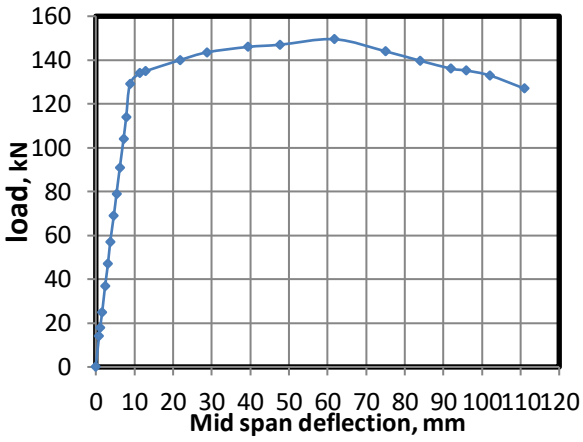

B4

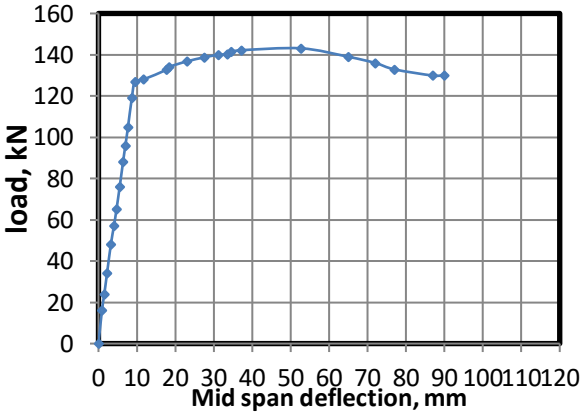

B5

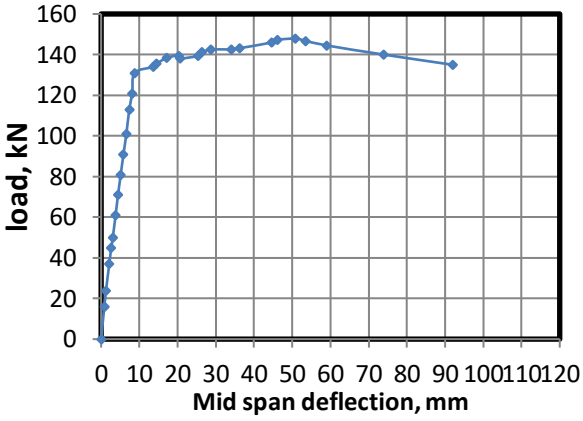

B6

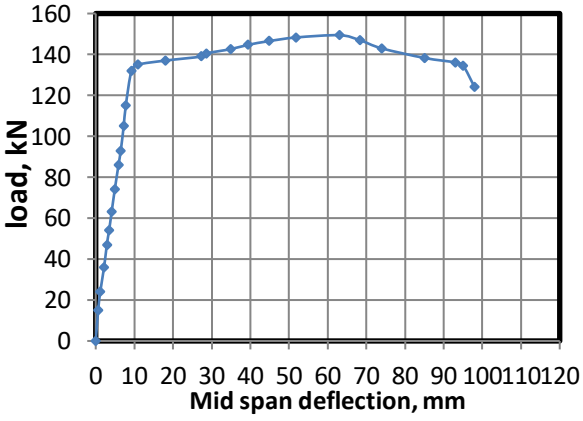

B7

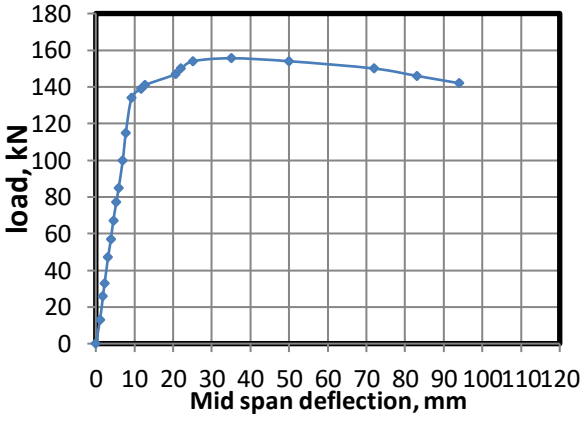

B8

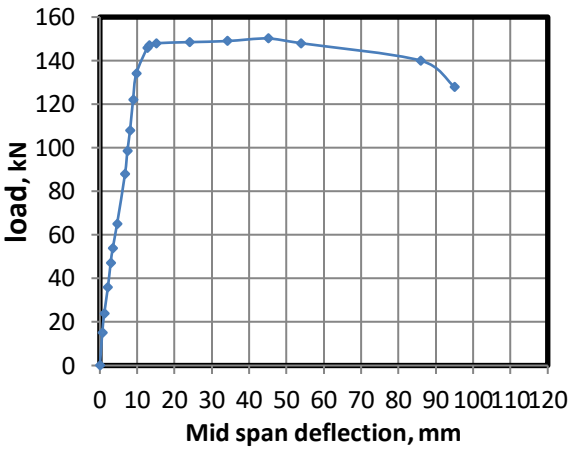

B9

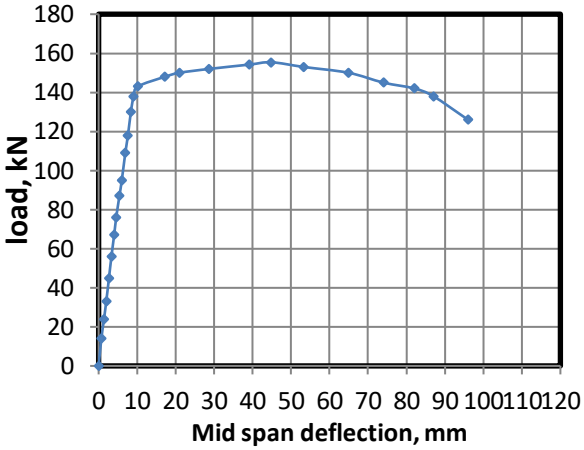

B10

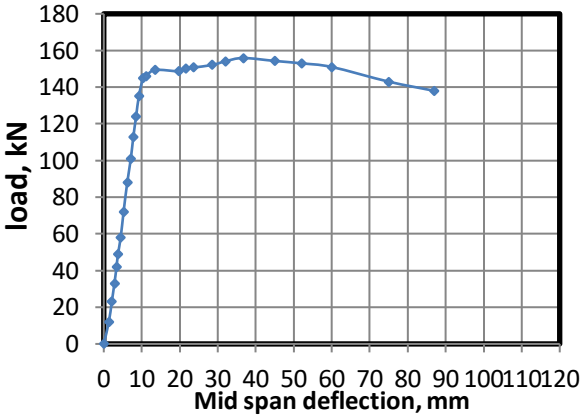

B11

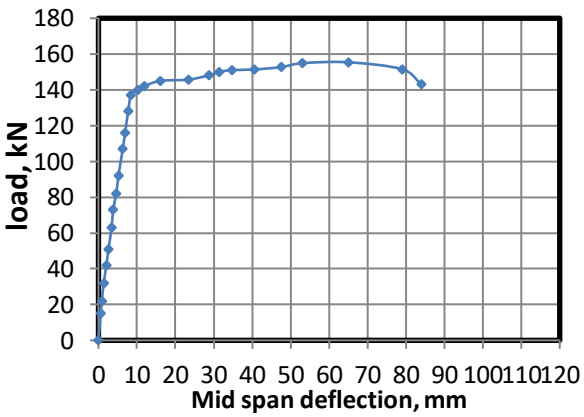

B12

Figure (4-6). Load –Mid span deflection relationship

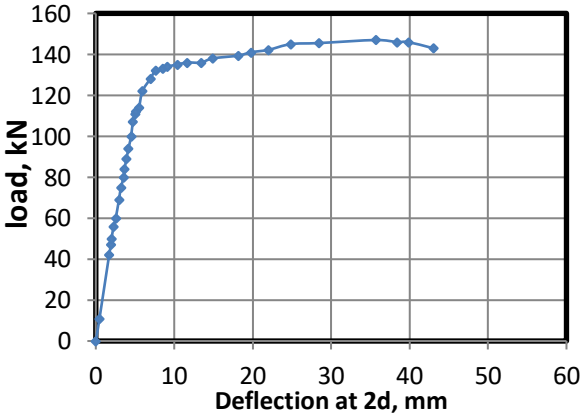

B1

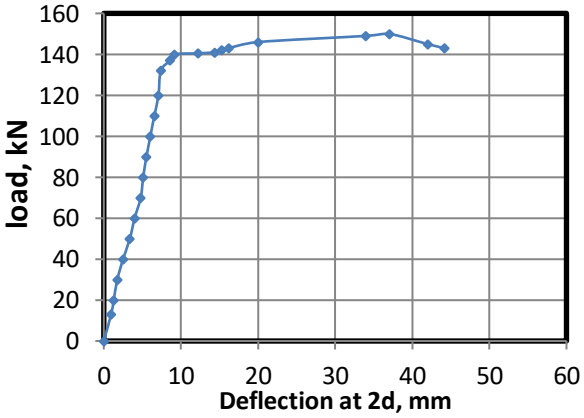

B2

Load -deflection relationships at 2d from midspan

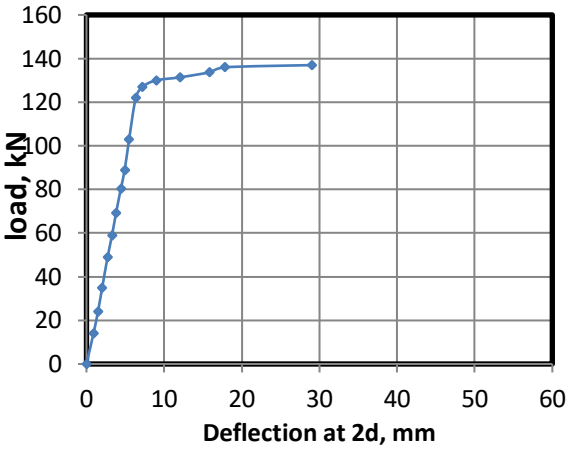

B3

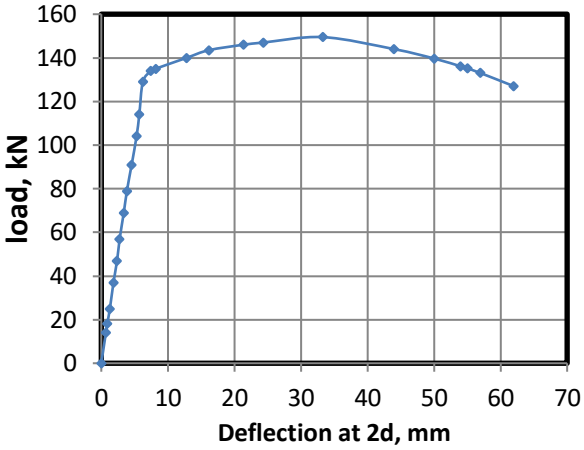

B4

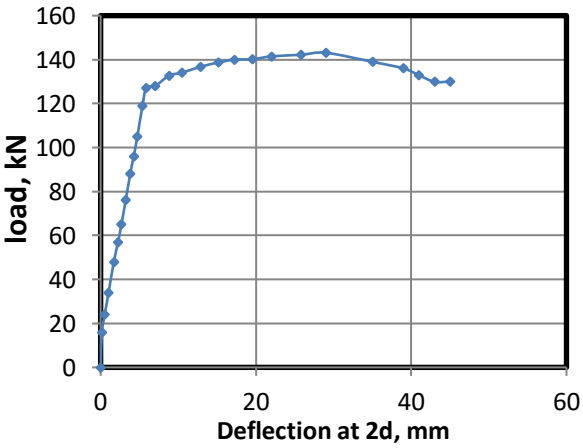

B5

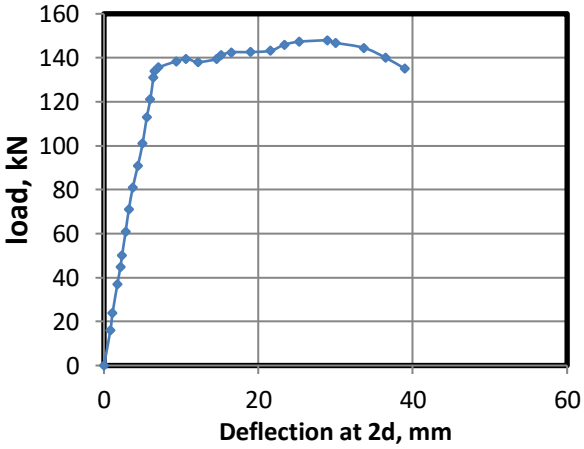

B6

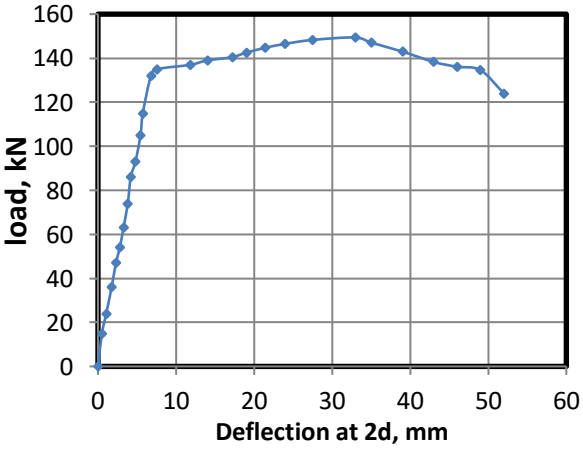

B7

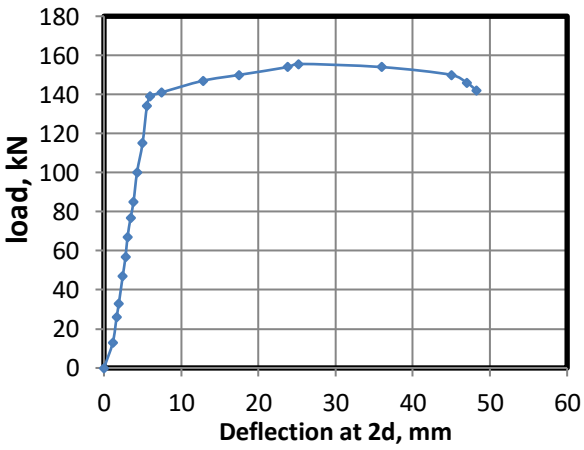

B8

Load-deflection relationships at 2d from midspan

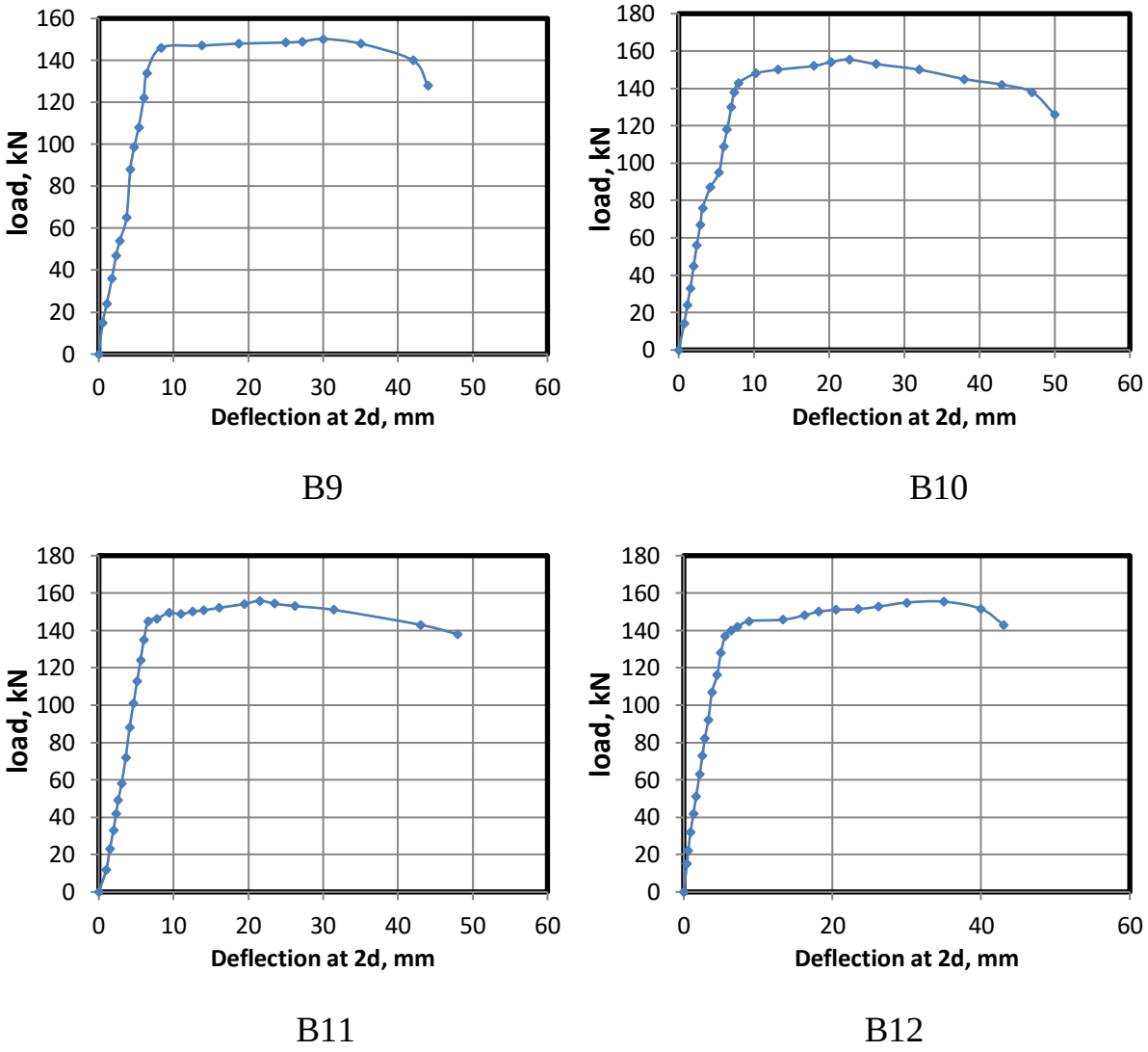

Figure (4-7) Load -deflection relationships at 2d from midspan

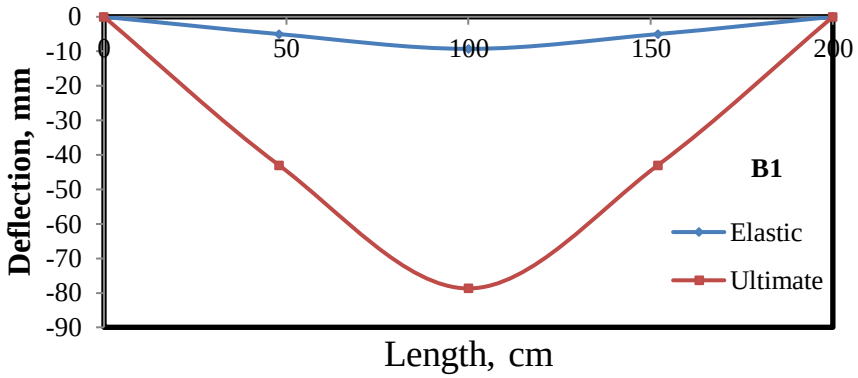

Deflection curve lines of B1

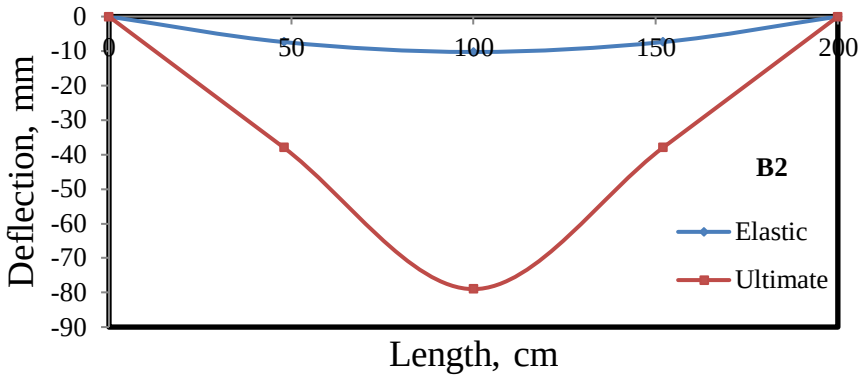

Deflection curve lines of B2

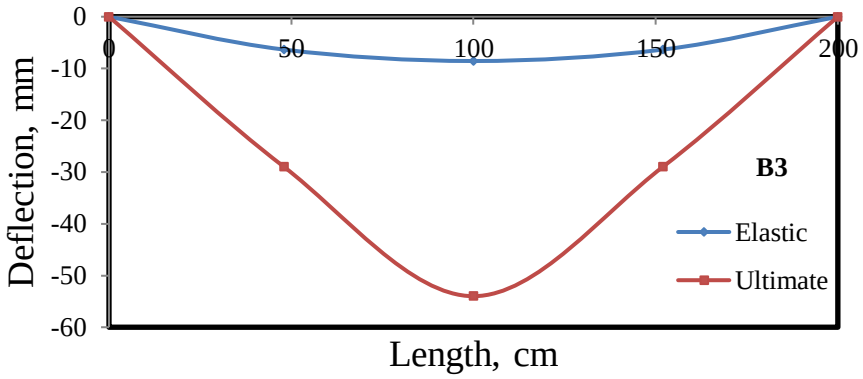

Deflection curve lines of B3

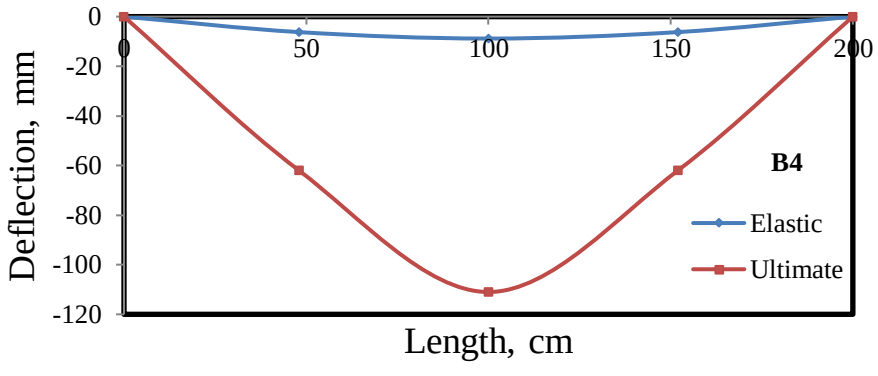

Deflection curve lines of B4

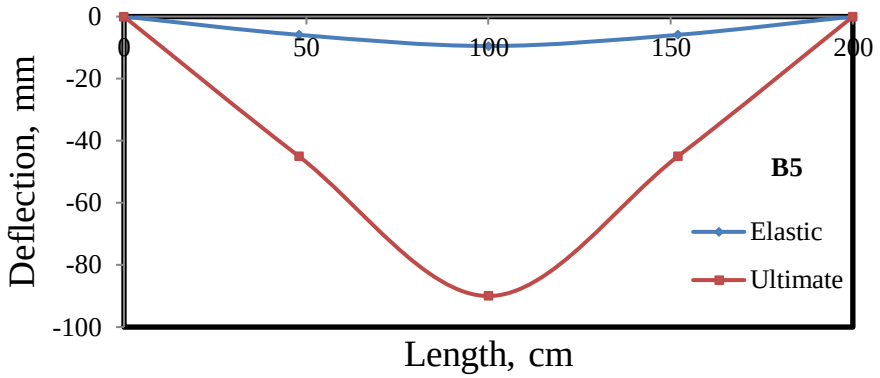

Deflection curve lines of B5

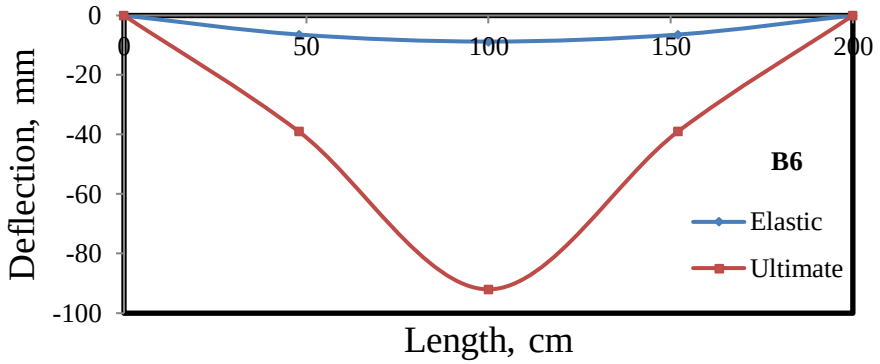

Deflection curve lines of B6

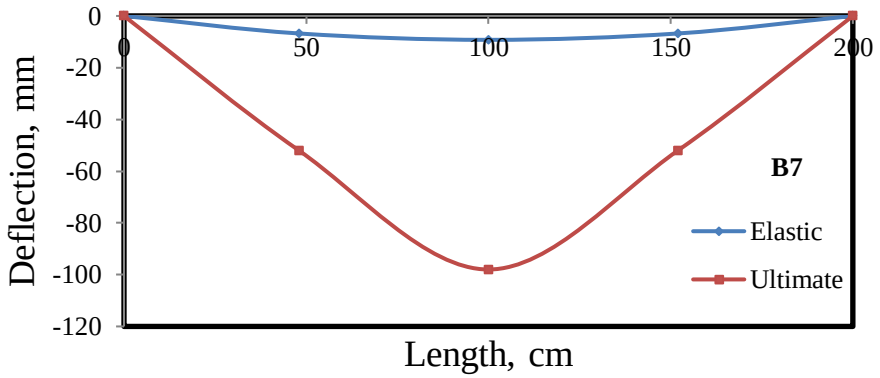

Deflection curve lines of B7

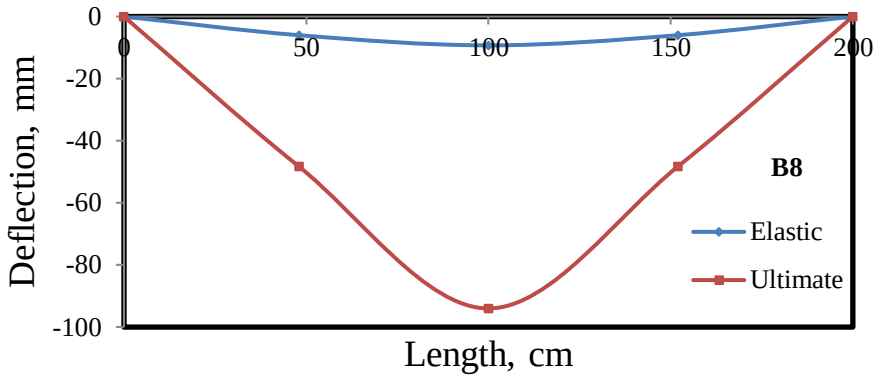

Deflection curve lines of B8

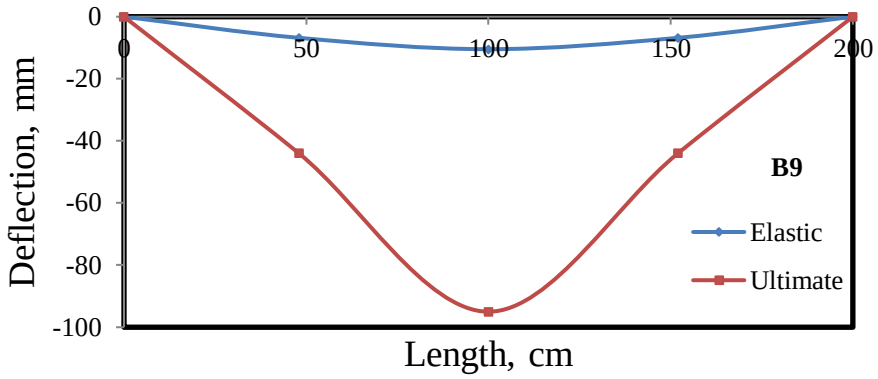

Deflection curve lines of B9

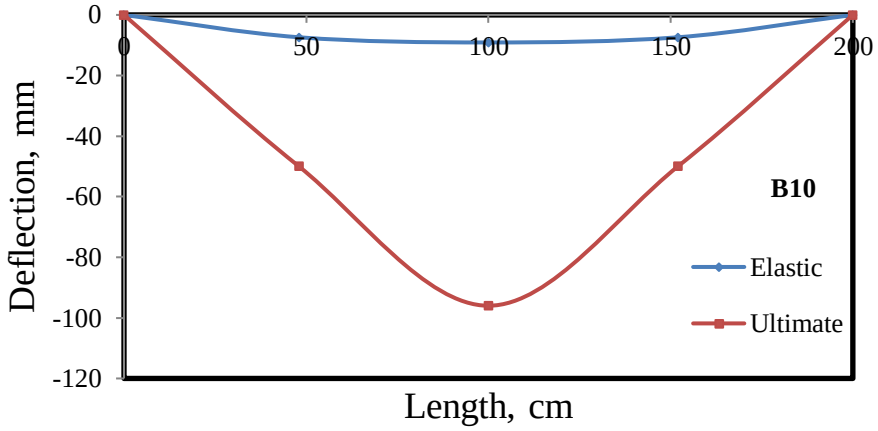

Deflection curve lines of B10

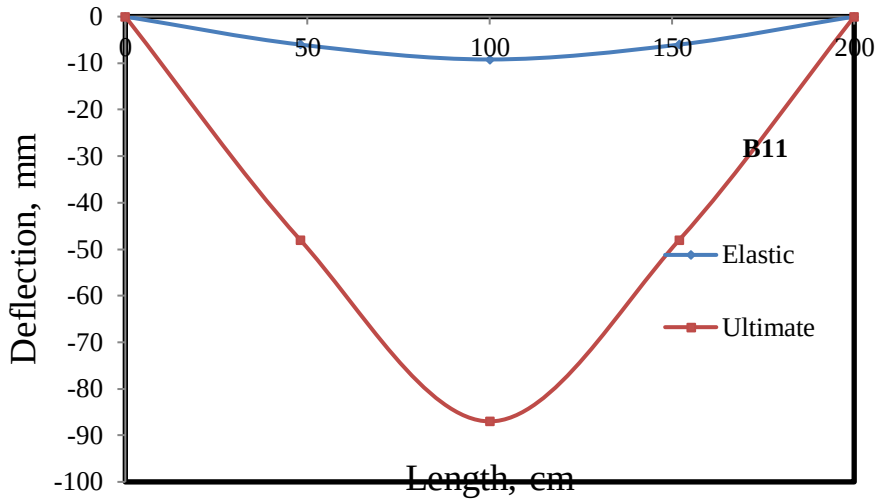

Deflection curve lines of B11

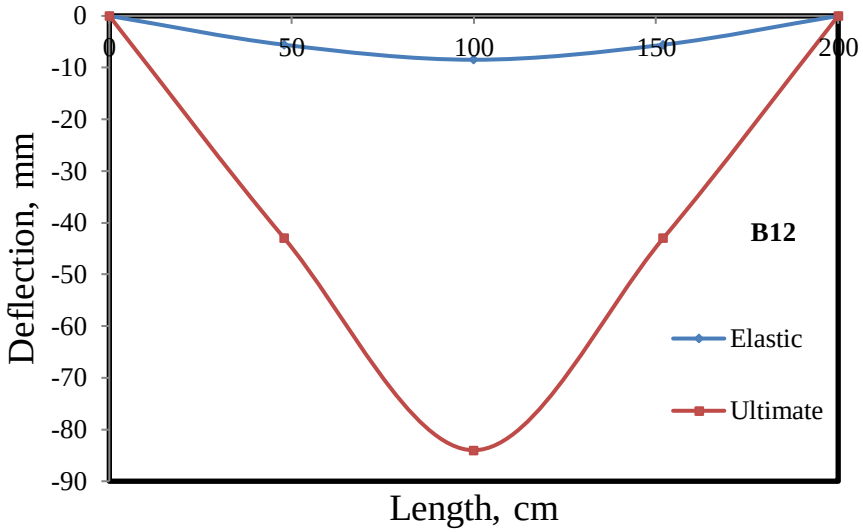

Deflection curve lines of B12

Figure (4-8a) Deflection curve lines

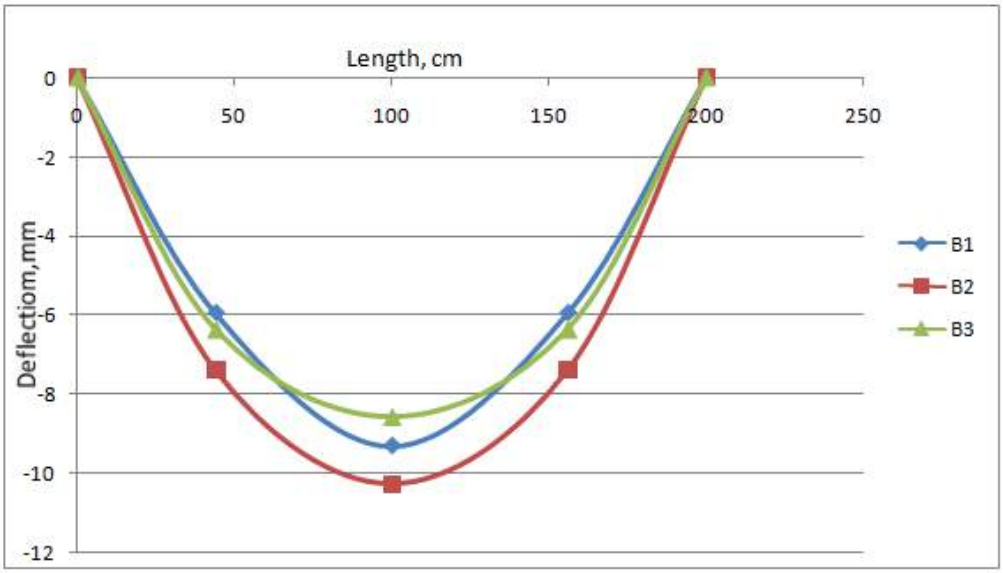

Deflection curve to B1,B2,B3

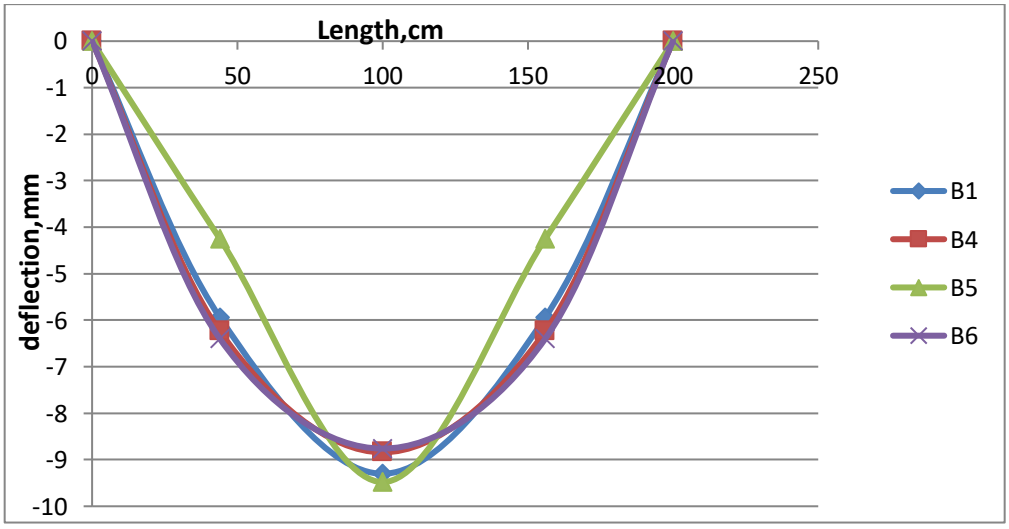

Deflection curve to B1,B4,B5,B6

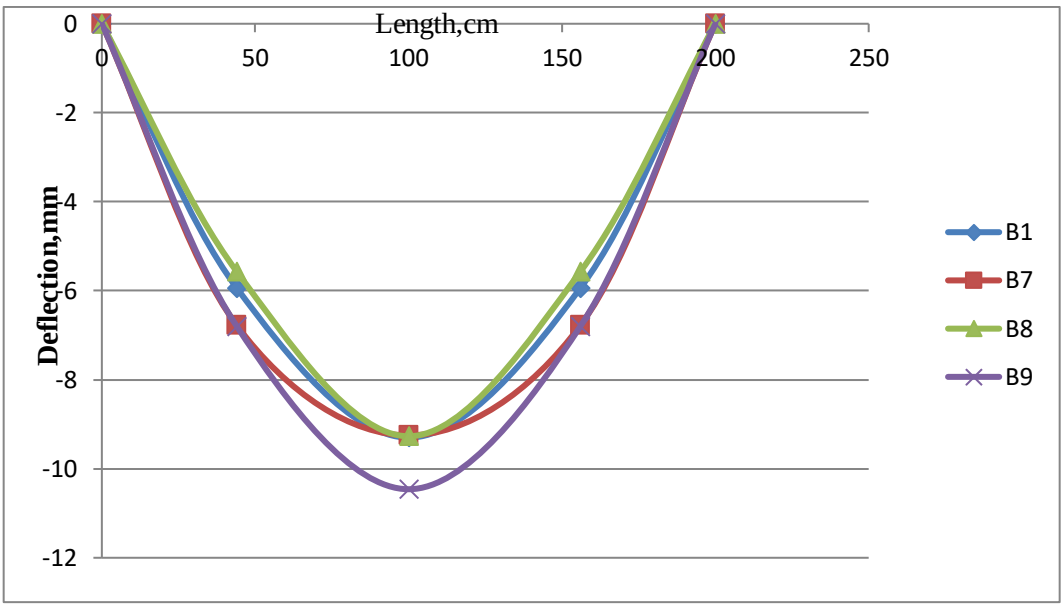

Deflection curve to B1,B7,B8,B9

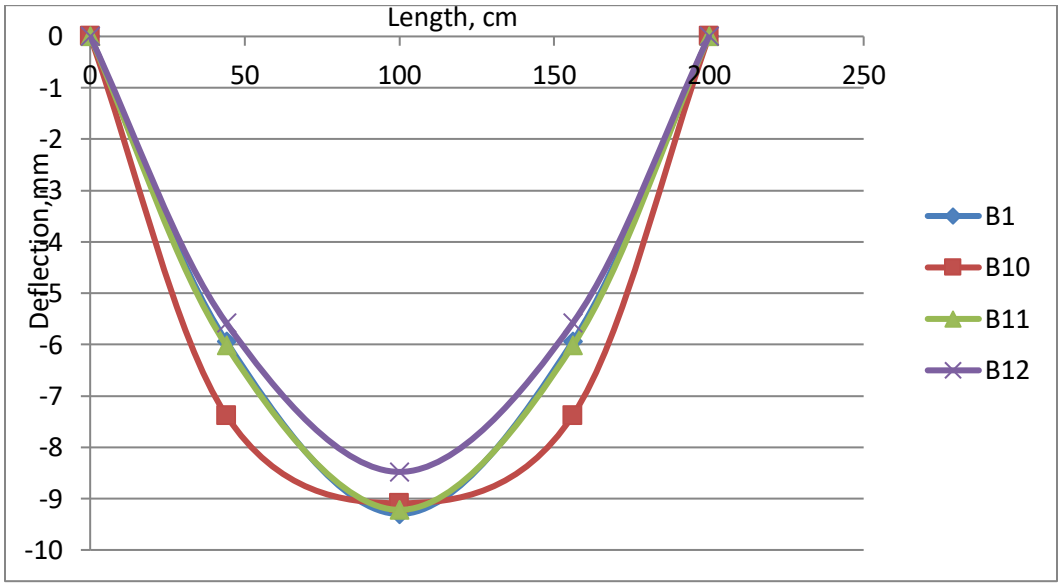

Deflection curve to B1,B10,B11,B12

Figure (4-8b)Deflection curve lines

4.7 Concrete Strains

The readings of concrete strains have been taken by data acquisition system, the positive reading sign refer to tension strain and negative sign refer to compression strain. It was used to measure surface concrete strain for every stage of loading at points located in mid span of beams in compression top adge (point 1) and tension bottom fiber (point 2) as well as along span within d and 2d from mid span point (point 3 and 4). They are measured by using electrical type strain gauges. The concrete strains were measured at every stage of loading, the process of measuring the strain was continued up to the failure of the beams. Fig. (4-9) clearly depicted compressive and tension strain distribution verse applied loading.

From the properties of concrete, the modulus of elasticity Ec could be equal to (27806)(N/mm^2) by using the equation of ACI-318[26]:

$$Ec = 4700\sqrt{f`_c}, \text{ (Mpa)} \qquad \text{……..(4-3)}$$

$f`_c$ is compression strength

for compressive strength obtained by cylinder specimens. So by using Hook`s law

$$E = \frac{\sigma}{\varepsilon} \qquad \text{……(4-4)}$$

The calculations for strain of concrete in tension and compression led to give :

Strain in tension approximately = 0.0001 mm/mm. where concrete strength in tension about ft = 2 N/mm2

Strain in compression approximately = 0.0011 mm/mm. where concrete strength in compression about f'c = 35 N/mm2

So when the reading for tension strains were reached to values limited to above values during the test was indicated that the reinforcement steel nearly to yield and initiate plastic behavior while for concrete when compressive strains were reached to values limited to above it is nearly failed.

For strain in point (1), generally did not reached to limited number in compression (not reached for maximum strain) so the charts were stable value except for B3.

For strain in point (2), generally was reached to limited value in tension and readings were not refer to strain after that (concrete failed in tension, while strain gauge still reading), for that the steel reinforcement yield and flexural bending maintained with gradually spreading of cracks companied with plastic behavior till failure occurring. (The locations of strain gage shown in Fig. (3-20) in chapter three).

For strain in point (3 and 4), generally did not reached to limited value in tension (Not reached for maximum strain) as illustrated in Fig. (4-9)

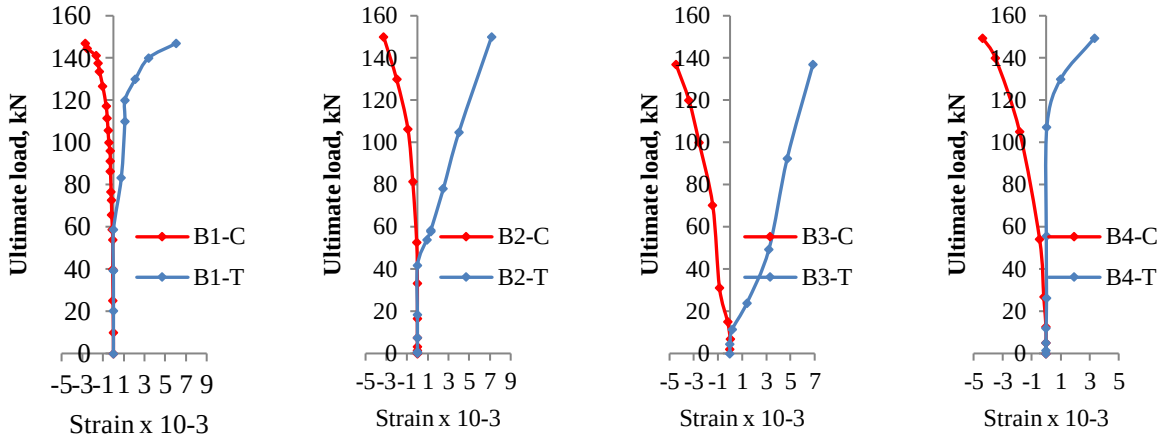

Load-Strain relations of beams B1, B2, B3and B4

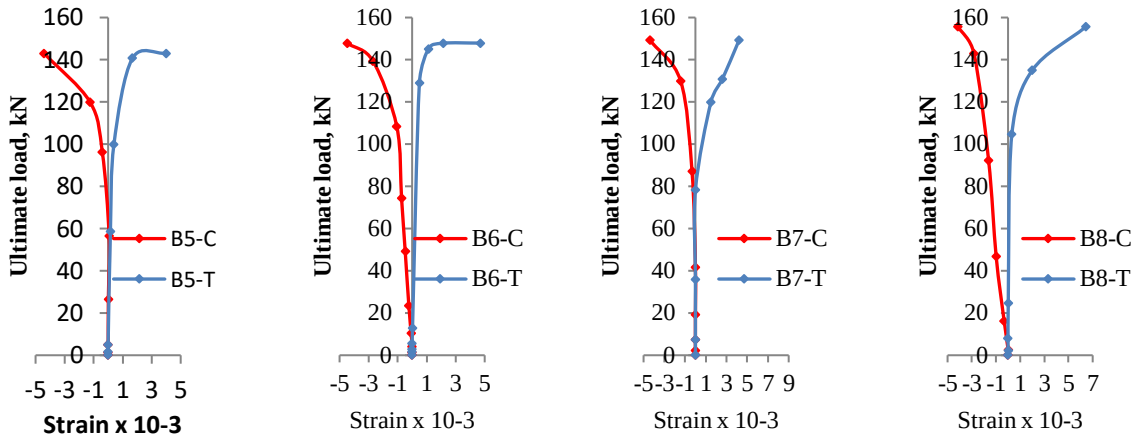

Load-Strain relations of beams B5, B6, B7 and B8

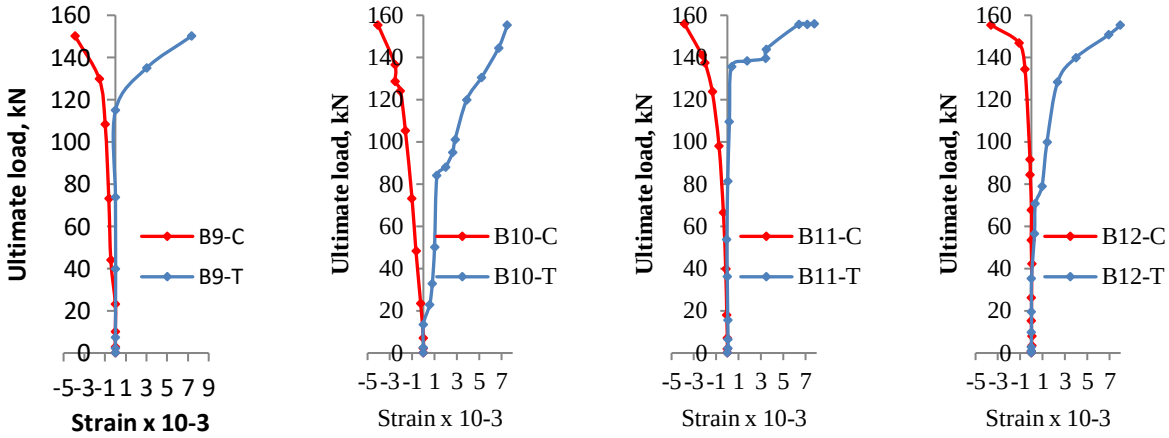

Load-Strain relations of beams B9, B10, B11 and B12

Figure (4-9) Load-Strain relations

4.8 Plastic rotation capacity

The rotation capacity depends mainly on the following [32]:

1. The ultimate strain capacity of concrete, ε'_c, experimental results assigned by stain gauges at upper compression fiber are considered.
2. The length of plastic hinge, lp , along which yielding occurs, in this study it is estimated by measuring plastically deformed region which is characteristic

by maintaining progress cracks after stopping other cracks, and continues toward compressive region.

3. The depth of the compressive block C of concrete at failure which is determined according to ACI concept:

$a = \beta_1 C$, where

β_1 is a function of concrete compressive strength and obtained from

$\beta_1 = 0.85 - 0.008(f'c - 30) \geq 0.65$ for $f'c > 30$ Mp

$$a = \frac{As\ fy}{0.85 f'c\ b} \qquad \text{.....(4-5)}$$

The rotation between any two points A and B of a member can be obtained by integrating the curvatures along the member length [33].

$$\theta_{AB} = \int_A^B \emptyset\, dx \qquad \text{.....(4-6)}$$

where *dx* is a length of an element of the member, and x is the distance of element *dx* from A as show in figure (4-10).

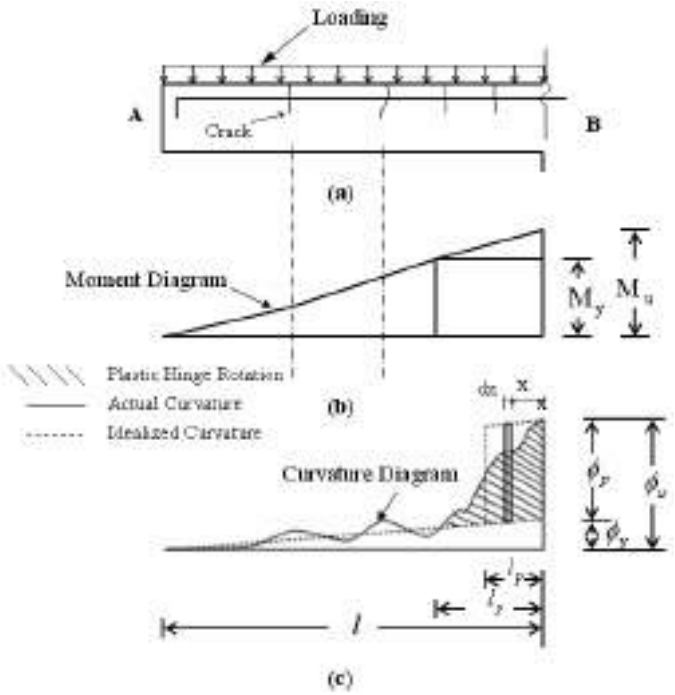

Figure (4-10) Schematic Curvature Distribution along Beam at Ultimate Stage.
(a) Beam, (b) Bending Moment Diagram, (c) Curvature Diagram[34]

For plastically deformed region which is extending in middle region along lp, the plastic rotation capacity (θ) could be estimated as follows:

$$\theta = \frac{\varepsilon p\ lp}{c} \qquad \text{.....(4-7)}$$

$$\theta = \frac{(0.0035 - \varepsilon cy)d}{\lambda d} = \frac{0.0035 - \varepsilon cy}{\lambda} \qquad \text{.....(4-8)}$$

In addition to the elastic rotation at the ultimate stage, the region of inelastic curvature, where the bending moment exceeds the yield moment of the section, is spread over a certain length of beams. In this region the curvature has oscillatory as like mutations because of the increased rigidity of the member between the cracks. However, for convenience, the inelastic area at the ultimate stage can be replaced by an equivalent rectangle of height (φu- φy) and width lp,(lp is the length of plastic hinge), having the same area as the actual inelastic curvature distribution[35]. As depicted in Fig. (4-11) where actual curvature distribution idealized into elastic and inelastic regions .

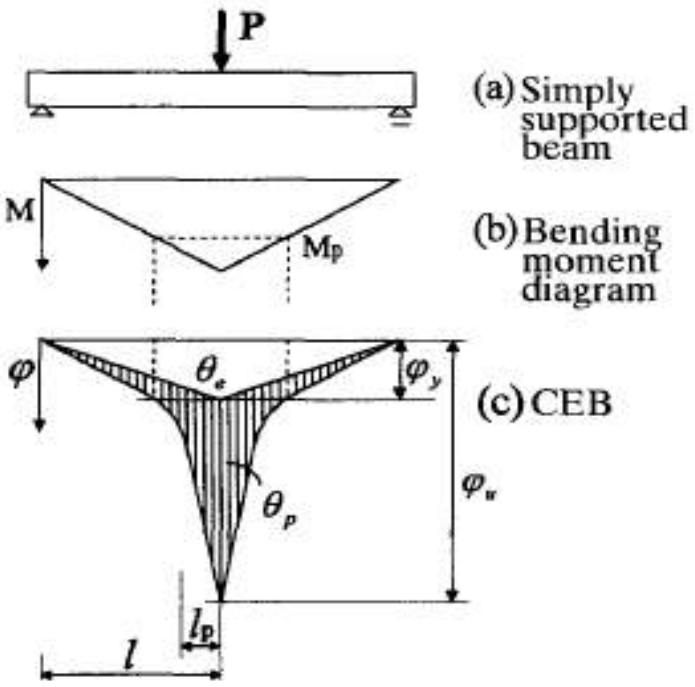

Figure(4-11) Plastic rotation of beam at ultimate states[33]

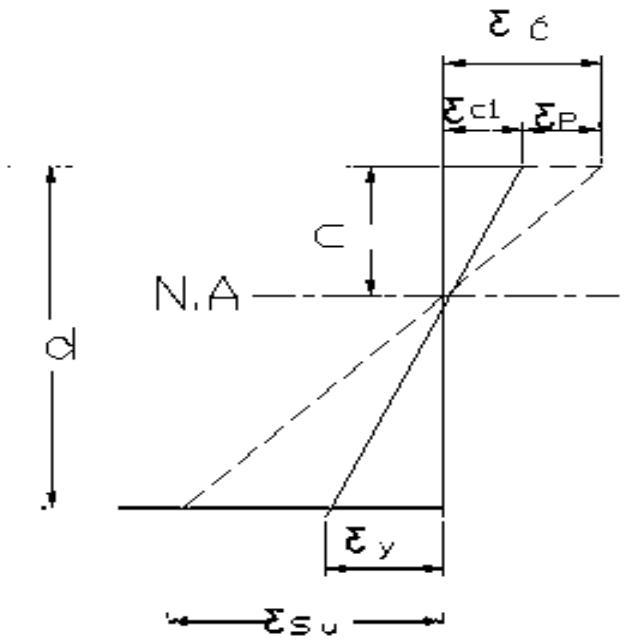

Figure (4-12) Strain diagram[36]

So, curvature and rotation are of particular interest in the plastic region. Hence the plastic rotation to one side of the critical section can be written as:

$$\theta_P = \emptyset_u - \emptyset_y \quad \text{..... (4-9)}$$

The curvatures at first yield of tension steel and at ultimate load of reinforced concrete member are expressed as:

$$\emptyset_y = \frac{fy/ES}{d(1-k)} \quad \text{.....(4-10)}$$

where k is the ratio of depth to centroid compression bars and effective depth

$$\emptyset_u = \varepsilon_{cu} / c \quad \text{.....(4-11)}$$

where ε_{cu} is the ultimate compressive strain of concrete, and c is the depth of the neutral axis at ultimate.

For reinforced concrete flexural members, the plastic deformation is localized in a small zone namely the plastic hinge zone after the yielding of the member. The performance of the plastic hinge zone is critical for flexural members as it governs

the load carrying and deformation capacities of the member. Therefore, plastic hinge has been of great interest to structural designers and researchers for decades [9]. The length of the plastic hinge zone is an important design parameter where intense confinement should be provided to increase the ductility of the member for survival from extreme events such as earthquakes. The behavior of plastic hinges is very complicated due to the high nonlinearity of materials, interaction and relative movement between the constituent materials, and strain localization.

As a result, most researchers investigated the problem through experimental testing, consume the time and cost involved in large tests, but very limited knowledge has been obtained up to date. The concrete ultimate compressive strain, εcu, was selected equal to 0.0078. The most widely used εcu formulations available in the literature were presented in Table (4-3). The values of ε_{cu}=0.0057, ε_{cu}=0.012, and ε_{cu}=0.00645 have been adopted from the works of Baker and Amarakone [37] (see Table 4 -3).

The neutral axis depth, *c*, was determined from the compatibility of the strains at the section. The ultimate curvature is then calculated as the ratio of ultimate concrete compressive strain at the top of beam to the neutral axis depth when the failure of structure occurs, i.e. $\varphi u=\varepsilon cu/c$. The influence of the tension reinforcement index on the ultimate curvature and curvature ductility ratio [30], for

$$\mu = \varphi u/\varphi y \qquad \text{.....(4-8)}$$

From equilibrium conditions of a beam subjected to bending moment, the moment curvature relationship can be obtained as follows[33]:

$$M = \frac{b}{\emptyset}\int_0^{\varepsilon c} fc\ \mathcal{E}c\ d\mathcal{E} + A's\ f's\ (\frac{\mathcal{E}c}{\emptyset d} - k')\,d + A_S f_s\,(1-\frac{\mathcal{E}c}{\emptyset\ d})\,d \qquad \text{.....(4-9)}$$

where εc is the strain of concrete, and k' is the ratio of depth to centroid of compression

bars and effective depth. The curvatures at first yield of tension steel and at ultimate load of reinforced concrete member are expressed as:

$$\emptyset_y = \frac{fy/ES}{d(1-k)} \quad \text{.....(4-10)}$$

$$\emptyset_u = \varepsilon cu \,/c \quad \text{.....(4-11)}$$

Where εcu is the ultimate compressive strain of concrete, and c is the depth of the neutral axis at ultimate. Table (4-3) depicts determined plastic Rotation Capacity

Table (4-3) Rotation Capacity Results Brevity

No.	Group	Code	Description	Moment Capacity kN.m	Ultimate tensile strain x 10^{-3}	Ultimate compressive strain x 10^{-3}	*lp*	ϕ	Rotation Capacity
1	G1	B1	Rectangular section	73.50	6.09	-2.72	428.50	0.00007	0.03182
2		B2	T-Section of prismatic flanges (upper limit)	75.00	7.16	-3.25	453.00	0.00009	0.04024
3		B3	T-Section of prismatic flanges (lower limt)	68.00	6.86	-4.47	N.A	0.00012	N.A
4	G2	B4	T-section of Non prismatic flanged	74.75	3.34	-4.39	536.80	0.00012	0.06442
5		B5	T-section of Non prismatic flanged	71.55	4.02	-4.42	485.70	0.00012	0.05872
6		B6	T-section of Non prismatic flanged	74.00	4.71	-4.49	450.00	0.00012	0.05527
7	G3	B7	T-section of Non prismatic flanged	74.70	4.23	-4.40	557.00	0.00012	0.06704
8		B8	T-section of Non prismatic flanged	77.80	6.43	-4.14	485.70	0.00011	0.05493

No.		Code	Description	Moment Capacity kN.m	Ultimate tensile strain x 10^{-3}	Ultimate compressive strain x 10^{-3}	*lp*	ϕ	Rotation Capacity
9		B9	T-section of Non prismatic flanged	75,10	7.36	-3.90	474.40	0.00011	0.05059
10	G4	B10	T-section of Non prismatic flanged	77.70	7.53	-4.06	540.00	0.00011	0.05997
11		B11	T-section of Non prismatic flanged	79.00	7.76	-3.85	480.00	0.00011	0.05053
12		B12	T-section of Non prismatic flanged	77.70	7.97	-3.62	450.00	0.00010	0.04450

The length of the plastic hinge is an important consideration, as it plays a significant role in the value of the total rotation. Theoretically, plastic rotations exist only at sections with yielded steel. The term ‘plastic hinge’ does not make sense when the steel has not yielded, but the model needs the definition of a length for the critical zone of the beam.

Taking into account these conclusions, which have been confirmed by other researchers, the assumption that the plastic hinge has a length equal to the effective depth of the section seems to be correct.

Euro code 2 makes a reference in Section5.6.3 that supports the proposition of this study, namely that the length of the plastic hinge is approximately 1.2 times the depth of the section. It is important to emphasis that the hypothesis of a constant plastic hinge length, adopted in this study, being an approximation to the actual behavior, is widely accepted as being sufficiently accurate for practical proposes.

In the case of simple bending, the region in study should be divided into small portions with short lengths to enable the evaluation of the influence of the bending moment.

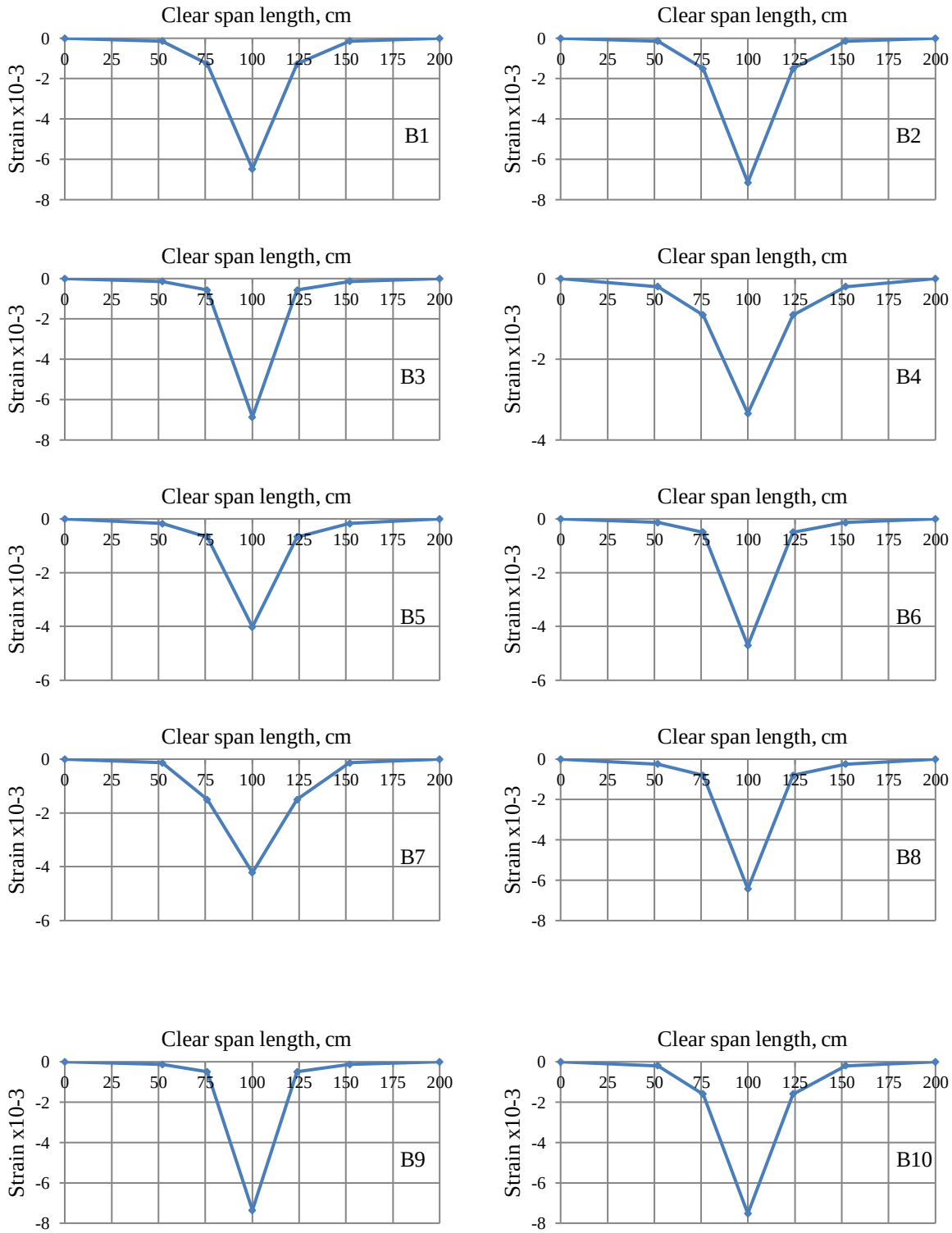

Strain distribution along clear span length for (B, B, B, B4, B5, B6, B7, B8, B9 and B10)

continued

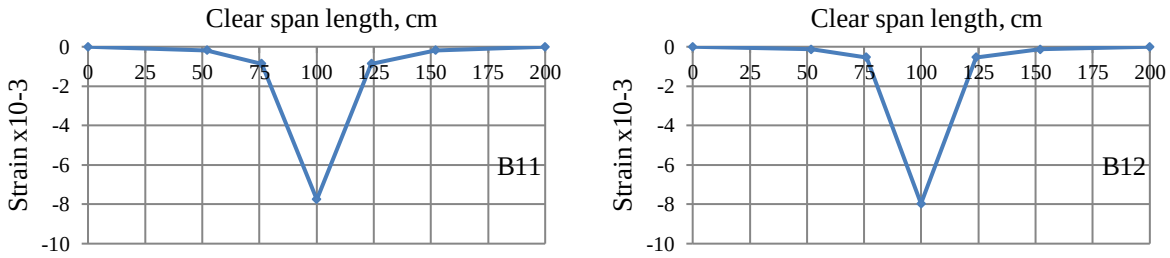

Strain distribution along clear span length for B11 and B12

Figure (4-13) Strain distribution along clear span length

4.9 Failure Modes

In all tests the load recorded by test machine dropped suddenly with increasing deflection when the specimens reach failure. The maximum load recorded by the machine was considered as the ultimate load. The failure modes for the tested composite beams are summarized in Table (4-4) and Fig. (4-14) shows typical failed specimens under test setting, Fig. (4-15) shows all tested beam sets while Fig. (4-16) reveal the beams after failure.

At early stages of loading, the deformations were initially within the elastic ranges (linear), then the applied load was increased until the first crack became visible which was observed in the maximum moment region under applied load. As the load was increased further, several flexural cracks initiated in the tension face at intervals throughout the beam, gradually increased in number, became wider and moved upwards reaching the compression face of the beam. For control specimens initiated cracks limited in approximately middle point which is corresponding to maximum moment while for developed section initiative cracks started within middle region which is corresponding to range of proportional moments.

For control specimens B1 and B2 one or two cracks start to widen more than the others, forming critical cracks where for developed section two or more than two cracks started to widen.

As the load was increased further, a loss of stiffness occurred and one mode of failure appeared which can be classified as flexural failure in tension by yielding of the steel reinforcement followed by crushing of concrete.

generally, Flexural cracks develop when the stress at the extreme tension fibers exceeds the modulus of rupture of concrete. Main cracks develop which caused by the difference in strains in steel and concrete at the section considered. First cracks initiated at mid span then spread gradually to both size till significant plastic deformation attaint where spreading stopped and cracks within middle region which is corresponding to plastic hinge progress to developed toward loading point as compression block decreased. This observation which is characteristic by tension failure mode is recorded for all tested beams except B3 which failed by flange Buckling compression mode.

Table(4-4) Failure modes

No.	Designation	Code	Description	Failure Mode	Configuration
1	G1	B1	Rectangular section	Flexural Mode- Tension failure	Fig. 4-16, B1
2		B2	T-Section of prismatic flanges (upper limit)	Flexural Mode- Tension failure	Fig. 4-16, B2
3		B3	T-Section of prismatic flanges (lower limit)	Flexural Mode- Flange Buckling Compression failure	Fig. 4-16, B3
4	G2	B4	T-section of Non prismatic flanges	Flexural Mode- Tension failure	Fig. 4-16, B4

No.		Code	Description	Failure Mode	Configuration
5		B5	T-section of Non prismatic flanges	Flexural Mode- Tension failure	Fig. 4-16, B5
6		B6	T-section of Non prismatic flanges	Flexural Mode- Tension failure	Fig. 4-16, B6
7	G3	B7	T-section of Non prismatic flanges	Flexural Mode- Tension failure	Fig. 4-16, B7
8		B8	T-section of Non prismatic flanges	Flexural Mode- Tension failure	Fig. 4-16, B8
9		B9	T-section of Non prismatic flanges	Flexural Mode- Tension failure	Fig. 4-16, B9
10	G4	B10	T-section of Non prismatic flanges	Flexural Mode- Tension failure	Fig. 4-16, B10
11		B11	T-section of Non prismatic flanges	Flexural Mode- Tension failure	Fig. 4-16, B11
12		B12	T-section of Non prismatic flanges	Flexural Mode- Tension failure	Fig. 4-16, B12

Figure (4-14) Typical failed specimens under test setting

Figure (4-15) Tested beam sets

Photo Overall tested specimens

B1

Mode failure of beams

B2

B3

B4

Mode failure of beams

B5

B6

B7

Mode failure of beams

B8

B9

B10

Mode failure of beams

B11

B12

Photo 4.Failure, Figure(4-16) Mode Exhibition of Tested Beams

Chapter Five

Conclusions and Recommendation

Chapter five

CONCLUSIONS AND RECOMMENDATIONS

5-1 Conclusions

Non prismatic flanged sections are developed and considered in this study to investigate their flexural strength, strength rating, flexural stiffness, flexural ductility and plastic rotational capacity. The strength and deformation characteristics of such members for both elastic and inelastic analysis were determined in adopted experimental program, and the following points have been assigned;

1. For developed non-prismatic flanged beams, the experimental results confirmed the upgrading strength rating, flexural ductility, and rotation capacity without significant effect upon ultimate load capacities, stiffness, and load deflection behavior.
2. The assigned ultimate capacity of non-prismatic section exhibited slightly increment in spite of they have the same middle cross section, the ultimate load ratio in respect to rectangular beam, the large ratio indicated is 1.057, These observations in the minimum limit confirming that the developed section maintains ultimate strength with slightly increment.
3. With regard to the important topic in this research; developed non-prismatic flanged section exhibits higher strength rating in comparison with related rectangular control beam section.
4. From the overall safety view point, flexural ductility is at least as urgent as strength importance in case of overloaded, generally all tested specimens of non-prismatic flanged exhibited higher plastic sustainability deformation and

more than corresponding control rectangular or ordinary Tee beams although all have constant steel ratio and same concrete grade.

5. Deflection curve lines at elastic region indicate that elastic curve lines are identical in spite of different section geometry while the deflection curve lines at ultimate loading level have significant different and flexural ductility increased in the three group of non-prismatic flanged beam in addition to comparison of all non-prismatic flanged beam curve lines in respect to these of control group, this observation enhancing that non-prismatic flanged efficiency to upgrade ductility thorough out non-prismatic flanged flexural element length.
6. The comparison of measured tensile strains with limit values indicated that; the reinforcement steel nearly to yield and initiate plastic behavior, while the measured compressive strain in point (1), did not reached to limited value in compression hence the responses were steady except for B3, while tensile strain in point (2), reached to limited value in tension and readings were not refer to strain after that (concrete failed in tension, while strain gauge still reading), for that the steel reinforcement yield and flexural bending maintained with gradually spreading of cracks companied with plastic behavior till failure occurring while strains in point (3 and 4), did not reached to limited value in tension.
7. The determined plastic rotation capacity in non-prismatic specimens (with corresponding plastic hinge length increment) improved in comparison with those of control specimens of rectangular or T sections, the best improvement assigned in group 2 of moderate web thickness (140 mm) while non-prismatic trend of entire length (Lfm=0) assigned as best mode in comparison with other modes of (Lfm =d or 2d) in all groups where the reinforcement steel bars are yielding in more progressive, the applied load

increases, the yielding affects the initial section and, more extensional neighboring sections.

8. As the load was increased further, a loss of stiffness occurred and one mode of failure appeared which can be classified as flexural failure in tension mode which is characteristic by yielding of the steel reinforcement followed by crushing of concrete. This observation which is assigned as tension failure mode is recorded for all tested beams except B3 which failed by flange buckling compression mode.

5-2 Recommendations

1. The further work require to develop Non prismatic flanged beam using hybird materials.
2. Different grade of strength of concrete can be studied to investigate the effect of diversity on the flexural strength, ductility and rotation capacity.
3. Shear capacity could be investigated in short span of Non prismatic flanged beam.
4. Non prismatic flanged beams of curve tapered could be consider.

References

Reference

[1] Hodeges, C. and Schwartz, B. T. , " Optimization in desgn", 2010.

[2] Computational Mechanics & Advanced Materials Group.

[3] Haluk S. "Reinforced Concrete Structures" 2012,pp.68-70.

[4] James K. Wight, "Reinforcement concrete, mechanics and design", 2005,pp,105-172.

[5] James, K. W., " Reinforced concrete, mechanics and design" F.E.Richart, Jr. Collegiate professor, Departement of civil & Environmental Engineering, University of Michign, 2005.

[6] Romano, F., "Deflections of Timoshenko beam with varying cross-section," International journal of mechanical sciences, vol. 38, pp. 1017-1035, 1996.

[7] Nadim, H. and Al- Manaseer, K., Structural concrete: theory and design: John wiley& sons, 2020.

[8] Kong and Evans, "Reinforced and Pre stressed Concrete".

[9] Zhao, X., Wu, Y. F., A. Yt. Leung, A. Y. and Lam, H. F., "Plastic hinge length in reinforced concrete flexural members," Procedia Engineering, vol. 14, pp. 1266-1274, 2011.

[10] Iraqi Standards No.45/1984, , "Aggregate from Natural Sources for Concrete and Construction", Ministry of Housing and Construction, Baghdad, 2004.

[11] Product data Sheet, "SikaFume®-HR, Concrete Additive", Lebanon, PP. 1−2.

[12] ASTM C33-2003, "Standard Specification for Concrete Aggregates", Vol. 4.2, 2003, PP. 1−11.

[13] B.S. 882 : 1992, "Specification for Aggregates from Natural Sources for Concrete", Dec.1992, PP. 1−9.

[14] Central Organization for Standardization and Quality Control, "Iraqi Standard Specification (IQS) No.1703/1992 Water used in concrete" ,Baghdad, Iraq.

[15] ASTM C494/C494M-1999a, "Standard Specification for Chemical Admixture for Concrete", Vol. 4.2, 1999, PP. 1−9.

[16] ASTM A615/A615M-04b, "Standard Specification for Deformed and Plain Carbon Steel Bars for Concrete Reinforcement ", 2004, PP. 1−6.

[17] ASTM C143/C143M-2003, "Standard Test Method for Slump of Hydraulic-Cement Concrete", Vol. 4.2, 2003, PP. 1−4.

[18] Arturo Tena-Colunga, "Stiffness formulation for nonprismatic beam elements," Journal of Structural Engineering, vol. 122, pp. 1484-1489, 1996.

[19] ASTM C39/C39M-2003, "Standard Test Method for Compressive Strength of Cylindrical Concrete Specimens", Vol. 4.2, 2003, PP. 1−5.

[20] B.S. 1881 : Part 116: 1983, "Methods for Determination of Compressive Strength of Concrete Cubes", January 1983, PP. 1−8.

[21] ASTM C496/C496M-04, "Standard Test Method for Splitting Tensile Strength of Cylindrical Concrete Specimens", Vol. 4.2, 2004, PP. 1−5.

[22] ASTM C78, " Standard Test Method for Flexural Strength of Concrete", American Society for Testing and Materials, (2002), (42) Env

206, Concrete-part 1, Specification, performance, production and conformity, European Standard, 1992.

[23] ASTM C469-02, "Standard Test Method for Static Modulus of Elasticity and Poisson's Ratio of Concrete in Compression", Vol. 4.2, 2002, PP. 1−5.

[24] ASTM C78-02, "Standard Test Method for Flexural Strength of Concrete (Using Simple Beam with Third-point Loading)", Vol. 4.2, 2002, PP. 1−3.

[25] ACI Committee-318, "Building Code Requirements for Structural Concrete (ACI 318M-14) and Commentary", American Concrete Institute, Farmington Hills, MI 48331, USA, 2019.

[26] ACI Committee-318, "Building Code Requirements for Structural Concrete (ACI 318-99) and Commentary (ACI 318R-99)", American Concrete Institute, Detriot, USA, 1999.

[27] Latifee, E. R., "Design and analysis of T and inverted L beams-Theory and Examples " Reference Book: Design of Reinforced Concrete by Jack C. McCormac and Russell H. Brown, Clemson University, 9th Edition, 2014, pp 1-14.

[28] ACI Committee 435, "Deflection of Reinforced Concrete Flexural Members", ACI Journal, Proc. Vol. 63, No. 6, June 1966, PP. 637−674.

[29] Tliouine, B. and Fedghouche, F., "Optimal Design of Reinforced Concrete T-Beams under Ultimate Loads," in 2nd International Conference on Engineering Optimization, 2010.

[30] Kwan, A. K. H., Ho, J. C. M. and Pam, H. J., "Flexural strength and ductility of reinforced concrete beams," Proceedings of the Institution of Civil Engineers-Structures and Buildings, vol. 152, pp. 361-369, 2002.

[31] Kwan, A. K. H., Ho, J. C. M. and Pam, H. J., "Effects of concrete grade and steel yield strength on flexural ductility of reinforced concrete beams," Australian Journal of Structural Engineering, vol. 5, pp. 1-20, 2004.

[32] Hillerborgi, A"Fracture mechanics concepts applied to moment capacity and rotational capacity of reinforced concrete beams," Engineering Fracture Mechanics, vol. 35, pp. 233-240, 1990.

[33]] Ko,M. Y., Kim, S. W. and Kim, J. K. "Experimental study on the plastic rotation capacity of reinforced high strength concrete beams," Materials and Structures, vol. 34, pp. 302-311, 2001.

[34] Ali Kheyroddin, A. and Naderpour, H., "Plastic hinge rotation capacity of reinforced concrete beams," 2007.

[35] Lee, J. Y. and Watanabe, F., "Predicting the longitudinal axial strain in the plastic hinge regions of reinforced concrete beams subjected to reversed cyclic loading," Engineering Structures, vol. 25, pp. 927-939, 2003.

[36] Kwan, A. K. H. and AU, F. T. K., "Flexural strength–ductility performance of flanged beam sections cast of high-strength concrete," The Structural Design of Tall and Special Buildings, vol. 13, pp. 29-43, 2004.

[37]] Baker, G., " Exact deflection in non prismatic members", St Lucia, Queensland 4067,Australia,1995.

[38] Romano, F., "Deflections of Timoshenko beam with varying cross-section," International journal of mechanical sciences, vol. 38, pp. 1017-1035, 1996.

[39] Mohammad, D. and AL-Sadder S., "A new technique for large deflection analysis of non-prismatic cantilever beams," Mechanics Research Communications, vol. 32, pp. 692-703, 2005.

[40] Veiskarami, M. and Pourzeynali, S., "Green's function for the deflection of non-prismatic simply supported beams by an analytical approach," Estonian Journal of Engineering, vol. 18, 2012.

[41] Beltempo,A. , Balduzzi, G., Alfano, G. and Auricchio, F., "Analytical derivation of a general 2D non-prismatic beam model based on the Hellinger–Reissner principle," Engineering Structures, vol. 101, pp. 88-98, 2015.

[42] Fertis, D. G. ASCE, and Keene, M. E., "Elastic and inelastic analysis of nonprismatic members," Journal of Structural Engineering, vol. 116, pp. 475-489, 1990.

[43] Stefanou, G. D., "Shear resistance of reinforced concrete beams with non-prismatic sections," Engineering Fracture Mechanics, vol. 18, pp. 643-666, 1983.

[44] Rinaldi, Z. Grimaldi, A. and Galli, G., "Ductility of RC beams reinforced with FRC," in 13th World conference on earthquake engineering, Vancouver, BC, Canada, August, 2004, pp. 1-6.

[45] Ferreira, C. C., Barros, M. and Barrosand, A. F., " Optimal design of reinforced concrete T-Sections in bending", 2002, PP951-964.

[46] Ayres, C., "16 Advantages and Disadvantages of Beam Bridges", Crystal Ayres has served as editor-in-chief the site of Kuora for the five years, May 16 2019.

[47] Shao-Yeh, M. M., Vitelmo V. B. and Egor P. P Experimental and analytical studies on the hysteretic behavior of reinforced concrete rectangular and T-beams: Earthquake Engineering Research Center, College of Engineering, University …, 1976.

[48] Wickline, J. E., "A Study of Effective Moment of Inertia Models for Full-Scale Reinforced Concrete T-Beams Subjected to A Tandem-Axle Load Configuration," ENGINEER RESEARCH AND DEVELOPMENT CENTER VICKSBURG MS GEOTECHNICAL …2003.

[49] A. Deifalla, A. and Ghobarah A. D., "Behavior and analysis of inverted T-shaped RC beams under shear and torsion," Engineering structures, vol. 68, pp. 57-70, 2014.

[50] Ismael, M. A. Hisham M. Al-Hassani, H. M. and Al-Kafaji, J. M. "Flexural Behavior of Reactive Powder Concrete Tee Beams," Journal of Engineering and Sustainable Development, vol. 18, pp. 20-35, 2014.

[51] Al-Hassani, H. M., Al-Kafaji, J. M. and Ismael, M. A"Flexural Behavior of Hybrid Tee Beams (Containing Reactive Powder Concrete and Normal Strength Concrete)," Journal of Engineering and Sustainable Development, vol. 19, pp. 123-140, 2015.

[52] do Carmo, R. N. F., Lopes, S. M. R. and Bernardo, L. F. A. "Theoretical model for the determination of plastic rotation capacity in reinforced concrete beams," Structural Concrete, vol. 4, pp. 75-83, 2003.

[53] Carpinteri, A. and Corrado, M., "Dimensional analysis approach to the plastic rotation capacity of over-reinforced concrete beams," Engineering Fracture Mechanics, vol. 77, pp. 1091-1100, 2010.

APPENDEX (A)

Design the beams

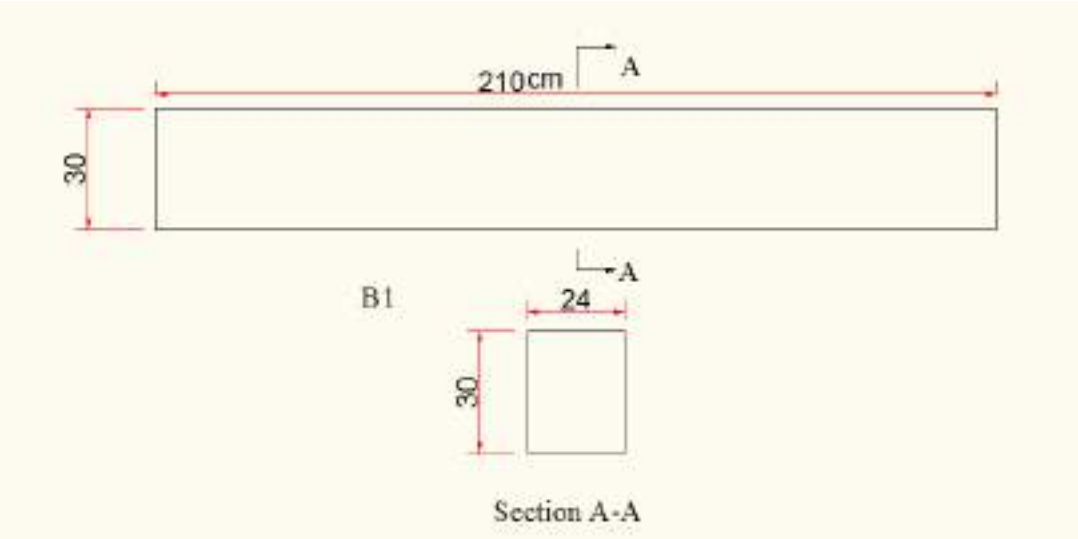

Beam No.(1)

Design flexural strength

fc´ =35 Mpa f_y=490 Mpa

$$\rho_b = 0.85\beta1 \frac{fc'}{fy}\left(\frac{600}{600+fy}\right)$$

β1 ={ 0.85-0.008(fc´-30)}≥0.65 for fc´ >30 Mpa

β1= {0.85-0.008(35-30)} =0.81

$$\rho_b = 0.85*0.81*\frac{35}{490}\left(\frac{600}{600+490}\right) = 0.0271$$

$\rho_{max} = 0.75\ \rho_b$

$\rho_{max} = 0.75*0.0271=0.02$

$$\rho_{min} = \frac{1.4}{fy} = \frac{1.4}{490} = 2.857*10^{-3}$$

Or $\rho_{min} = \frac{\sqrt{fc'}}{4fy} = \frac{\sqrt{35}}{4*490} = 3*10^{-3}$

APPENDEX (A)

use $\rho_{min} = 3*10^{-3}$

As = ρ b d= $3*10^{-3}$* 240 * 260 =188.35 mm^2

Use Ø 10 A= $\frac{\pi}{4}*10^2$ A= 78.54 mm^2

n= $\frac{As}{A} = \frac{188.35}{78.54} \approx 3$ bars

use 5Ø 10mm

As= 5*78.54= 392.7 mm^2

$\rho = \frac{392.7}{240*260}$ = 6.3* $10^{-3} < \rho_{max} > \rho_{min}$ O.K

a = $\frac{As*fy}{0.85fc' b} = \frac{392.7*490}{0.85*35*240}$ =27mm

c = $\frac{a}{0.85} = \frac{27}{0.85}$ = 31.76 mm

Mu = Ø Mn = Ø ρ b d^2 f_y (1- 0.59 ρ $\frac{fy}{fc'}$)

Mu= 0.9 *6.3*10^{-3}*240*$(260)^2$ *490(1- 0.59*6.3* $10^{-3}*\frac{490}{35}$)

Mu= 42.73 kN-m

Mu= $PL/_4$ » P = $\frac{Mu*4}{L} = \frac{42.73*4}{2}$

P= 85.46 kN

Design the shear

fc´ =35 Mpa f_y=420 Mpa

Vu= 85.46/2 = 42.73 kN

$\frac{vu*d}{mu} = \frac{42.73*0.26}{42.37}$ =0.262< 1

APPENDEX (A)

$v_c = 0.17 * \sqrt{fc'} * b * d$

$v_c = 0.17 * \sqrt{35} * 240 * 260 = 62757.77$ N

use ∅ 8 mm→ Av = no.$* \frac{\pi\, ds^2}{4} = 2 * \frac{\pi}{4} * 8^2$

Av=100.48 mm^2

$\frac{Vu}{\emptyset} = \frac{42.73}{0.85}$ =50.27 kN =50270 N = $0.8V_C$

$S = \frac{d}{2} = \frac{260}{2}$ =130 mm

S = 600mm

$S = \frac{Av * fy}{0.34\, b} = \frac{100.48 * 420}{0.34 * 240}$ =517.18mm

S_{min} = 130 mm

Use ∅ 8 mm @50mm

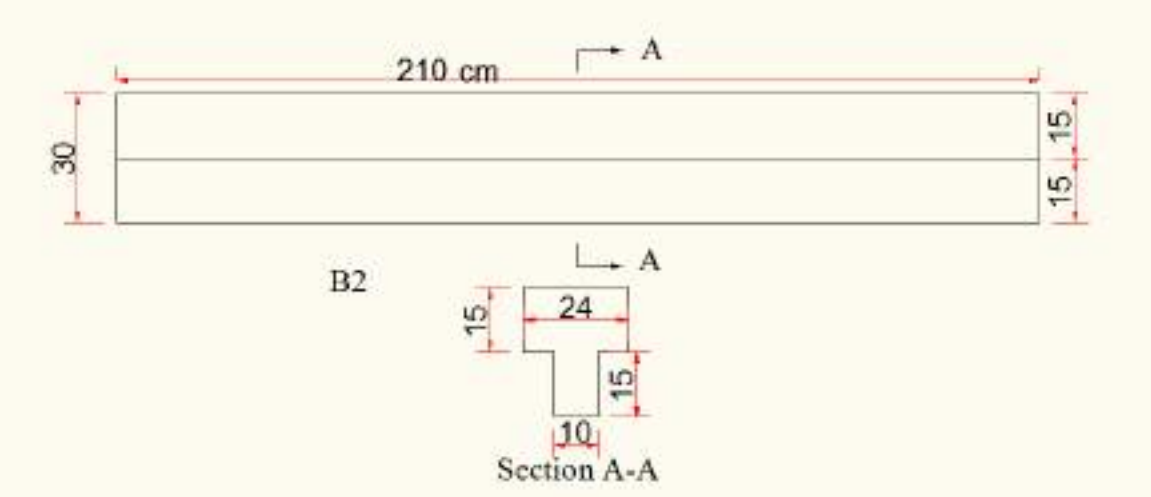

Beam No.(2)

Design flexural strength No.(1)

fc´ =35 Mpa f_y=490 Mpa

APPENDEX (A)

$\rho_b = 0.85\beta 1 \frac{fc'}{fy}(\frac{600}{600+fy})$

$\beta 1 = \{0.85-0.008(fc'-30)\} \geq 0.65$ for $fc' > 30$ Mpa

$\beta 1 = \{0.85-0.008(35-30)\} = 0.81$

$\rho_b = 0.85*0.81*\frac{35}{490}(\frac{600}{600+490}) = 0.0271$

$\rho_{max} = 0.75\ \rho_b$

$\rho_{max} = 0.75*0.0271 = 0.02$

$\rho_{min} = \frac{1.4}{fy}\frac{bw}{b} = \frac{1.4}{490}\frac{100}{240} = 1.19*10^{-3}$

Or $\rho_{min} = \frac{\sqrt{fc'}}{4fy}\frac{bw}{b} = \frac{\sqrt{35}}{4*490}\frac{100}{240} = 1.26*10^{-3}$

Use $\rho_{min} = 1.26*10^{-3}$

As = ρ b d= $1.26*10^{-3}*$ 240 * 260 =78.62 mm^2

Use Ø 10 A= $\frac{\pi}{4}*10^2$ A= 78.54 mm^2

$n = \frac{As}{A} = \frac{78.62}{78.54} \approx 2$ bars

use 5Ø 10mm

$As = 5*78.54 = 392.7\ mm^2$

$\rho = \frac{392.7}{240*260} = 6.3*10^{-3} < \rho_{max} > \rho_{min}$ O.K

$a = \frac{As*fy}{0.85fc'\ b} = \frac{392.7*490}{0.85*35*240} = 27mm \rightarrow a < h_f$

$c = \frac{a}{0.85} = \frac{27}{0.85} = 31.76$ mm

$Mu = Ø\ Mn = Ø\ \rho\ b\ d^2\ f_y(1- 0.59\ \rho\ \frac{fy}{fc'})$

APPENDEX (A)

Mu= 0.9 *6.3*10^{-3}*240*$(260)^2$ *490(1- 0.59*6.3* 10^{-3}*$\frac{490}{35}$)

Mu= 42.73 kN-m

Mu= $PL/4$ » P = $\frac{\text{Mu}*4}{\text{L}} = \frac{42.37*4}{2}$

P= 85.46 kN

Design the shear of beam No.(2)

fc´ =35 Mpa f_y=420 Mpa

Vu= 85.46/2 = 42.73 kN

$\frac{\text{vu}*\text{d}}{\text{mu}} = \frac{42.73*0.26}{42.73}$ =0.26< 1

v_c = 0.17* $\sqrt{\text{fc}'}$ * bw * d

v_c= 0.17*$\sqrt{35}$ * 100 * 260 = 26149.1 N

use ∅ 8 mm→ Av =no. $\frac{\pi\, ds^2}{4}$ =2*$\frac{\pi}{4}$ *8^2

Av=100.48 mm^2

$v_n = \frac{\text{Vu}}{\emptyset} = \frac{42.73}{0.85}$ =50.27 kN =50270 N = 1.92V_C

$S = \frac{d}{2} = \frac{260}{2}$ =130 mm

S = 600 mm

$S = \frac{\text{Av}*\text{fy}}{0.34\ bw} = \frac{100.48*420}{0.34*100}$ =1241.22mm

v_n= v_s+v_c → v_s= 50270-26149.1=24120.9 N

S= $\frac{\text{Av}*\text{fy}*\text{d}}{\text{vs}} = \frac{100.48*420*260}{24120.9}$ = 454.9 mm

S_{min} = 130 mm

Use Ø 8 mm @50mm

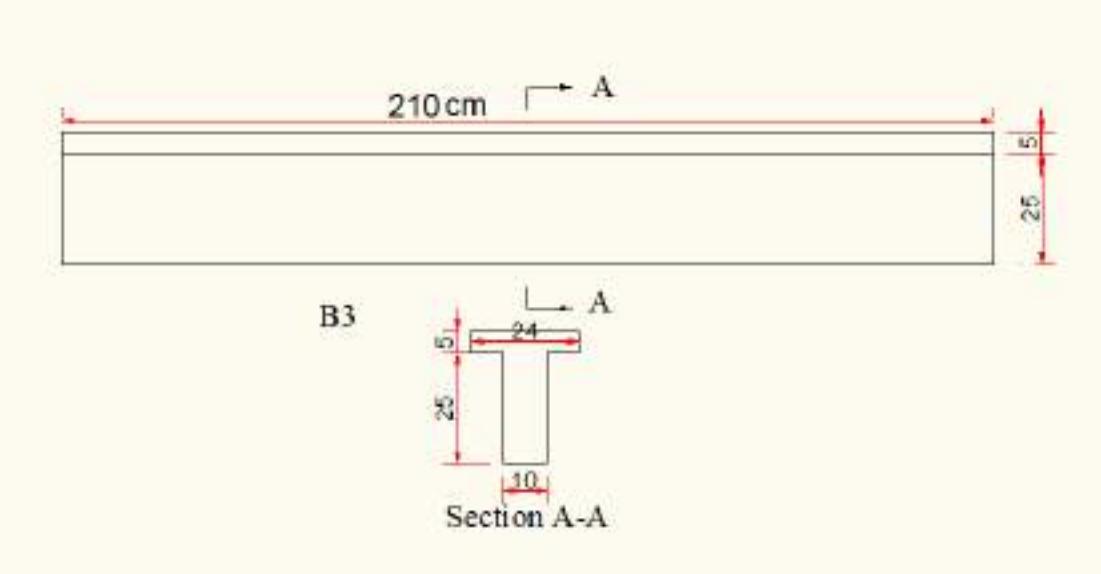

Beam No.(3)

Design of flexural strength

fc´ =35 Mpa f_y=490 Mpa

$\rho_b = 0.85\beta1 \frac{fc'}{fy}(\frac{600}{600+fy})$

β1 ={ 0.85-0.008(fc´-30)}≥0.65 for fc´ >30 Mpa

β1= {0.85-0.008(35-30)} =0.81

$\rho_b = 0.85*0.81*\frac{35}{490}(\frac{600}{600+490}) = 0.0271$

$\rho_{max} = 0.75\ \rho_b$

$\rho_{max} = 0.75*0.0271 = 0.02$

$\rho_{min} = \frac{1.4}{fy}\frac{bw}{b} = \frac{1.4}{490}\frac{100}{240} = 1.19*10^{-3}$

Or $\rho_{min} = \frac{\sqrt{fc'}}{4fy}\frac{bw}{b} = \frac{\sqrt{35}}{4*490}\frac{100}{240} = 1.26*10^{-3}$

Use $\rho_{min} = 1.26*10^{-3}$

APPENDEX (A)

As = ρ b d= $1.26*10^{-3}*$ 240 * 260 =78.62 mm^2

Use Ø 10 A= $\frac{\pi}{4}*10^2$ A= 78.54 mm^2

n = $\frac{As}{A} = \frac{78.62}{78.54} \approx$ 2 bars

use 5Ø 10mm

As= 5*78.54= 392.7 mm^2

$\rho = \frac{392.7}{240*260}$ = $6.3*10^{-3} < \rho_{max} > \rho_{min}$ O.K

a = $\frac{As*fy}{0.85fc' b} = \frac{392.7*490}{0.85*35*240}$ =27mm $\rightarrow a < h_f$

c = $\frac{a}{0.85} = \frac{27}{0.85}$ = 31.76 mm

Mu = Ø Mn = Ø ρ b d^2 $f_y(1- 0.59 \rho \frac{fy}{fc'})$

Mu= 0.9 $*6.3*10^{-3}*240*(260)^2$ $*490(1- 0.59*6.3*10^{-3}*\frac{490}{35})$

Mu= 42.73 kN-m

Mu= $PL/4$ » P = $\frac{Mu*4}{L} = \frac{42.73*4}{2}$

P= 85.46 KN

Design the shear of beam No.(3)

fc´ =35 Mpa f_y=420 Mpa

Vu= 85.46/2 = 42.73 kN

$\frac{vu*d}{mu} = \frac{42.73*0.26}{42.73}$ =0.26 < 1

v_c = 0.17* $\sqrt{fc'} * bw * d$

v_c= $0.17*\sqrt{35} * 100 * 260 = 26149.1$ N

APPENDEX (A)

use ∅ 8 mm→ Av =no. $\frac{\pi\, ds^2}{4}$ $=2*\frac{\pi}{4}*8^2$

Av=100.48 mm^2

$v_n = \frac{Vu}{\emptyset} = \frac{42.73}{0.85}$ =50.27 kN =50270 N = 1.92V_C

$S = \frac{d}{2} = \frac{260}{2}$ =130 mm

S = 600 mm

$S = \frac{Av*fy}{0.34\ bw} = \frac{100.84*420}{0.34*100}$ =1245.67mm

$v_n = v_s + v_c \rightarrow v_s$=50270-26149.1=24120.9 N

$S = \frac{Av*fy*d}{vs} = \frac{100.48*420*260}{24120.9}$ = 454.9 mm

S_{min} = 130 mm

Use ∅ 8 mm @50mm

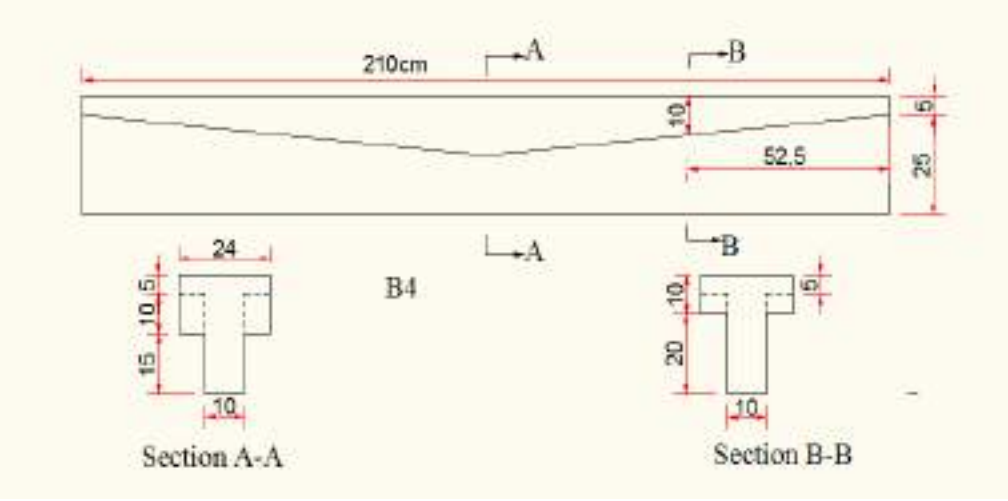

Beam No.4

Design flexural strength of section (A-A)

APPENDEX (A)

fc´ =35 Mpa f_y=490 Mpa

$\rho_b = 0.85\beta 1 \frac{fc'}{fy}(\frac{600}{600+fy})$

β1 ={ 0.85-0.008(fc´-30)}≥0.65 for fc´ >30 Mpa

β1= {0.85-0.008(35-30)} =0.81

$\rho_b = 0.85*0.81*\frac{35}{490}(\frac{600}{600+490}) = 0.0271$

$\rho_{max} = 0.75\ \rho_b$

$\rho_{max} = 0.75*0.0271 = 0.02$

$\rho_{min} = \frac{1.4}{fy}\frac{bw}{b} = \frac{1.4}{490}\frac{100}{240} = 1.19*10^{-3}$

Or $\rho_{min} = \frac{\sqrt{fc'}}{4fy}\frac{bw}{b} = \frac{\sqrt{35}}{4*490}\frac{100}{240} = 1.26*10^{-3}$

Use $\rho_{min} = 1.26*10^{-3}$

As = ρ b d= $1.26*10^{-3}$* 240 * 260 =78.62 mm^2

Use Ø 10 A= $\frac{\pi}{4}*10^2$ A= 78.54 mm^2

$n = \frac{As}{A} = \frac{78.62}{78.54} \approx 2$ bars

use 5Ø 10mm

$As = 5*78.54 = 392.7\ mm^2$

$\rho = \frac{392.7}{240*260} = 6.3*10^{-3} < \rho_{max} > \rho_{min}$ O.K

$a = \frac{As*fy}{0.85fc'\ b} = \frac{392.7*490}{0.85*35*240} = 27mm \rightarrow a < h_f$

$c = \frac{a}{0.85} = \frac{27}{0.85} = 31.76$ mm

APPENDEX (A)

$Mu = Ø\ Mn = Ø\ \rho\ b\ d^2\ f_y\left(1- 0.59\ \rho\ \frac{fy}{fc'}\right)$

$Mu= 0.9 *6.3*10^{-3}*240*(260)^2 *490\left(1- 0.59*6.3* 10^{-3}*\frac{490}{35}\right)$

Mu= 42.73 kN-m

$Mu= {}^{PL}/_{4}$ » $P = \frac{Mu*4}{L} = \frac{42.73*4}{2}$

P= 85.46 kN

Design flexural strength of section (B-B)

$fc' =35$ Mpa $f_y=490$ Mpa

M=0.5*P*0.475= 0.5*85.46*0.475= 20.3 KN-m

$$\rho= \frac{1-\sqrt{1-2.622M/(fc'bd^2)}}{1.18fy/fc'} =\frac{1-\sqrt{1-2.622*20.3*10^6/(35*240*260^2)}}{1.18*490/35}$$

$\rho= 2.9*10^{-3}$

$As= \rho bd= 2.9*10^{-3}*240*260= 181 mm^2$

Use Ø 10 $A= \frac{\pi}{4} *10^2$ $A= 78.54\ mm^2$

$n = \frac{As}{A} = \frac{181}{78.54} \approx 3$ bars

$\rho_b = 0.85\beta1\ \frac{fc'}{fy}\left(\frac{600}{600+fy}\right)$

$\beta1 =\{ 0.85-0.008(fc'-30)\}\geq 0.65$ for $fc' >30$ Mpa

$\beta1= \{0.85-0.008(35-30)\} =0.81$

$\rho_b = 0.85*0.81*\frac{35}{490}\left(\frac{600}{600+490} \right)=0.0271$

$\rho_{max} = 0.75\ \rho_b$

APPENDEX (A)

ρ_{max} =0.75*0.0271= 0.02

$\rho_{min} = \frac{1.4}{fy}\frac{bw}{b} = \frac{1.4}{490}\frac{100}{240} = 1.19*10^{-3}$

Or $\rho_{min} = \frac{\sqrt{fc'}}{4fy}\frac{bw}{b} = \frac{\sqrt{35}}{4*490}\frac{100}{240} = 1.26*10^{-3}$

Use $\rho_{min} = 1.26*10^{-3}$

use 5Ø 10mm

As= 5*78.54= 392.7 mm^2

$\rho = \frac{392.7}{240*260} = 6.3*10^{-3} < \rho_{max} > \rho_{min}$ O.K

$a = \frac{As*fy}{0.85fc'\,b} = \frac{392.7*490}{0.85*35*240} = 27mm \rightarrow a < h_f$

$c = \frac{a}{0.85} = \frac{27}{0.85} = 31.76$ mm

Shear design of beam No.(4)

$fc' = 35$ Mpa $f_y = 420$ Mpa

Vu= 85.46/2 = 42.73 kN

$\frac{vu*d}{mu} = \frac{42.73*0.26}{42.73} = 0.26 < 1$

$v_c = 0.17*\sqrt{fc'}*bw*d$

$v_c = 0.17*\sqrt{35}*100*260 = 26149.1$ N

use Ø 8 mm→ Av =no. $\frac{\pi\, ds^2}{4} = 2*\frac{\pi}{4}*8^2$

Av=100.48 mm^2

$v_n = \frac{Vu}{\emptyset} = \frac{42.73}{0.85} = 50.27$ kN =50270 N = $1.9V_C$

APPENDEX (A)

$S = \frac{d}{2} = \frac{260}{2}$ =130 mm

S = 600 mm

$S = \frac{Av*fy}{0.34\ bw} = \frac{100.48*420}{0.34*100}$ =1241mm

$v_n = v_s + v_c \rightarrow v_s$=50270-26149.1=24120.9 N

$S = \frac{Av*fy*d}{vs} = \frac{100.48*420*260}{24120.9}$ = 455 mm

S_{min} = 130 mm

Use Ø 8 mm @50mm

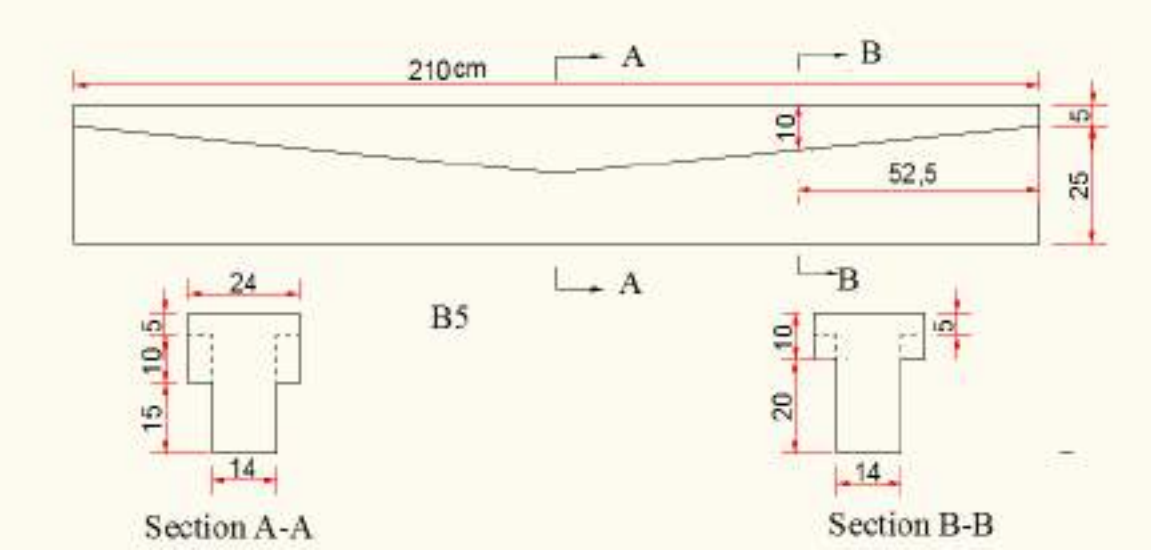

Beam No. (5)

Design flexural strength of section (A-A)

fc´ =35 Mpa f_y=490 Mpa

$\rho_b = 0.85\beta1 \frac{fc'}{fy}(\frac{600}{600+fy})$

β1 ={ 0.85-0.008(fc´-30)}≥0.65 for fc´ >30 Mpa

β1= {0.85-0.008(35-30)} =0.81

APPENDEX (A)

$\rho_b = 0.85*0.81*\frac{35}{490}\left(\frac{600}{600+490}\right)=0.0271$

$\rho_{max} = 0.75\ \rho_b$

$\rho_{max} = 0.75*0.0271= 0.02$

$\rho_{min} = \frac{1.4}{fy}\frac{bw}{b} = \frac{1.4}{490}\frac{140}{240} = 1.67*10^{-3}$

Or $\rho_{min} = \frac{\sqrt{fc'}}{4fy}\frac{bw}{b} = \frac{\sqrt{35}}{4*490}\frac{140}{240} = 1.76*10^{-3}$

Use $\rho_{min} = 1.76*10^{-3}$

As = ρ b d= $1.76*10^{-3}$* 240 * 260 =109.82 mm^2

Use Ø 10 A= $\frac{\pi}{4}*10^2$ A= 78.54 mm^2

$n = \frac{As}{A} = \frac{109.82}{78.54} \approx 2$ bars

use 5Ø 10mm

As= 5*78.54= 392.7 mm^2

$\rho = \frac{392.7}{240*260}$ = $6.3*10^{-3} < \rho_{max} > \rho_{min}$ O.K

$a = \frac{As*fy}{0.85fc'\ b} = \frac{392.7*490}{0.85*35*240}$ =27mm $\rightarrow a < h_f$

$c = \frac{a}{0.85} = \frac{27}{0.85}$ = 31.76 mm

$Mu = Ø\ Mn = Ø\ \rho\ b\ d^2\ f_y\left(1- 0.59\ \rho\ \frac{fy}{fc'}\right)$

$Mu= 0.9*6.3*10^{-3}*240*(260)^2*490\left(1- 0.59*6.3*10^{-3}*\frac{490}{35}\right)$

Mu= 42.73 kN-m

$Mu= {PL}/{4}$ » $P = \frac{Mu*4}{L} = \frac{42.73*4}{2}$

APPENDEX (A)

P= 85.46 kN

Design flexural strength of section (B-B)

fc´ =35 Mpa f_y=490 Mpa

M=0.5*P*0.475= 0.5*85.46*0.475= 20.3 KN-m

$$\rho = \frac{1-\sqrt{1-2.622M/(fc'bd^2)}}{1.18fy/fc'} = \frac{1-\sqrt{1-2.622*20.3*10^6/(35*240*260^2)}}{1.18*490/35}$$

$\rho = 2.9*10^{-3}$

As= ρbd= $2.9*10^{-3}*240*260= 181mm^2$

Use Ø 10 A= $\frac{\pi}{4}*10^2$ A= 78.54 mm^2

$$n = \frac{As}{A} = \frac{181}{78.54} \approx 3 \text{ bars}$$

$$\rho_b = 0.85\beta1 \frac{fc'}{fy}\left(\frac{600}{600+fy}\right)$$

β1 ={ 0.85-0.008(fc´-30)}≥0.65 for fc´ >30 Mpa

β1= {0.85-0.008(35-30)} =0.81

$$\rho_b = 0.85*0.81*\frac{35}{490}\left(\frac{600}{600+490}\right)=0.0271$$

$\rho_{max} = 0.75\ \rho_b$

ρ_{max} =0.75*0.0271= 0.02

$$\rho_{min} = \frac{1.4}{fy}\frac{bw}{b} = \frac{1.4}{490}\frac{140}{240} = 1.67*10^{-3}$$

Or $\rho_{min} = \frac{\sqrt{fc'}}{4fy}\frac{bw}{b} = \frac{\sqrt{35}}{4*490}\frac{140}{240} = 1.76*10^{-3}$

Use $\rho_{min} = 1.76*10^{-3}$

use 5Ø 10mm

As= 5*78.54= 392.7 mm^2

$\rho = \frac{392.7}{240*260}$ = 6.3* 10^{-3} < ρ_{max}> ρ_{min} O.K

$a = \frac{As*fy}{0.85fc' b} = \frac{392.7*490}{0.85*35*240}$ =27mm →$a < h_f$

$c = \frac{a}{0.85} = \frac{27}{0.85}$ = 31.76 mm

Shear design of beam No.(5)

fc´ =35 Mpa f_y=420 Mpa

Vu= 85.46/2 = 42.73 kN

$\frac{vu*d}{mu} = \frac{42.73*0.26}{42.73}$ =0.26 < 1

$v_c = 0.17* \sqrt{fc'} * bw * d$

v_c= $0.17*\sqrt{35} * 140 * 260 = 36608.7$ N

use Ø 8 mm→ Av =no. $\frac{\pi\, ds^2}{4} = 2*\frac{\pi}{4}*8^2$

Av=100.48 mm^2

$v_n = \frac{Vu}{\emptyset} = \frac{42.73}{0.85}$ = 50.27 kN =50270 N = 1.9V_C

$S = \frac{d}{2} = \frac{260}{2}$ =130 mm

S = 600 mm

$S = \frac{Av*fy}{0.34\ bw} = \frac{100.48*420}{0.34*140}$ =887mm

$v_n = v_s + v_c \rightarrow v_s$=50270-36608.7=13661.3 N

APPENDEX (A)

$$S=\frac{Av*fy*d}{vs}=\frac{100.48*420*260}{13661.3}=803\ mm$$

$S_{min}=130$ mm

Use Ø 8 mm @50mm

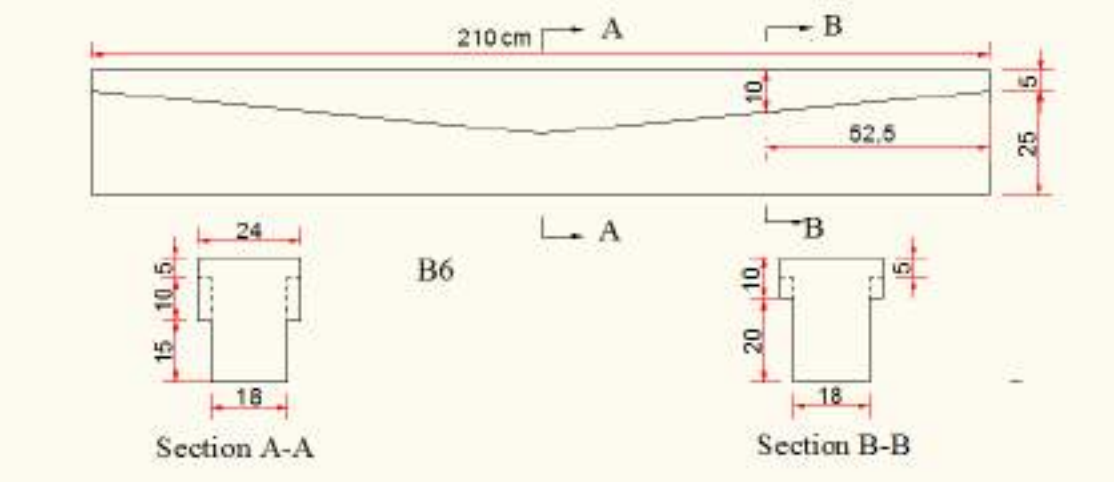

Beam No. (6)

Design flexural strength of section (A-A)

$f_c' = 35$ Mpa $f_y = 490$ Mpa

$$\rho_b = 0.85\beta 1 \frac{fc'}{fy}\left(\frac{600}{600+fy}\right)$$

$\beta 1 = \{0.85-0.008(fc'-30)\} \geq 0.65$ for $fc' > 30$ Mpa

$\beta 1 = \{0.85-0.008(35-30)\} = 0.81$

$$\rho_b = 0.85*0.81*\frac{35}{490}\left(\frac{600}{600+490}\right)=0.0271$$

$\rho_{max} = 0.75\ \rho_b$

$\rho_{max} = 0.75*0.0271 = 0.02$

$$\rho_{min} = \frac{1.4}{fy}\frac{bw}{b} = \frac{1.4}{490}\frac{180}{240} = 2.14*10^{-3}$$

APPENDEX (A)

Or $\rho_{min} = \frac{\sqrt{fc'}}{4fy}\frac{bw}{b} = \frac{\sqrt{35}}{4*490}\frac{180}{240} = 2.26*10^{-3}$

Use $\rho_{min} = 2.26*10^{-3}$

As = ρ b d= $2.26*10^{-3}$* 240 * 260 =141.02 mm^2

Use Ø 10 A= $\frac{\pi}{4}*10^2$ A= 78.54 mm^2

$n = \frac{As}{A} = \frac{141.02}{78.54} \approx 2$ bars

use 5Ø 10mm

As= 5*78.54= 392.7 mm^2

$\rho = \frac{392.7}{240*260} = 6.3*10^{-3} < \rho_{max} > \rho_{min}$ O.K

$a = \frac{As*fy}{0.85fc' b} = \frac{392.7*490}{0.85*35*240}$ =27mm $\rightarrow a < h_f$

$c = \frac{a}{0.85} = \frac{27}{0.85}$ = 31.76 mm

Mu = Ø Mn = Ø ρ b d^2 $f_y(1- 0.59\rho\frac{fy}{fc'})$

Mu= $0.9*6.3*10^{-3}*240*(260)^2*490(1- 0.59*6.3*10^{-3}*\frac{490}{35})$

Mu= 42.73 kN-m

Mu= $PL/_4$ » $P = \frac{Mu*4}{L} = \frac{42.73*4}{2}$

P= 85.46 kN

Design flexural strength of section (B-B)

fc´ =35 Mpa f_y=490 Mpa

M=0.5*P*0.475= 0.5*85.46*0.475= 20.3 KN-m

APPENDEX (A)

$$\rho = \frac{1-\sqrt{1-2.622M/(fc'bd^2)}}{1.18fy/fc'} = \frac{1-\sqrt{1-2.622*20.3*10^6/(35*240*260^2)}}{1.18*490/35}$$

$\rho = 2.9*10^{-3}$

As= ρbd= $2.9*10^{-3}*240*260 = 181mm^2$

Use Ø 10 A= $\frac{\pi}{4}*10^2$ A= 78.54 mm^2

$n = \frac{As}{A} = \frac{181}{78.54} \approx 3$ bars

$\rho_b = 0.85\beta1 \frac{fc'}{fy}(\frac{600}{600+fy})$

$\beta1 = \{0.85-0.008(fc'-30)\} \geq 0.65$ for fc′ >30 Mpa

$\beta1 = \{0.85-0.008(35-30)\} = 0.81$

$\rho_b = 0.85*0.81*\frac{35}{490}(\frac{600}{600+490}) = 0.0271$

$\rho_{max} = 0.75\ \rho_b$

$\rho_{max} = 0.75*0.0271 = 0.02$

$\rho_{min} = \frac{1.4}{fy}\frac{bw}{b} = \frac{1.4}{490}\frac{180}{240} = 2.14*10^{-3}$

Or $\rho_{min} = \frac{\sqrt{fc'}}{4fy}\frac{bw}{b} = \frac{\sqrt{35}}{4*490}\frac{180}{240} = 2.26*10^{-3}$

Use $\rho_{min} = 2.26*10^{-3}$

use 5Ø 10mm

$As = 5*78.54 = 392.7\ mm^2$

$\rho = \frac{392.7}{240*260} = 6.3*10^{-3} < \rho_{max} > \rho_{min}$ O.K

$a = \frac{As*fy}{0.85fc'\,b} = \frac{392.7*490}{0.85*35*240} = 27mm \rightarrow a < h_f$

APPENDEX (A)

$c = \frac{a}{0.85} = \frac{27}{0.85}$ = 31.76 mm

Shear design of beam No.(6)

fc´ =35 Mpa f_y=420 Mpa

Vu= 85.46/2 = 42.73 kN

$\frac{vu*d}{mu} = \frac{42.73*0.26}{42.73}$ =0.26 < 1

$v_c = 0.17* \sqrt{fc'} * bw * d$

$v_c = 0.17*\sqrt{35} * 180 * 260 = 47068$ N

use ∅ 8 mm→ Av =no. $\frac{\pi\, ds^2}{4} = 2*\frac{\pi}{4} *8^2$

Av=100.48 mm^2

$v_n = \frac{Vu}{\emptyset} = \frac{42.73}{0.85}$ = 50.27 kN =50270 N = 1.07V_C

$S = \frac{d}{2} = \frac{260}{2}$ =130 mm

S = 600 mm

$S = \frac{Av*fy}{0.34\, bw} = \frac{100.48*420}{0.34*180}$ =690mm

$v_n = v_s+v_c \rightarrow v_s$=50270-47068=3202 N

$S = \frac{Av*fy*d}{vs} = \frac{100.48*420*260}{3202}$ =3427 mm

S_{min} = 130 mm

Use ∅ 8 mm @50mm

APPENDEX (A)

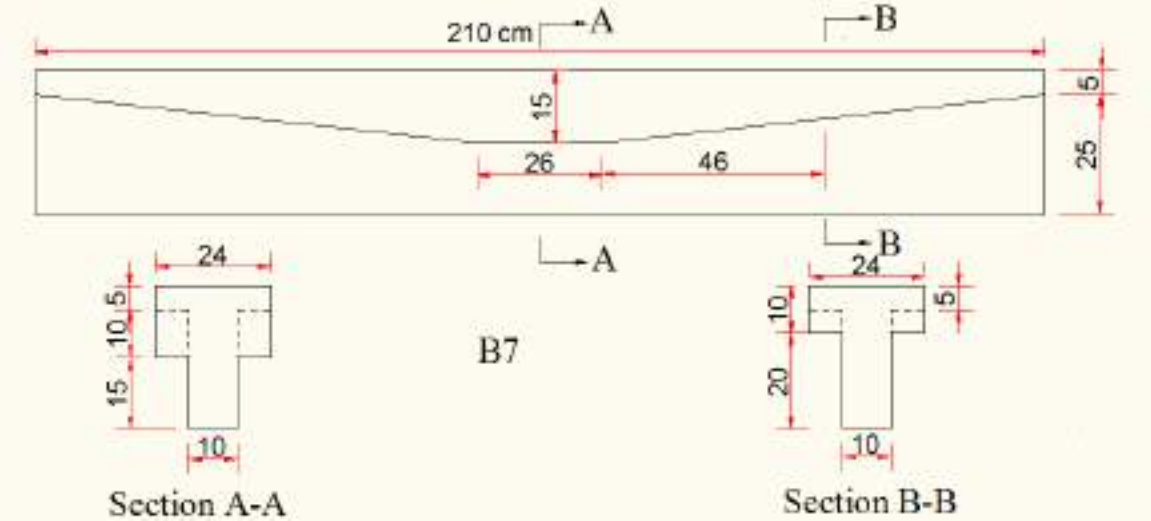

Beam No.(7)

Design flexural strength of section (A-A)

fc´ =35 Mpa f_y=490 Mpa

$\rho_b = 0.85\beta1 \frac{fc'}{fy}(\frac{600}{600+fy})$

β1 ={ 0.85-0.008(fc´-30)}≥0.65 for fc´ >30 Mpa

β1= {0.85-0.008(35-30)} =0.81

$\rho_b = 0.85*0.81*\frac{35}{490}(\frac{600}{600+490}) = 0.0271$

$\rho_{max} = 0.75\ \rho_b$

$\rho_{max} = 0.75*0.0271 = 0.02$

$\rho_{min} = \frac{1.4}{fy}\frac{bw}{b} = \frac{1.4}{490}\frac{100}{240} = 1.19*10^{-3}$

Or $\rho_{min} = \frac{\sqrt{fc'}}{4fy}\frac{bw}{b} = \frac{\sqrt{35}}{4*490}\frac{100}{240} = 1.26*10^{-3}$

Use $\rho_{min} = 1.26*10^{-3}$

As = ρ b d= $1.26*10^{-3}$* 240 * 260 =78.62 mm^2

APPENDEX (A)

Use Ø 10 A= $\frac{\pi}{4}$ *10^2 A= 78.54 mm^2

n = $\frac{As}{A} = \frac{78.62}{78.54} \approx$ 2 bars

use 5Ø 10mm

As= 5*78.54= 392.7 mm^2

$\rho = \frac{392.7}{240*260}$ = 6.3* 10^{-3} < ρ_{max} > ρ_{min} O.K

a = $\frac{As*fy}{0.85fc' b} = \frac{392.7*490}{0.85*35*240}$ =27mm →a < h_f

c = $\frac{a}{0.85} = \frac{27}{0.85}$ = 31.76 mm

Mu = Ø Mn = Ø ρ b d^2 $f_y(1- 0.59 \rho \frac{fy}{fc'})$

Mu= 0.9 *6.3*10^{-3}*240*$(260)^2$ *490(1- 0.59*6.3* 10^{-3}*$\frac{490}{35}$)

Mu= 42.73 kN-m

Mu= $PL/_4$ » P = $\frac{Mu*4}{L} = \frac{42.73*4}{2}$

P= 85.46 kN

Design flexural strength of section (B-B)

fc´ =35 Mpa f_y=490 Mpa

M=0.5*P*0.41= 0.5*85.46*0.41= 17.52 KN-m

$\rho = \frac{1-\sqrt{1-2.622M/(fc'bd^2)}}{1.18fy/fc'} = \frac{1-\sqrt{1-2.622*17.52*10^6/(35*240*260^2)}}{1.18*490/35}$

ρ= 2.5*10^{-3}

As= ρbd= 2.5*10^{-3}*240*260= 156mm^2

APPENDEX (A)

Use Ø 10 A= $\frac{\pi}{4}$ *10^2 A= 78.54 mm^2

n = $\frac{As}{A} = \frac{156}{78.54} \approx$ 2 bars

ρ_b =0.85β1 $\frac{fc'}{fy}(\frac{600}{600+fy})$

β1 ={ 0.85-0.008(fc´-30)}≥0.65 for fc´ >30 Mpa

β1= {0.85-0.008(35-30)} =0.81

ρ_b = 0.85*0.81*$\frac{35}{490}(\frac{600}{600+490})$=0.0271

ρ_{max} = 0.75 ρ_b

ρ_{max} =0.75*0.0271= 0.02

$\rho_{min} = \frac{1.4}{fy}\frac{bw}{b} = \frac{1.4}{490}\frac{100}{240} = 1.19*10^{-3}$

Or $\rho_{min} = \frac{\sqrt{fc'}}{4fy}\frac{bw}{b} = \frac{\sqrt{35}}{4*490}\frac{100}{240} = 1.26*10^{-3}$

Use $\rho_{min} = 1.26*10^{-3}$

use 5Ø 10mm

As= 5*78.54= 392.7 mm^2

$\rho = \frac{392.7}{240*260}$ = 6.3* 10^{-3} < ρ_{max}> ρ_{min} O.K

a = $\frac{As*fy}{0.85fc'\,b} = \frac{392.7*490}{0.85*35*240}$ =27mm →a < h_f

c = $\frac{a}{0.85} = \frac{27}{0.85}$ = 31.76 mm

Shear design of beam No.(7)

fc´ =35 Mpa f_y=420 Mpa

Vu= 85.46/2 = 42.73 kN

APPENDEX (A)

$\frac{vu*d}{mu} = \frac{42.73*0.26}{42.73}$ =0.26 < 1

$v_c = 0.17* \sqrt{fc'} * bw * d$

$v_C = 0.17*\sqrt{35} * 100 * 260 = 26149.1$ N

use ∅ 8 mm→ Av =no. $\frac{\pi\, ds^2}{4} = 2*\frac{\pi}{4} *8^2$

Av=100.48 mm^2

$v_n = \frac{Vu}{\emptyset} = \frac{42.73}{0.85}$ = 50.27 kN =50270 N = $1.9V_C$

$S = \frac{d}{2} = \frac{260}{2}$ =130 mm

S = 600 mm

$S = \frac{Av*fy}{0.34\ bw} = \frac{100.48*420}{0.34*100}$ =1241mm

$v_n = v_s + v_c \rightarrow v_s$=50270-26149.1=24120.9 N

$S = \frac{Av*fy*d}{vs} = \frac{100.48*420*260}{24120.9}$ = 455 mm

S_{min} = 130 mm

Use ∅ 8 mm @50mm

APPENDEX (A)

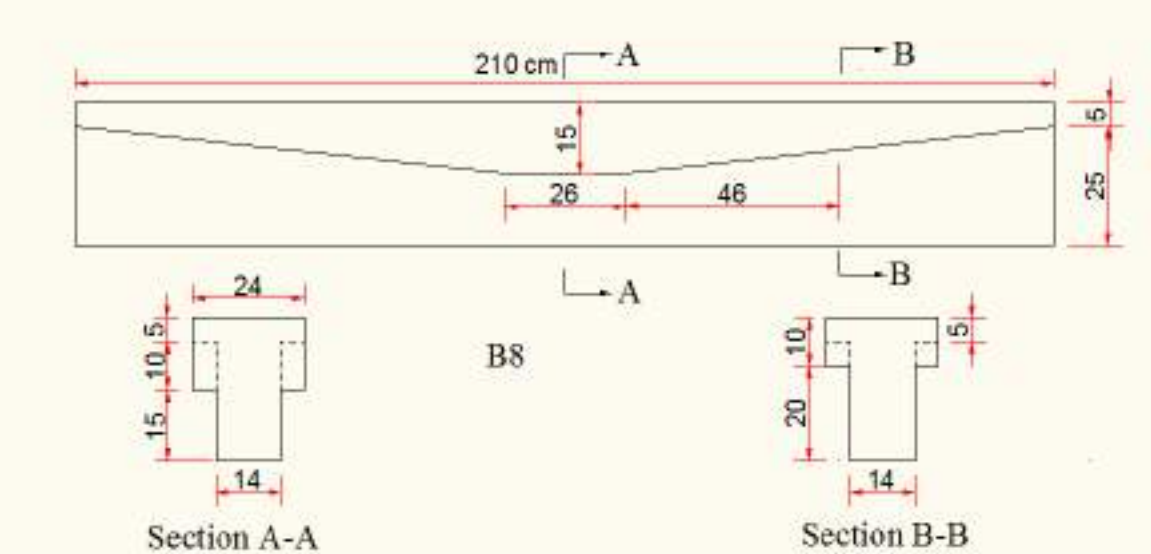

Beam No. (8)

Design flexural strength of section (A-A)

fc´ =35 Mpa f_y=490 Mpa

$\rho_b = 0.85\beta1 \frac{fc'}{fy}\left(\frac{600}{600+fy}\right)$

β1 ={ 0.85-0.008(fc´-30)}≥0.65 for fc´ >30 Mpa

β1= {0.85-0.008(35-30)} =0.81

$\rho_b = 0.85*0.81*\frac{35}{490}\left(\frac{600}{600+490}\right)=0.0271$

$\rho_{max} = 0.75\ \rho_b$

$\rho_{max} = 0.75*0.0271= 0.02$

$\rho_{min} = \frac{1.4}{fy}\frac{bw}{b} = \frac{1.4}{490}\frac{140}{240} = 1.67*10^{-3}$

Or $\rho_{min} = \frac{\sqrt{fc'}}{4fy}\frac{bw}{b} = \frac{\sqrt{35}}{4*490}\frac{140}{240} = 1.76*10^{-3}$

Use $\rho_{min} = 1.76*10^{-3}$

As = ρ b d= $1.76*10^{-3}$* 240 * 260 =109.82 mm^2

APPENDEX (A)

Use Ø 10 A= $\frac{\pi}{4}$ *10^2 A= 78.54 mm^2

n = $\frac{As}{A} = \frac{109.82}{78.54} \approx$ 2 bars

use 5Ø 10mm

As= 5*78.54= 392.7 mm^2

$\rho = \frac{392.7}{240*260}$ = 6.3* 10^{-3} < ρ_{max} > ρ_{min} O.K

a = $\frac{As*fy}{0.85fc' b} = \frac{392.7*490}{0.85*35*240}$ =27mm →a < h_f

c = $\frac{a}{0.85} = \frac{27}{0.85}$ = 31.76 mm

Mu = Ø Mn = Ø ρ b d^2 $f_y(1- 0.59 \rho \frac{fy}{fc'})$

Mu= 0.9 *6.3*10^{-3}*240*$(260)^2$ *490$(1- 0.59*6.3* 10^{-3}*\frac{490}{35})$

Mu= 42.73 kN-m

Mu= $PL/_4$ » P = $\frac{Mu*4}{L} = \frac{42.73*4}{2}$

P= 85.46 kn

Design flexural strength of section (B-B)

fc´ =35 Mpa f_y=490 Mpa

M=0.5*P*0.41= 0.5*85.46*0.41= 17.52 KN-m

$\rho = \frac{1-\sqrt{1-2.622M/(fc'bd^2)}}{1.18fy/fc'} = \frac{1-\sqrt{1-2.622*17.52*10^6/(35*240*260^2)}}{1.18*490/35}$

ρ= 2.5*10^{-3}

As= ρbd= 2.5*10^{-3}*240*260= 156mm^2

APPENDEX (A)

Use Ø 10 A= $\frac{\pi}{4}$ *10^2 A= 78.54 mm^2

n = $\frac{As}{A} = \frac{156}{78.54} \approx$ 2 bars

ρ_b =0.85β1 $\frac{fc'}{fy}(\frac{600}{600+fy})$

β1 ={ 0.85-0.008(fc´-30)}≥0.65 for fc´ >30 Mpa

β1= {0.85-0.008(35-30)} =0.81

ρ_b = 0.85*0.81*$\frac{35}{490}(\frac{600}{600+490})$=0.0271

ρ_{max} = 0.75 ρ_b

ρ_{max} =0.75*0.0271= 0.02

$\rho_{min} = \frac{1.4}{fy}\frac{bw}{b} = \frac{1.4}{490}\frac{140}{240} = 1.67*10^{-3}$

Or $\rho_{min} = \frac{\sqrt{fc'}}{4fy}\frac{bw}{b} = \frac{\sqrt{35}}{4*490}\frac{140}{240} = 1.76*10^{-3}$

Use $\rho_{min} = 1.76*10^{-3}$

use 5Ø 10mm

As= 5*78.54= 392.7 mm^2

$\rho = \frac{392.7}{240*260}$ = 6.3* 10^{-3} < ρ_{max}> ρ_{min} O.K

a = $\frac{As*fy}{0.85fc'\,b} = \frac{392.7*490}{0.85*35*240}$ =27mm →a < h_f

c = $\frac{a}{0.85} = \frac{27}{0.85}$ = 31.76 mm

Shear design of beam No.(8)

fc´ =35 Mpa f_y=420 Mpa

APPENDEX (A)

Vu= 85.46/2 = 42.73 kN

$\frac{vu*d}{mu} = \frac{42.73*0.26}{42.73}$ =0.26 < 1

$v_c = 0.17* \sqrt{fc'} * bw * d$

$v_C = 0.17*\sqrt{35} * 140 * 260 = 36608.7$ N

use ∅ 8 mm→ Av =no. $\frac{\pi\, ds^2}{4} = 2*\frac{\pi}{4} *8^2$

Av=100.48 mm^2

$v_n = \frac{Vu}{\emptyset} = \frac{42.73}{0.85}$ = 50.27 kN =50270 N = $1.9V_C$

$S = \frac{d}{2} = \frac{260}{2}$ =130 mm

S = 600 mm

$S = \frac{Av*fy}{0.34\ bw} = \frac{100.48*420}{0.34*140}$ =887mm

$v_n = v_s+v_c \rightarrow v_s$=50270-36608.7=13661.3 N

$S = \frac{Av*fy*d}{vs} = \frac{100.48*420*260}{13661.3}$ = 803 mm

S_{min} = 130 mm

Use ∅ 8 mm @50mm

APPENDEX (A)

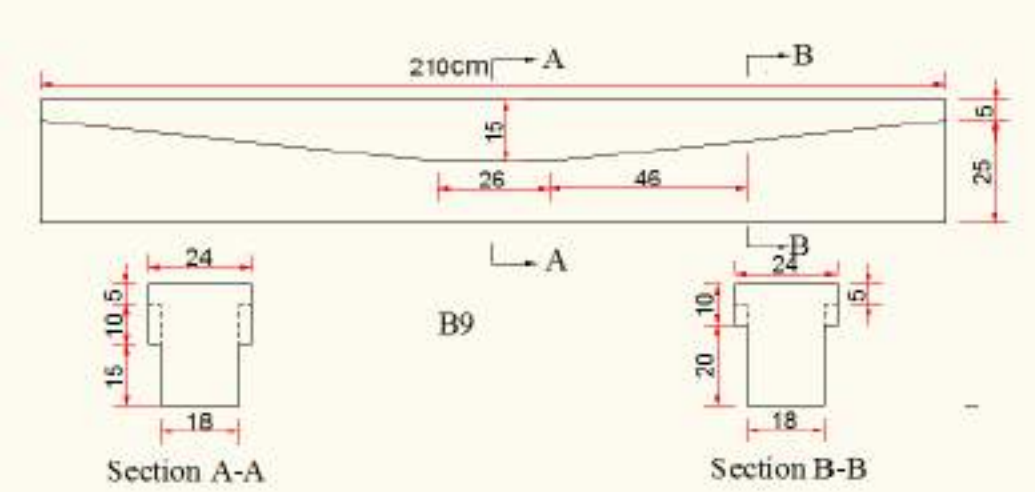

Beam No. (9)

Design flexural strength of section (A-A)

fc´ =35 Mpa f_y=490 Mpa

$\rho_b = 0.85\beta 1 \frac{fc'}{fy}\left(\frac{600}{600+fy}\right)$

β1 ={ 0.85-0.008(fc´-30)}≥0.65 for fc´ >30 Mpa

β1= {0.85-0.008(35-30)} =0.81

$\rho_b = 0.85*0.81*\frac{35}{490}\left(\frac{600}{600+490}\right)=0.0271$

$\rho_{max} = 0.75\ \rho_b$

$\rho_{max} = 0.75*0.0271= 0.02$

$\rho_{min} = \frac{1.4}{fy}\frac{bw}{b} = \frac{1.4}{490}\frac{180}{240} = 2.14*10^{-3}$

Or $\rho_{min} = \frac{\sqrt{fc'}}{4fy}\frac{bw}{b} = \frac{\sqrt{35}}{4*490}\frac{180}{240} = 2.26*10^{-3}$

Use $\rho_{min} = 2.26*10^{-3}$

As = ρ b d= $2.26*10^{-3}$* 240 * 260 =141.02 mm^2

APPENDEX (A)

Use Ø 10 A= $\frac{\pi}{4}$ *10^2 A= 78.54 mm^2

n = $\frac{As}{A} = \frac{141.02}{78.54} \approx$ 2 bars

use 5Ø 10mm

As= 5*78.54= 392.7 mm^2

$\rho = \frac{392.7}{240*260}$ = 6.3* 10^{-3} < ρ_{max}> ρ_{min} O.K

a = $\frac{As*fy}{0.85fc' b} = \frac{392.7*490}{0.85*35*240}$ =27mm →a < h_f

c = $\frac{a}{0.85} = \frac{27}{0.85}$ = 31.76 mm

Mu = Ø Mn = Ø ρ b d^2 $f_y(1- 0.59 \rho \frac{fy}{fc'})$

Mu= 0.9 *6.3*10^{-3}*240*$(260)^2$ *490(1- 0.59*6.3* 10^{-3}*$\frac{490}{35}$)

Mu= 42.73 kN-m

Mu= $PL/_4$ » P = $\frac{Mu*4}{L} = \frac{42.73*4}{2}$

P= 85.46 kN

Design flexural strength of section (B-B)

fc´ =35 Mpa f_y=490 Mpa

M=0.5*P*0.41= 0.5*85.46*0.41= 17.52 KN-m

$\rho = \frac{1-\sqrt{1-2.622M/(fc'bd^2)}}{1.18fy/fc'} = \frac{1-\sqrt{1-2.622*17.52*10^6/(35*240*260^2)}}{1.18*490/35}$

ρ= 2.5*10^{-3}

As= ρbd= 2.5*10^{-3}*240*260= 156mm^2

APPENDEX (A)

Use Ø 10 A= $\frac{\pi}{4}$ *10^2 A= 78.54 mm^2

$n = \frac{As}{A} = \frac{156}{78.54} \approx 2$ bars

$\rho_b = 0.85\beta1 \frac{fc'}{fy}(\frac{600}{600+fy})$

$\beta1 = \{0.85-0.008(fc'-30)\} \geq 0.65$ for $fc' > 30$ Mpa

$\beta1 = \{0.85-0.008(35-30)\} = 0.81$

$\rho_b = 0.85*0.81*\frac{35}{490}(\frac{600}{600+490}) = 0.0271$

$\rho_{max} = 0.75\ \rho_b$

$\rho_{max} = 0.75*0.0271 = 0.02$

$\rho_{min} = \frac{1.4}{fy}\frac{bw}{b} = \frac{1.4}{490}\frac{180}{240} = 2.14*10^{-3}$

Or $\rho_{min} = \frac{\sqrt{fc'}}{4fy}\frac{bw}{b} = \frac{\sqrt{35}}{4*490}\frac{180}{240} = 2.26*10^{-3}$

Use $\rho_{min} = 2.26*10^{-3}$

use 5Ø 10mm

$As = 5*78.54 = 392.7\ mm^2$

$\rho = \frac{392.7}{240*260} = 6.3*10^{-3} < \rho_{max} > \rho_{min}$ O.K

$a = \frac{As*fy}{0.85fc'\,b} = \frac{392.7*490}{0.85*35*240} = 27mm \rightarrow a < h_f$

$c = \frac{a}{0.85} = \frac{27}{0.85} = 31.76$ mm

Shear design of beam No.(9)

$fc' = 35$ Mpa $f_y = 420$ Mpa

APPENDEX (A)

Vu= 85.46/2 = 42.73 kN

$\frac{vu*d}{mu} = \frac{42.73*0.26}{42.73}$ =0.26 < 1

$v_c = 0.17* \sqrt{fc'} * bw * d$

$v_C = 0.17*\sqrt{35} * 180 * 260 = 47068$ N

use ∅ 8 mm→ Av =no. $\frac{\pi\, ds^2}{4} = 2*\frac{\pi}{4} *8^2$

Av=100.48 mm^2

$v_n = \frac{Vu}{\emptyset} = \frac{42.73}{0.85}$ = 50.27 kN =50270 N = 1.07V_C

$S = \frac{d}{2} = \frac{260}{2}$ =130 mm

S = 600 mm

$S = \frac{Av*fy}{0.34\ bw} = \frac{100.48*420}{0.34*180}$ =690mm

$v_n = v_s+v_c \rightarrow v_s$=50270-47068=3202 N

$S = \frac{Av*fy*d}{vs} = \frac{100.48*420*260}{3202}$ =3427 mm

S_{min} = 130 mm

Use ∅ 8 mm @50mm

APPENDEX (A)

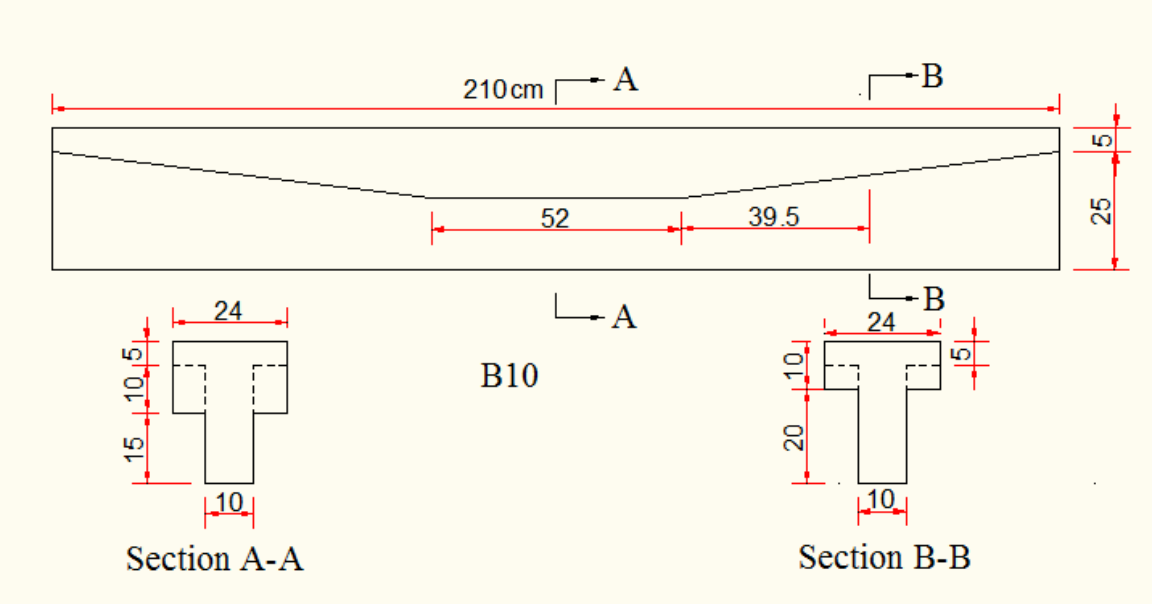

Beam No.(10)

Design flexural strength of section (A-A)

fc´ =35 Mpa f_y=490 Mpa

$\rho_b = 0.85\beta1 \frac{fc'}{fy}\left(\frac{600}{600+fy}\right)$

β1 ={ 0.85-0.008(fc´-30)}≥0.65 for fc´ >30 Mpa

β1= {0.85-0.008(35-30)} =0.81

$\rho_b = 0.85*0.81*\frac{35}{490}\left(\frac{600}{600+490}\right)=0.0271$

$\rho_{max} = 0.75\ \rho_b$

$\rho_{max} = 0.75*0.0271= 0.02$

$\rho_{min} = \frac{1.4}{fy}\frac{bw}{b} = \frac{1.4}{490}\frac{100}{240} = 1.19*10^{-3}$

Or $\rho_{min} = \frac{\sqrt{fc'}}{4fy}\frac{bw}{b} = \frac{\sqrt{35}}{4*490}\frac{100}{240} = 1.26*10^{-3}$

Use $\rho_{min} = 1.26*10^{-3}$

APPENDEX (A)

As = ρ b d= $1.26*10^{-3}*$ 240 * 260 =78.62 mm^2

Use Ø 10 A= $\frac{\pi}{4}*10^2$ A= 78.54 mm^2

n = $\frac{As}{A} = \frac{78.62}{78.54} \approx$ 2 bars

use 5Ø 10mm

As= 5*78.54= 392.7 mm^2

$\rho = \frac{392.7}{240*260} = 6.3*10^{-3} < \rho_{max} > \rho_{min}$ O.K

a = $\frac{As*fy}{0.85fc' b} = \frac{392.7*490}{0.85*35*240}$ =27mm $\rightarrow a < h_f$

c = $\frac{a}{0.85} = \frac{27}{0.85}$ = 31.76 mm

Mu = Ø Mn = Ø ρ b d^2 $f_y(1- 0.59 \rho \frac{fy}{fc'})$

Mu= 0.9 $*6.3*10^{-3}*240*(260)^2 *490(1- 0.59*6.3*10^{-3}*\frac{490}{35})$

Mu= 42.73 kN-m

Mu= $PL/4$ » P = $\frac{Mu*4}{L} = \frac{42.73*4}{2}$

P= 85.46 kN

Design flexural strength of section (B-B)

fc´ =35 Mpa f_y=490 Mpa

M=0.5*P*0.345= 0.5*85.46*0.345= 14.74 KN-m

$\rho = \frac{1-\sqrt{1-2.622M/(fc'bd^2)}}{1.18fy/fc'} = \frac{1-\sqrt{1-2.622*14.74*10^6/(35*240*260^2)}}{1.18*490/35}$

$\rho = 2.23*10^{-3}$

APPENDEX (A)

As= ρbd= $2.23*10^{-3}*240*260= 139mm^2$

Use Ø 10 A= $\frac{\pi}{4}*10^2$ A= 78.54 mm^2

$$n = \frac{As}{A} = \frac{139}{78.54} \approx 2 \text{ bars}$$

$$\rho_b = 0.85\beta1 \frac{fc'}{fy}\left(\frac{600}{600+fy}\right)$$

$\beta1 = \{0.85-0.008(fc'-30)\} \geq 0.65$ for $fc' > 30$ Mpa

$\beta1 = \{0.85-0.008(35-30)\} = 0.81$

$$\rho_b = 0.85*0.81*\frac{35}{490}\left(\frac{600}{600+490}\right)=0.0271$$

$\rho_{max} = 0.75\ \rho_b$

$\rho_{max} = 0.75*0.0271= 0.02$

$$\rho_{min} = \frac{1.4}{fy}\frac{bw}{b} = \frac{1.4}{490}\frac{100}{240} = 1.19*10^{-3}$$

Or $$\rho_{min} = \frac{\sqrt{fc'}}{4fy}\frac{bw}{b} = \frac{\sqrt{35}}{4*490}\frac{100}{240} = 1.26*10^{-3}$$

Use $\rho_{min} = 1.26*10^{-3}$

use 5Ø 10mm

$As = 5*78.54= 392.7\ mm^2$

$$\rho = \frac{392.7}{240*260} = 6.3*10^{-3} < \rho_{max} > \rho_{min}$$ O.K

$$a = \frac{As*fy}{0.85fc'\,b} = \frac{392.7*490}{0.85*35*240} = 27mm \rightarrow a < h_f$$

$$c = \frac{a}{0.85} = \frac{27}{0.85} = 31.76 \text{ mm}$$

APPENDEX (A)

Shear design of beam No.(10)

$fc' = 35$ Mpa $f_y = 420$ Mpa

Vu= 85.46/2 = 42.73 kN

$$\frac{vu*d}{mu} = \frac{42.73*0.26}{42.73} = 0.26 < 1$$

$$v_c = 0.17* \sqrt{fc'} * bw * d$$

$$v_c = 0.17*\sqrt{35} * 100 * 260 = 26149.1 \text{ N}$$

use ∅ 8 mm→ Av =no. $\frac{\pi\, ds^2}{4} = 2*\frac{\pi}{4} *8^2$

$Av = 100.48 \text{ mm}^2$

$$v_n = \frac{vu}{\emptyset} = \frac{42.73}{0.85} = 50.27 \text{ kN} = 50270 \text{ N} = 1.9V_C$$

$$S = \frac{d}{2} = \frac{260}{2} = 130 \text{ mm}$$

S = 600 mm

$$S = \frac{Av*fy}{0.34\, bw} = \frac{100.48*420}{0.34*100} = 1241 \text{mm}$$

$v_n = v_s + v_c \rightarrow v_s = 50270 - 26149.1 = 24120.9$ N

$$S = \frac{Av*fy*d}{vs} = \frac{100.48*420*260}{24120.9} = 455 \text{ mm}$$

$S_{min} = 130$ mm

Use ∅ 8 mm @50mm

APPENDEX (A)

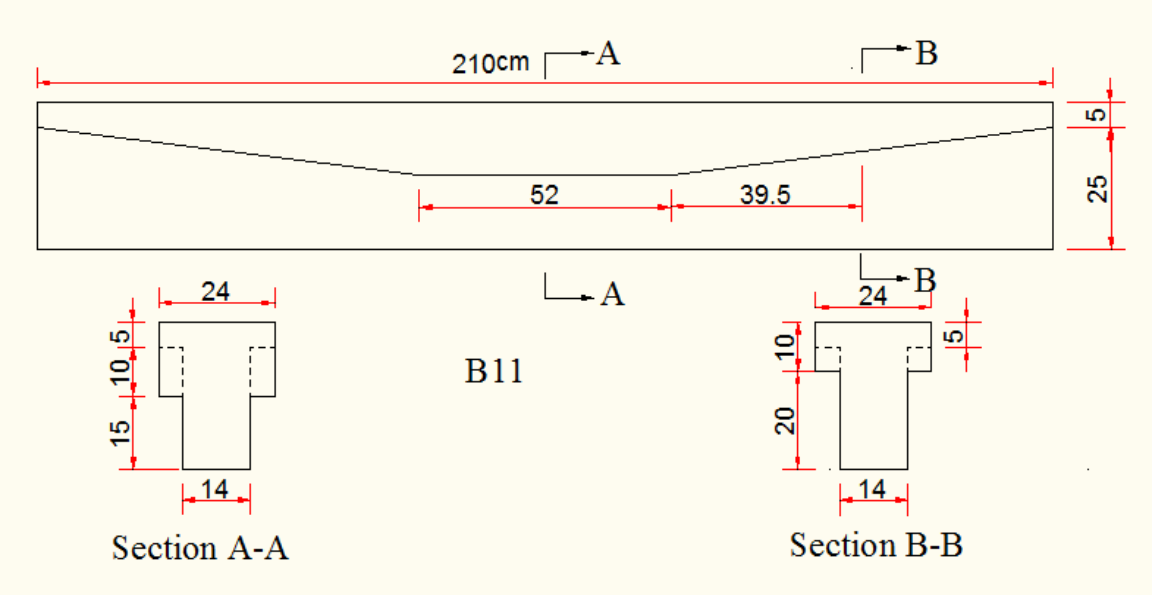

Beam No. (11)

Design flexural strength of section (A-A)

fc´ =35 Mpa f_y=490 Mpa

$$\rho_b = 0.85\beta1 \frac{fc'}{fy}\left(\frac{600}{600+fy}\right)$$

β1 ={ 0.85-0.008(fc´-30)}≥0.65 for fc´ >30 Mpa

β1= {0.85-0.008(35-30)} =0.81

$$\rho_b = 0.85*0.81*\frac{35}{490}\left(\frac{600}{600+490}\right)=0.0271$$

$$\rho_{max} = 0.75\ \rho_b$$

$$\rho_{max} = 0.75*0.0271= 0.02$$

$$\rho_{min} = \frac{1.4}{fy}\frac{bw}{b} = \frac{1.4}{490}\frac{140}{240} = 1.67*10^{-3}$$

Or $$\rho_{min} = \frac{\sqrt{fc'}}{4fy}\frac{bw}{b} = \frac{\sqrt{35}}{4*490}\frac{140}{240} = 1.76*10^{-3}$$

Use $$\rho_{min} = 1.76*10^{-3}$$

APPENDEX (A)

As = ρ b d= $1.76*10^{-3}$* 240 * 260 =109.82 mm^2

Use Ø 10 A= $\frac{\pi}{4}$ *10^2 A= 78.54 mm^2

n = $\frac{As}{A} = \frac{109.82}{78.54} \approx$ 2 bars

use 5Ø 10mm

As= 5*78.54= 392.7 mm^2

$\rho = \frac{392.7}{240*260}$ = 6.3* 10^{-3} < ρ_{max} > ρ_{min} O.K

a = $\frac{As*fy}{0.85fc' b} = \frac{392.7*490}{0.85*35*240}$ =27mm →a < h_f

c = $\frac{a}{0.85} = \frac{27}{0.85}$ = 31.76 mm

Mu = Ø Mn = Ø ρ b d^2 $f_y(1- 0.59 \rho \frac{fy}{fc'})$

Mu= 0.9 *6.3*10^{-3}*240*$(260)^2$ *490$(1- 0.59*6.3* 10^{-3}*\frac{490}{35})$

Mu= 42.73 kN-m

Mu= $PL/_4$ » P = $\frac{Mu*4}{L} = \frac{42.73*4}{2}$

P= 85.46 kN

Design flexural strength of section (B-B)

fc´ =35 Mpa f_y=490 Mpa

M=0.5*P*0.345= 0.5*85.46*0.345= 14.74 KN-m

$\rho = \frac{1-\sqrt{1-2.622M/(fc'bd^2)}}{1.18fy/fc'} = \frac{1-\sqrt{1-2.622*14.74*10^6/(35*240*260^2)}}{1.18*490/35}$

ρ= $2.23*10^{-3}$

APPENDEX (A)

As= ρbd= $2.23*10^{-3}*240*260= 139mm^2$

Use Ø 10 A= $\frac{\pi}{4}*10^2$ A= 78.54 mm^2

$$n = \frac{As}{A} = \frac{139}{78.54} \approx 2 \text{ bars}$$

$$\rho_b = 0.85\beta1 \frac{fc'}{fy}\left(\frac{600}{600+fy}\right)$$

$\beta1 = \{0.85-0.008(fc'-30)\} \geq 0.65$ for $fc' > 30$ mpa

$\beta1 = \{0.85-0.008(35-30)\} = 0.81$

$$\rho_b = 0.85*0.81*\frac{35}{490}\left(\frac{600}{600+490}\right)=0.0271$$

$\rho_{max} = 0.75\ \rho_b$

$\rho_{max} = 0.75*0.0271= 0.02$

$$\rho_{min} = \frac{1.4}{fy}\frac{bw}{b} = \frac{1.4}{490}\frac{140}{240} = 1.67*10^{-3}$$

Or $\rho_{min} = \frac{\sqrt{fc'}}{4fy}\frac{bw}{b} = \frac{\sqrt{35}}{4*490}\frac{140}{240} = 1.76*10^{-3}$

Use $\rho_{min} = 1.76*10^{-3}$

use 5Ø 10mm

$As = 5*78.54= 392.7\ mm^2$

$$\rho = \frac{392.7}{240*260} = 6.3*10^{-3} < \rho_{max} > \rho_{min}$$ O.K

$$a = \frac{As*fy}{0.85fc'\,b} = \frac{392.7*490}{0.85*35*240} = 27mm \rightarrow a < h_f$$

$$c = \frac{a}{0.85} = \frac{27}{0.85} = 31.76 \text{ mm}$$

APPENDEX (A)

Shear design of beam No.(11)

$fc' = 35$ Mpa $f_y = 420$ Mpa

Vu= 85.46/2 = 42.73 kN

$$\frac{vu*d}{mu} = \frac{42.73*0.26}{42.73} = 0.26 < 1$$

$$v_c = 0.17*\sqrt{fc'}*bw*d$$

$$v_c = 0.17*\sqrt{35}*140*260 = 36608.7 \text{ N}$$

use ∅ 8 mm→ Av =no. $\frac{\pi\, ds^2}{4} = 2*\frac{\pi}{4}*8^2$

$Av = 100.48 \text{ mm}^2$

$$v_n = \frac{vu}{\emptyset} = \frac{42.73}{0.85} = 50.27 \text{ kN} = 50270 \text{ N} = 1.9V_C$$

$$S = \frac{d}{2} = \frac{260}{2} = 130 \text{ mm}$$

S = 600 mm

$$S = \frac{Av*fy}{0.34\, bw} = \frac{100.48*420}{0.34*140} = 887 \text{mm}$$

$v_n = v_s + v_c \rightarrow v_s = 50270 - 36608.7 = 13661.3$ N

$$S = \frac{Av*fy*d}{vs} = \frac{100.48*420*260}{13661.3} = 803 \text{ mm}$$

$S_{min} = 130$ mm

Use ∅ 8 mm @50mm

APPENDEX (A)

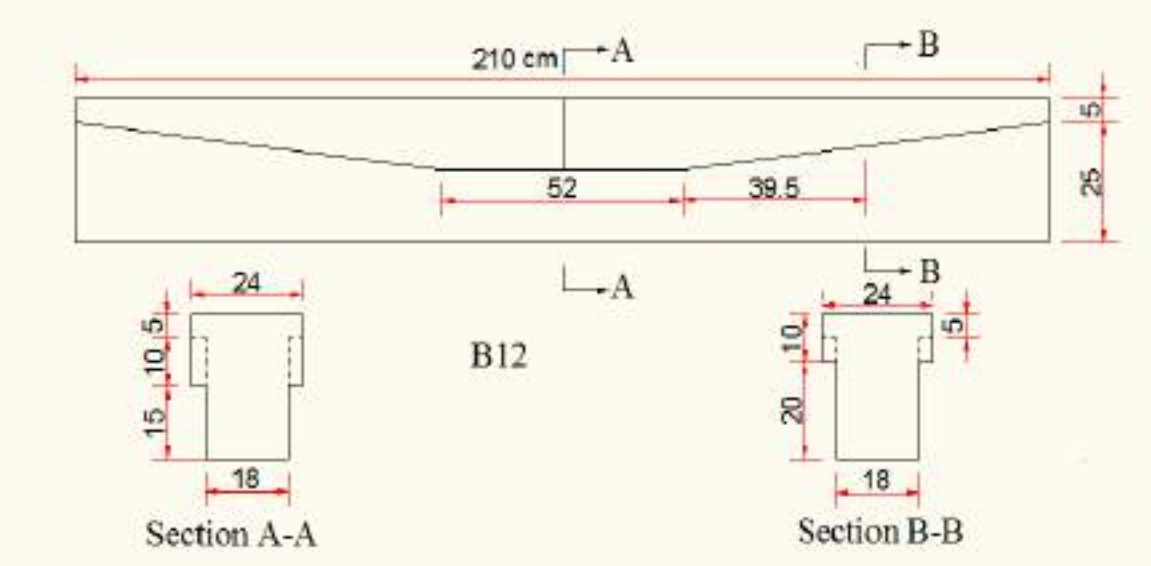

Beam No. (12)

Design flexural strength of section (A-A)

fc´ =35 Mpa f_y=490 Mpa

$\rho_b = 0.85\beta 1 \frac{fc'}{fy}(\frac{600}{600+fy})$-

β1 ={ 0.85-0.008(fc´-30)}≥0.65 for fc´ >30 Mpa

β1= {0.85-0.008(35-30)} =0.81

$\rho_b = 0.85*0.81*\frac{35}{490}(\frac{600}{600+490}) = 0.0271$

$\rho_{max} = 0.75\ \rho_b$

$\rho_{max} = 0.75*0.0271 = 0.02$

$\rho_{min} = \frac{1.4}{fy}\frac{bw}{b} = \frac{1.4}{490}\frac{180}{240} = 2.14*10^{-3}$

Or $\rho_{min} = \frac{\sqrt{fc'}}{4fy}\frac{bw}{b} = \frac{\sqrt{35}}{4*490}\frac{180}{240} = 2.26*10^{-3}$

Use $\rho_{min} = 2.26*10^{-3}$

As = ρ b d= $2.26*10^{-3}$* 240 * 260 =141.02 mm^2

APPENDEX (A)

Use Ø 10 A= $\frac{\pi}{4}$ *10^2 A= 78.54 mm^2

n = $\frac{As}{A} = \frac{141.02}{78.54} \approx$ 2 bars

use 5Ø 10mm

As= 5*78.54= 392.7 mm^2

$\rho = \frac{392.7}{240*260}$ = 6.3* 10^{-3} < ρ_{max} > ρ_{min} O.K

a = $\frac{As*fy}{0.85fc' b} = \frac{392.7*490}{0.85*35*240}$ =27mm →a < h_f

c = $\frac{a}{0.85} = \frac{27}{0.85}$ = 31.76 mm

Mu = Ø Mn = Ø ρ b d^2 $f_y(1- 0.59 \rho \frac{fy}{fc'})$

Mu= 0.9 *6.3*10^{-3}*240*$(260)^2$ *490$(1- 0.59*6.3* 10^{-3}*\frac{490}{35})$

Mu= 42.73 kN-m

Mu= $PL/_4$ » P = $\frac{Mu*4}{L} = \frac{42.73*4}{2}$

P= 85.46 kN

Design flexural strength of section (B-B)

fc´ =35 Mpa f_y=490 Mpa

M=0.5*P*0.345= 0.5*85.46*0.345= 14.74 KN-m

$\rho = \frac{1-\sqrt{1-2.622M/(fc'bd^2)}}{1.18fy/fc'} = \frac{1-\sqrt{1-2.622*14.74*10^6/(35*240*260^2)}}{1.18*490/35}$

ρ= 2.23*10^{-3}

As= ρbd= 2.23*10^{-3}*240*260= 139mm^2

APPENDEX (A)

Use Ø 10 A= $\frac{\pi}{4}$ *10^2 A= 78.54 mm^2

$n = \frac{As}{A} = \frac{139}{78.54} \approx 2$ bars

$\rho_b = 0.85\beta1 \frac{fc'}{fy}(\frac{600}{600+fy})$

$\beta1 = \{0.85-0.008(fc'-30)\} \geq 0.65$ for $fc' > 30$ Mpa

$\beta1 = \{0.85-0.008(35-30)\} = 0.81$

$\rho_b = 0.85*0.81*\frac{35}{490}(\frac{600}{600+490}) = 0.0271$

$\rho_{max} = 0.75\ \rho_b$

$\rho_{max} = 0.75*0.0271 = 0.02$

$\rho_{min} = \frac{1.4}{fy}\frac{bw}{b} = \frac{1.4}{490}\frac{180}{240} = 2.14*10^{-3}$

Or $\rho_{min} = \frac{\sqrt{fc'}}{4fy}\frac{bw}{b} = \frac{\sqrt{35}}{4*490}\frac{180}{240} = 2.26*10^{-3}$

Use $\rho_{min} = 2.26*10^{-3}$

use 5Ø 10mm

$As = 5*78.54 = 392.7\ mm^2$

$\rho = \frac{392.7}{240*260} = 6.3*10^{-3} < \rho_{max} > \rho_{min}$ O.K

$a = \frac{As*fy}{0.85fc'\,b} = \frac{392.7*490}{0.85*35*240} = 27mm \rightarrow a < h_f$

$c = \frac{a}{0.85} = \frac{27}{0.85} = 31.76$ mm

Shear design of beam No.(12)

$fc' = 35$ Mpa $f_y = 420$ Mpa

APPENDEX (A)

Vu= 85.46/2 = 42.73 kn

$\frac{vu*d}{mu} = \frac{42.73*0.26}{42.73}$ =0.26 < 1

$v_c = 0.17* \sqrt{fc'} * bw * d$

$v_C = 0.17*\sqrt{35} * 180 * 260 = 47068$ N

use ∅ 8 mm→ Av =no. $\frac{\pi\, ds^2}{4} = 2*\frac{\pi}{4} *8^2$

Av=100.48 mm^2

$v_n = \frac{Vu}{\emptyset} = \frac{42.73}{0.85}$ = 50.27 kN =50270 N = 1.07V_C

$S = \frac{d}{2} = \frac{260}{2}$ =130 mm

S = 600 mm

$S = \frac{Av*fy}{0.34\ bw} = \frac{100.48*420}{0.34*180}$ =690mm

$v_n = v_s+v_c \rightarrow v_s$=50270-47068=3202 N

$S = \frac{Av*fy*d}{vs} = \frac{100.48*420*260}{3202}$ =3427 mm

S_{min} = 130 mm

Use ∅ 8 mm @50mm

Appendex (B)

beam	Section	Moment (KN-M)	As (mm^2)	ρ	ρmax	ρmin
B1	A-A	42.73	392.7	$6.3* 10^{-3}$	0.02	$3* 10^{-3}$
B2	A-A	42.73	392.7	$6.3* 10^{-3}$	0.02	$1.26* 10^{-3}$
B3	A-A	42.72	392.7	$6.3* 10^{-3}$	0.02	$1.26* 10^{-3}$
B4	A-A	42.73	392.7	$6.3* 10^{-3}$	0.02	$1.26* 10^{-3}$
	B-B	20.3	181	$2.9* 10^{-3}$	0.02	$1.26* 10^{-3}$
B5	A-A	42.73	392.7	$6.3* 10^{-3}$	0.02	$1.76* 10^{-3}$
	B-B	20.3	181	$2.9* 10^{-3}$	0.02	$1.76* 10^{-3}$
B6	A-A	42.73	392.7	$6.3* 10^{-3}$	0.02	$2.26* 10^{-3}$
	B-B	20.3	181	$2.9* 10^{-3}$	0.02	$2.26* 10^{-3}$
B7	A-A	42.73	392.7	$6.3* 10^{-3}$	0.02	$1.26* 10^{-3}$
	B-B	17.52	156	$2.5* 10^{-3}$	0.02	$1.26* 10^{-3}$
B8	A-A	42.73	392.7	$6.3* 10^{-3}$	0.02	$1.76* 10^{-3}$
	B-B	17.52	156	$2.5* 10^{-3}$	0.02	$1.76* 10^{-3}$
B9	A-A	42.73	392.7	$6.3* 10^{-3}$	0.02	$2.26* 10^{-3}$
	B-B	17.52	156	$2.5* 10^{-3}$	0.02	$2.26* 10^{-3}$
B10	A-A	42.73	392.7	$6.3* 10^{-3}$	0.02	$1.26* 10^{-3}$
	B-B	14.74	139	$2.23* 10^{-3}$	0.02	$1.26* 10^{-3}$
B11	A-A	42.73	392.7	$6.3* 10^{-3}$	0.02	$1.76* 10^{-3}$
	B-B	14.74	139	$2.23* 10^{-3}$	0.02	$1.76* 10^{-3}$
B12	A-A	42.73	392.7	$6.3* 10^{-3}$	0.02	$2.26* 10^{-3}$
	B-B	14.74	139	$2.23* 10^{-3}$	0.02	$2.26* 10^{-3}$

الخلاصه

الهدف الاساسي من هذه الدراسه هو لتحري الكفاءه للعتبات ذات الشفاه غير الموشوريه على زيادة التحمل وليونة الانثناء وقابلية الدوران دون تاثير كبير على قابلية التحمل القصوى والصلاده وسلوك الحمل المسبب للانحناء للعتبات الخرسانيه المسلحه، لهذا الهدف اختيرت المتغيرات لتتناسب مع هذه الفكره، ان المتغيرات العمليه في هذه الدراسه كانت هي باستخدام شفه مسلوبة الشكل اي سمكها متغير تقريبا على طول العتبات وكذلك سمك الجزء الاسفل من العتبه متغير بين عتبه واخرى وبما انه مقاومة الانثناء للعتبات تتناسب مع المسافه المقاسه من وسط العتبه الخرسانيه لذلك فان الشفاه الغير موشوريه والجزء الاسفل المتغيرمن العتبه الخرسانيه تم اختيارهما لهذا الهدف وللمقارنه مع عتبات المقارنه وهو الجسر ذو المقطع المستطيل والجسور ذات الشفاه الاعتياديه.

هذه الدراسه تضمنت صب وفحص اثناعشر عتبه خرسانيه متماثله في توزيع وكمية الحديد الطولي وكذلك الحلقي، صنفت العتبات الى اربعة مجاميع كل مجموعه تحتوي على ثلاثة عتبات،المجموعه الاولى تتكون من عتبه ذات مقطع مستطيل ثابت واثنين ذات شفاه ثابتة السماكه على طول العتبه الاولى بسمك ١٥ سم اما الاخرى فسماكتها ٥ سم اما باقي المجاميع كانت عباره عن عتبات ذات شفاه غير موشوريه وكانت المتغيرات فيها هو سمك الجزء الاسفل من العتبه وبناءا على ذلك يكون عرض الشفه متغير من الاسفل اضافة الى ذلك الشكل الهندسي للشفة المسلوب الشكل والمتغير من مجموعه الى اخرى حيث يبدأ سمك الشفه ب ٥ سم عند الحافه حتى يصل الى ١٥ سم في منتصف العتبه هذا بالتسبه للمجموعه الثانيه اما بالنسبه للمجموعه الثالثه فيصل سمك الشفه المتغير الى ١٥ سم على بعد نصف عمق الحديد الفعال ويستمر بنفس السمك حتى منتصف العتبه اما المجموعه الرابعه فهي مشابهه للمجموعه الثالثه ولكن وصول السمك لل ١٥ سم يكون على بعد مساوي لعمق الحديد الفعال ويستمر حتى منتصف العتبه، لقد تم تنفيذ العمل من صب ومعالجه تحت نفس الظروف وطبقا للمواصفات ولتحري سلوك العتبات الخرسانيه تم تثبيت مقياسين لقراءة مقدار الانحناء والازاحه في العتبات وكذلك تم تثبيت اربعة مقاييس الكترونيه في مناطق مختلفه من العتبات لتسجيل مقدار الانفعال، بينت هذه الدراسه ان هناك زياده في معدل المقاومه ومرونة الانثناء وسعة الدوران دون تاثير على مقدار الحمل الاقصى والصلاده وسلوك حمل الانحناء للنماذج ذات الشفاه غير الموشوريه.

الخلاصه

أن نسبة الحمل الاقصى للعتبات غير الموشوريه هي الأكبر مقارنة بالعتبه ذات المقطع المستطيل، كما أكدت تلك الدراسه على أن التغير بالشكل يحافظ على المقاومة القصوى مع زياده طفيفه وكذلك زياده في نسبة المقاومه بالنسبه للحجم للعتبات ذات الشفاه غير الموشوريه وهذا الموضوع يجب أن يؤخذ بنظر الأعتبار لأنتاج مقاطع خفيفة الوزن وأقتصاديه كما أن هناك زياده كبيره في ليونة الأنثناء وكذلك أستدامه بلاستيكيه أعلى مقارنة بالعتبه ذات المقطع المستطيل وكذلك أكبر من العتبات ذات الشفاه الثابته أو العاديه بالرغم أن نسبة حديد التسليح متماثله في التوزيع والكميه في كل العتبات وكذلك درجة المقاومه والصنف للخرسانه هي نفسها لكل العتبات، خطوط منحني الأنحناء عند مستوى التحميل الأقصى تمتلك ليونه مختلفه وسجلت زياده ملحوظه في سعة الأنحناء في المجموعات الثلاث التي هي عتبات ذات الشفاه غير الموشوريه.

من خلال المراقبه لوحظ أن للعتبات الخرسانيه غير الموشوريه كفاءه عاليه في زيادة الليونه على طول العتبه وهذا ناتج من تناسب تغير الشكل مع تناقص عزم الأنحناء كلما أبتعدنا من منتصف العتبه بأتجاه المسند كما أن الخضوع لحديد التسليح والأنحناء المرن حافضوا على الأنتشار التدريجي للتشققات المرافقه للسلوك البلاستيكي حتى حدوث الفشل.

أن قيم سعة الدوران البلاستيكي(θ) زادت بشكل ملحوظ للعتبات ذات الشفاه غير الموشوريه مقارنة مع العتبات الأخرى (ذات المقطع المستطيل والعتبات ذات الشفاه الثابته) كما أكدت هذه الدراسه بأن طول المفصل البلاستيكي تقريبا يساوي ١,٢ مره من عمق المقطع بدلا من الشائع والمتداول وهو العمق الفعال لحديد التسليح.

بالتحري لنمط الفشل بالنسبه لعينات المقارنه (ذات المقطع المتطيل والثابتة الشفاه) لوحظ أن التشقق الأبتدائي كان تقريبا في المنطقه الوسطى للعتبه التي تقابل أكبر عزم أنحناء بينما في بقية المجموات نشأت شقوق في المنطقه الوسطيه وواحد أو تشققين أستمرا بالأتساع أكثر من الباقي.

جمهورية العراق
وزارة التعليم العالي والبحث العلمي
جامعة ميسان / كلية الهندسة
قسم الهندسة المدنية

السلوك الانشائي للعتبات الخرسانيه المسلحه الكونكريتيه بسيطةالاسناد ذات الشفاه غير الموشوريه

رسالة
مقدمة إلى قسم الهندسة المدنية في جامعة ميسان كجزء من متطلبات نيل
شهادة الماجستير في علوم الهندسة المدنية/انشاءات

من قبل

جاسم كاظم زامل العبادي
(بكالوريوس هندسة مدنية ١٩٩١)

باشراف

ا.م.د. سعد فهد رسن

محرم ١٤٤١ أيلول ٢٠١٩